IAEA TECDOC SERIES

IAEA-TECDOC-1761

Performance Analysis Review of Thorium TRISO Coated Particles during Manufacture, Irradiation and Accident Condition Heating Tests

IAEA
International Atomic Energy Agency

PERFORMANCE ANALYSIS REVIEW OF THORIUM TRISO COATED PARTICLES DURING MANUFACTURE, IRRADIATION AND ACCIDENT CONDITION HEATING TESTS

The following States are Members of the International Atomic Energy Agency:

AFGHANISTAN
ALBANIA
ALGERIA
ANGOLA
ARGENTINA
ARMENIA
AUSTRALIA
AUSTRIA
AZERBAIJAN
BAHAMAS
BAHRAIN
BANGLADESH
BELARUS
BELGIUM
BELIZE
BENIN
BOLIVIA
BOSNIA AND HERZEGOVINA
BOTSWANA
BRAZIL
BRUNEI DARUSSALAM
BULGARIA
BURKINA FASO
BURUNDI
CAMBODIA
CAMEROON
CANADA
CENTRAL AFRICAN REPUBLIC
CHAD
CHILE
CHINA
COLOMBIA
CONGO
COSTA RICA
CÔTE D'IVOIRE
CROATIA
CUBA
CYPRUS
CZECH REPUBLIC
DEMOCRATIC REPUBLIC OF THE CONGO
DENMARK
DOMINICA
DOMINICAN REPUBLIC
ECUADOR
EGYPT
EL SALVADOR
ERITREA
ESTONIA
ETHIOPIA
FIJI
FINLAND
FRANCE
GABON
GEORGIA
GERMANY
GHANA
GREECE
GUATEMALA
GUYANA
HAITI
HOLY SEE
HONDURAS
HUNGARY
ICELAND
INDIA
INDONESIA
IRAN, ISLAMIC REPUBLIC OF
IRAQ
IRELAND
ISRAEL
ITALY
JAMAICA
JAPAN
JORDAN
KAZAKHSTAN
KENYA
KOREA, REPUBLIC OF
KUWAIT
KYRGYZSTAN
LAO PEOPLE'S DEMOCRATIC REPUBLIC
LATVIA
LEBANON
LESOTHO
LIBERIA
LIBYA
LIECHTENSTEIN
LITHUANIA
LUXEMBOURG
MADAGASCAR
MALAWI
MALAYSIA
MALI
MALTA
MARSHALL ISLANDS
MAURITANIA, ISLAMIC REPUBLIC OF
MAURITIUS
MEXICO
MONACO
MONGOLIA
MONTENEGRO
MOROCCO
MOZAMBIQUE
MYANMAR
NAMIBIA
NEPAL
NETHERLANDS
NEW ZEALAND
NICARAGUA
NIGER
NIGERIA
NORWAY
OMAN
PAKISTAN
PALAU
PANAMA
PAPUA NEW GUINEA
PARAGUAY
PERU
PHILIPPINES
POLAND
PORTUGAL
QATAR
REPUBLIC OF MOLDOVA
ROMANIA
RUSSIAN FEDERATION
RWANDA
SAN MARINO
SAUDI ARABIA
SENEGAL
SERBIA
SEYCHELLES
SIERRA LEONE
SINGAPORE
SLOVAKIA
SLOVENIA
SOUTH AFRICA
SPAIN
SRI LANKA
SUDAN
SWAZILAND
SWEDEN
SWITZERLAND
SYRIAN ARAB REPUBLIC
TAJIKISTAN
THAILAND
THE FORMER YUGOSLAV REPUBLIC OF MACEDONIA
TOGO
TRINIDAD AND TOBAGO
TUNISIA
TURKEY
UGANDA
UKRAINE
UNITED ARAB EMIRATES
UNITED KINGDOM OF GREAT BRITAIN AND NORTHERN IRELAND
UNITED REPUBLIC OF TANZANIA
UNITED STATES OF AMERICA
URUGUAY
UZBEKISTAN
VENEZUELA, BOLIVARIAN REPUBLIC OF
VIET NAM
YEMEN
ZAMBIA
ZIMBABWE

The Agency's Statute was approved on 23 October 1956 by the Conference on the Statute of the IAEA held at United Nations Headquarters, New York; it entered into force on 29 July 1957. The Headquarters of the Agency are situated in Vienna. Its principal objective is "to accelerate and enlarge the contribution of atomic energy to peace, health and prosperity throughout the world".

IAEA-TECDOC-1761

PERFORMANCE ANALYSIS REVIEW OF THORIUM TRISO COATED PARTICLES DURING MANUFACTURE, IRRADIATION AND ACCIDENT CONDITION HEATING TESTS

INTERNATIONAL ATOMIC ENERGY AGENCY
VIENNA, 2015

For further information on this publication, please contact:

Nuclear Fuel Cycle and Materials Section
International Atomic Energy Agency
Vienna International Centre
PO Box 100
1400 Vienna, Austria
Email: Official.Mail@iaea.org

Printed by the IAEA in Austria
March 2015

IAEA Library Cataloguing in Publication Data

Performance analysis review of thorium TRISO coated particles during manufacture, irradiation and accident condition heating tests.
— Vienna : International Atomic Energy Agency, 2015.
p. ; 30 cm. — (IAEA-TECDOC series, ISSN 1011–4289 ; no. 1761)
ISBN 978–92–0–100715–5
Includes bibliographical references.

1. Nuclear reactors — Materials. 2. Nuclear fuels — Testing. 3. Gas cooled reactors — Research. I. International Atomic Energy Agency. II. Series.

IAEAL 15–00960

FOREWORD

Thorium, in combination with high enriched uranium, was used in all early high temperature reactors (HTRs). Initially, the fuel was contained in a kernel of coated particles. However, particle quality was low in the 1960s and early 1970s.

Modern, high quality, tristructural isotropic (TRISO) fuel particles with thorium oxide and uranium dioxide (UO_2) had been manufactured since 1978 and were successfully demonstrated in irradiation and accident tests. In 1980, HTR fuels changed to low enriched uranium UO_2 TRISO fuels. The wide ranging development and demonstration programme was successful, and it established a worldwide standard that is still valid today.

During the process, results of the thorium work with high quality TRISO fuel particles had not been fully evaluated or documented. This publication collects and presents the information and demonstrates the performance of thorium TRISO fuels.

This publication is an outcome of the technical contract awarded under the IAEA Coordinated Research Project on Near Term and Promising Long Term Options for Deployment of Thorium Based Nuclear Energy, initiated in 2012. It is based on the compilation and analysis of available results on thorium TRISO coated particle performance in manufacturing and during irradiation and accident condition heating tests.

The IAEA expresses its appreciation to H. Nabielek (Germany) for the preparation of this publication. The IAEA officer responsible for this publication was U. Basak of the Division of Nuclear Fuel Cycle and Waste Technology.

EDITORIAL NOTE

This publication has been prepared from the original material as submitted by the contributors and has not been edited by the editorial, staff of the IAEA. The views expressed remain the responsibility of the contributors and do not necessarily represent the views of the IAEA or its Member States.

Neither the IAEA nor its Member States assume any responsibility for consequences which may arise from the use of this publication.

This publication does not address questions of responsibility, legal or otherwise, for acts or omissions on the part of any person.

The use of particular designations of countries or territories does not imply any judgement by the publisher, the IAEA, as to the legal status of such countries or territories, of their authorities and institutions or of the delimitation of their boundaries.

The mention of names of specific companies or products (whether or not indicated as registered) does not imply any intention to infringe proprietary rights, nor should it be construed as an endorsement or recommendation on the part of the IAEA.

The IAEA has no responsibility for the persistence or accuracy of URLs for external or third party Internet web sites referred to in this publication and does not guarantee that any content on such web sites is, or will remain, accurate or appropriate.

CONTENTS

1. THORIUM IN HIGH TEMPERATURE REACTORS

1.1. INTRODUCTION

^{235}U is the initial and primary fissile material to drive nuclear power generation. Other fissile materials are ^{233}U, ^{239}Pu and ^{241}Pu.

Natural uranium contains 99.3% of ^{238}U and 0.7% of ^{235}U. Therefore, most reactors use enriched uranium.

With uranium fuels, ^{238}U produces fissile plutonium during reactor irradiation:

$$^{238}_{92}U + n \rightarrow ^{239}_{92}U \xrightarrow{\beta^-} ^{239}_{93}Np \xrightarrow{\beta^-} ^{239}_{94}Pu$$

with 65% fission and 35% capture cross section for incoming neutrons. Neutron capture leads to ^{241}Pu as additional fissile isotope.

Thorium containing nuclear fuels produces fissile ^{233}U during reactor irradiation:

$$^{232}_{90}Th + n \rightarrow ^{233}_{90}Th \xrightarrow{\beta^-} ^{233}_{91}Pa \xrightarrow{\beta^-} ^{233}_{92}U$$

with 90% fission and 10% capture cross section for incoming neutrons.

All early high temperature reactors (HTRs) used thorium and high enriched uranium as fuels. The main problem in utilizing thorium today is the difficulty of handling high enriched fissile materials that are required for the start of a thorium-containing system.

The original advantages of thorium fuels are found in many reports [1–7].

ThO_2 is very stable and is one of the highest known refractories. It melts at 3390°C (UO_2 at 2865°C) thereby allowing high burnup and high temperatures. At the same time, this complicates chemical treatment for the separation of Th compounds and their dissolution for reprocessing.

Oxide fuels of Th, U, and Pu have similar physical characteristics enabling the manufacture of hybrid oxide fuels that may be promising for a wide range of applications.

Between fissile materials ^{233}U, ^{235}U and ^{239}Pu, ^{233}U is best in terms of the ratio of neutron yield per fission to neutrons absorbed. Its fission products have less poisoning neutronic effects and are less aggressive in HTR coated particle fuels. ^{233}U also retains its good neutronic properties with higher temperatures.

Thorium cycle fuels generate at least one order of magnitude less long lived minor actinides [8, 9] than plutonium fuel cycles.

^{233}U, with its superior nuclear properties vs. ^{235}U and ^{239}Pu, might be misused for weapons production. However, the decay products of ^{232}Th and ^{232}U (Fig. 1) contain 1 – 2.6 MeV hard gamma emitters. This necessitates remote manufacture, but can also be considered as a safeguard against malicious use. In practice, it is significantly more proliferation resistant due to the presence of ^{232}U and its daughters because of associated handling difficulties and easy tracing.

For Th utilization, next to ^{235}U fissile contributions in a thorium nuclear power plant, also Pu from LWRs or ^{233}U bred in Th reactors might be used.

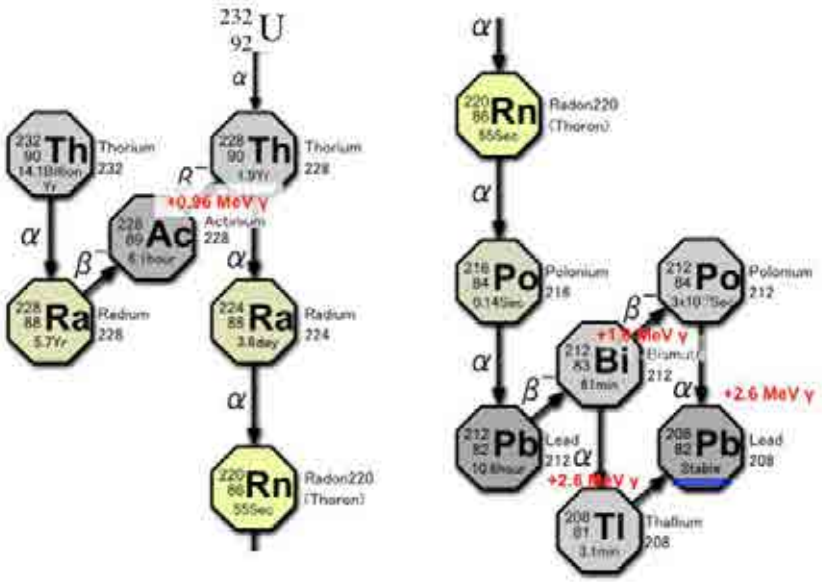

FIG. 1. ^{232}Th and ^{232}U decay products with hard gamma ray emitting isotopes.

A Th-U fuel cycle is more amenable to multiple recycling of ^{233}U compared to Pu recycling in U-Pu fuel cycle. This is caused by the lower non-fissile absorption of neutrons in ^{233}U than in ^{235}U and ^{239}Pu while the fission cross-sections are similar leading to lower generation of higher isotopes in the Th-U fuel cycle. Furthermore, in the case of application of a pure $^{233}U/^{232}Th$ mix in fuel composition, i.e. absence of ^{238}U and plutonium in 'fresh' fuel, the amount of minor actinides in spent fuel drops significantly.

In addition to the elimination of the need for an enrichment process, a fuel cycle based on thorium/^{233}U has other proliferation resistance related peculiarities. Unlike the plutonium case one more barrier for potential proliferation of ^{233}U can be created by denaturising it by mixing it with the non-fissile isotope ^{238}U (in practice with depleted uranium) to create 'reactor grade' but not a 'weapon grade' $^{233}U/^{238}U$ mixture not adherent to chemical separation. The critical configuration (i.e. mass, geometry etc.) of the mixture of 12% ^{233}U with ^{238}U approximately corresponds to 20% enriched $^{235}U/^{238}U$ compound.

Once irradiated, the fuel of a Th-U cycle contains an admixture of ^{232}U whose radioactive decay chain includes emitters (particularly ^{208}Tl) of high energy gamma radiation. This makes spent Th fuel treatment more difficult, requires remote handling/control during the reprocessing as well as during further fuel fabrication, but may be considered as an additional non-proliferation barrier.

Thorium fuel may be utilised either in a once-through manner (also called open fuel cycle), i.e. via breeding ^{233}U in a fuel element and afterwards burning it up in the same element, or in a mode with spent fuel reprocessing, i.e. in a closed fuel cycle.

The breeding ratio of ^{233}U depends on the type of the reactor utilising thorium and on the mode chosen (obviously a once through fuel cycle is not able to achieve breeding ratios as high as one with reprocessing). Historically, in the USA at the Shipping Port 72 MW(e) light water reactor, a breeding ratio of 1.01 was achieved. According to design calculations, a light

water breeding reactor (LWBR) could theoretically reach a breeding ratio of 1.06. According to preliminary studies, due to even better neutron efficiency in a core of a heavy water moderated reactor (HWR), one is able to reach a breeding ratio higher than 1 in a HWR with Th-U fuel. HWR is long known to have a high Th/^{233}U conversion ratio, and innovative HWR concepts can be designed to have at least (semi-self-breeding) possibility of a self-sustaining fuel cycle.

Thorium and ^{233}U utilization is technically feasible in most of existing and prospective reactor types, including gas cooled, light water and heavy water reactors, fast breeders, and molten salt reactors. For the majority of thorium introduction options, only reactor physics studies have been performed and there are other aspects in the use of thorium that may require more detailed investigations as well as several technological developments are necessary for their commercial implementation. Especially, the incorporation of Th-U fuel into cores of existing reactors requires modifications in engineered systems, such as reactor and reactivity control devices, mainly because of the difference in the effective fractions of delayed neutrons per fission that are the basis for power control of a reactor. For ^{235}U-the fraction is ~0.0065 but only ~0.00266 for ^{233}U.

Some countries consider the application of thorium in thermal reactors as a short to middle term option. E.g. the natural resources of cheap uranium in the Russian Federation may be exhausted by the Russian nuclear energy system based on thermal reactors by the middle of the current century. At that time Russian fleet of reactors will consist of WWER (Vodo-Vodyanoi Energetichesky Reactor = water water power reactor) type reactors to large extent, which consume low enriched uranium. The significant part of WWER reactors will not exceed their design life and the smooth change-over of operating WWERs to denaturized ^{233}U based fuel cycle is considered as possible option for the procurement of fuel for this good mastered technology. Denaturized uranium, i.e. the mixture of ^{233}U and depleted or regenerated uranium, may have higher resistance against the proliferation of nuclear materials. ^{233}U can be produced either in thermal reactors using mixed uranium and thorium oxides fuel or in thorium blankets of fast reactors of BN type (fast neutron reactors with sodium coolant) with MOX fuel used in a core. Comparison of thermal and fast reactors features on effectiveness to use plutonium based fuel for ^{233}U accumulation showed that the efficiency of thermal neutron spectrum breeder of WWER type is significantly worse than fast neutron spectrum of BN type reactor. Besides, fast reactor allows producing uranium with significantly less content of ^{233}U.

Advanced heavy water reactor (AHWR) under design is a 920 MW(th) nuclear installation destined especially for effective utilization of thorium fuel. It is vertical pressure tube type thorium based reactor cooled by boiling light water and moderated by heavy water. The main objectives are to achieve relatively higher fraction of power from Th/^{233}U, negative void reactivity coefficient, minimisation of initial inventory and consumption of plutonium, self-sustaining characteristics in ^{233}U and high discharge burnup. Plutonium is used as makeup fuel to achieve high discharge burnup and self-sustaining characteristics of Th-^{233}U fuel cycle. The ^{233}U required is to be bred in situ. However, the calculations show that there will be annual deficit of about 22 kg of ^{233}U if the core is refuelled with the composite clusters having 30 (Th-^{233}U) MOX and 24 (Th-Pu) MOX pins alone. Hence, an alternate cluster was designed to generate the required ^{233}U to make the AHWR core self-sustaining in ^{233}U. The reactor, however, offers enough flexibility to accommodate different kinds of fuel cycles. Few cases were studied to achieve high discharge burnup by using LEU as external feed in thorium oxide fuel in AHWR. The enriched uranium with initial configuration 19.75% ^{235}U and 80.25% ^{238}U was used along with thorium in all the 54 pins of the AHWR fuel cluster and

calculations were done for the equilibrium fuel cycle. It was found that in a case with the average LEU content of 21.3% gives high burnup of about 64 GWd/t. There is better utilization of natural uranium resources. Also, the discharged fuel contains less plutonium and less minor actinides.

In a short term prospective implementation of Th/U based fuel in operating reactors in a once-through mode may become technically available. However, fuel cycle services like reprocessing and recycled fuel fabrication demand the development of several new technologies to provide the necessary economic competitiveness at a commercial scale of operation, and will be available, apparently, only in long term prospective. Nonetheless, multi-fold growth of electricity demand and a tentatively rapid increase of nuclear capacity may change the priorities for nuclear power and accelerate development of technologies needed.

Taking into account a high potential growth of nuclear power, there are some concerns in the nuclear community on the availability of reasonable priced nuclear fuel based on U/Pu fuel cycles, which may not be sustainable on their own in the long term future. A collaborative effort among interested INPRO members to study possibilities of introducing thorium could therefore be expected to be worthwhile6. It also generates a new perspective and/or clarification to the potential contribution of thorium to sustainable global growth in the 21st century.

1.2. HIGH TEMPERATURE REACTORS AND THEIR FUELS

The high temperature reactor (HTR) is characterized by an all ceramic core structure made of nuclear grade graphite as the moderator, reflector, core support and primary fuel element material. The nuclear fuel is also a ceramic with a number of ceramic coatings surrounding an oxide or carbide fuel. The use of refractory core materials combined with a single phase inert helium coolant allows high coolant temperatures up to 950°C and a high thermal efficiency. Together, these design selections present a number of inherent safety advantages, including: a reactor core with a low power density and a large heat capacity; the absence of coolant phase changes; and the prompt negative temperature coefficient. These features ease reactor siting constrains by reducing both cooling water requirements and the consequences of postulated accidents [10–12].

Early development of HTRs proceeded in two directions: (1) the pebble bed concept in Germany and the Russian Federation, and (2) the prismatic core concept in the United States of America (USA), the United Kingdom (UK) and the Japan pin-in-block type.

Although both the pebble bed and the prismatic core concepts employ an all ceramic core, ceramic fuel and use helium as coolant, the differ substantially with respect to the type of fuel elements employed by each.

The pebble bed HTR concept employs a spherical fuel element, 60 mm diameter, manufactured by a cold isostatic moulding process. This element is of two-part design with an inner 50 mm diameter fuel zone surrounded by a 5 mm thick fuel free shell of graphitized carbonaceous material (Fig. 2). The fuel zone contains the coated particles, overcoated with matrix material and then homogenously dispersed within the graphitized matrix. The pebble bed concept was initially pursued in Germany and Russia, and today China [10–12].

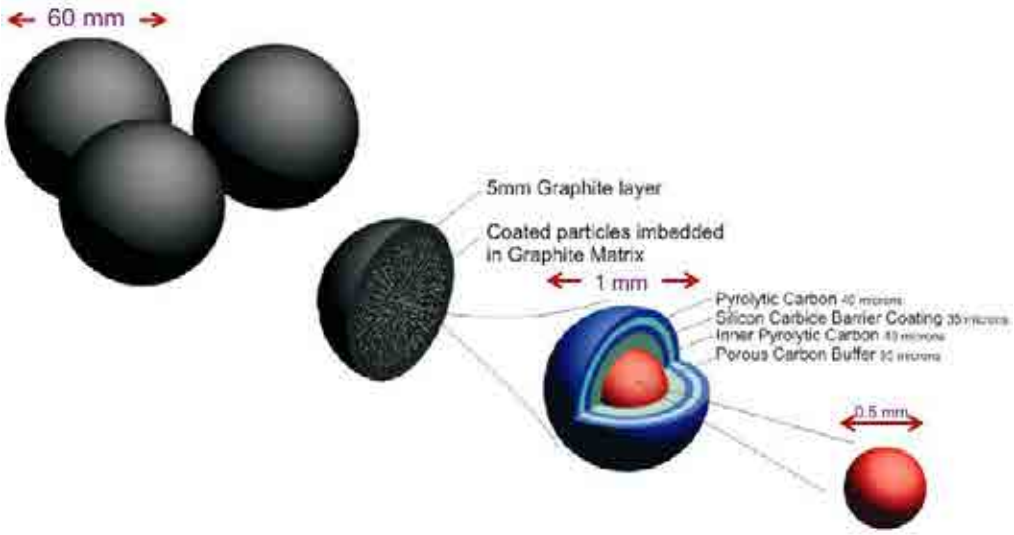

FIG. 2. Spherical fuel element consisting of ~50 mm diameter fuel zone and ~5 mm thick fuel free zone, the TRISO coated particle and the 0.5 mm diameter fuel kernel.

In the prismatic core HTR concept (sometimes called the HTGR — high temperature gas cooled reactor), the fuel elements are fabricated from nuclear grade graphite machined into a hexagonal shape, 800 mm high by 360 mm across flats. Separate fuel and coolant holes are drilled into the graphite block with six fuel holes surrounding each coolant hole in a hexagonal pattern (Fig. 3). Prefabricated fuel compacts, 12.5 mm diameter by 50 mm long contain the coated fuel particles in a close-packed array, dispersed within a carbonaceous matrix. These fuel compacts are then stacked in the fuel holes. The prismatic core concept was initially pursued in the United States of America, United Kingdom and Japan [10–12].

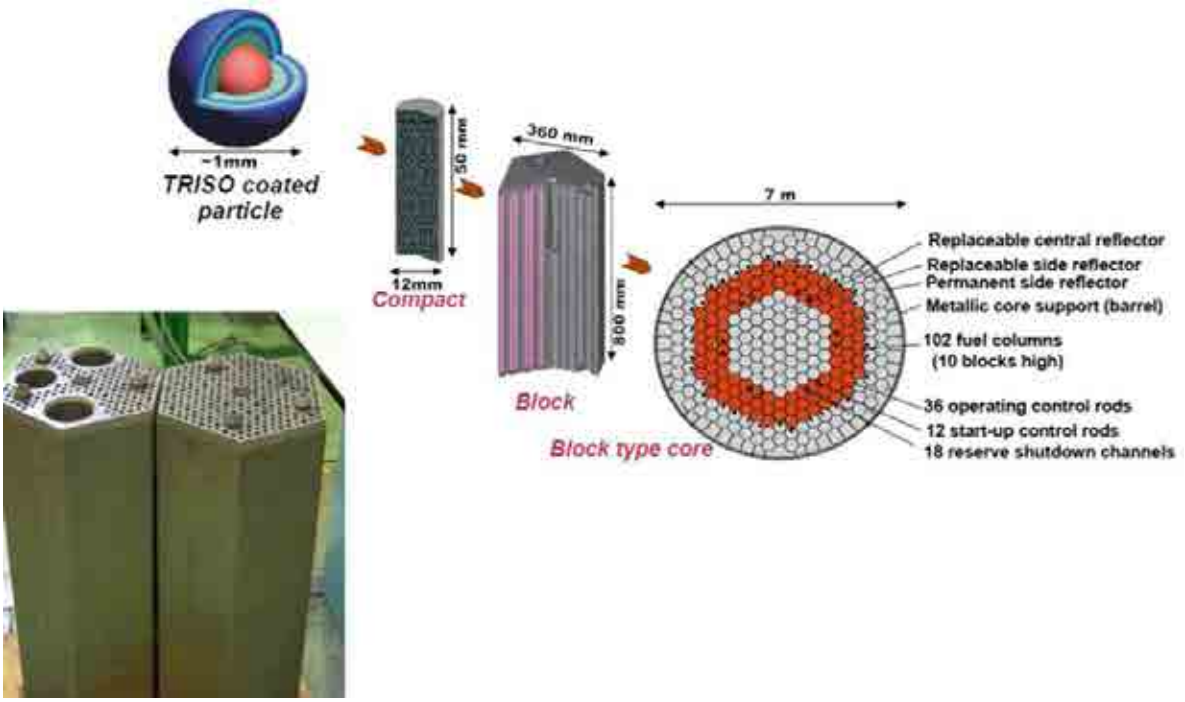

FIG. 3. Fuel element designs for the prismatic core concepts. Both pebble and block HTR core concepts employ the fuel particle as the basic fuel-containing unit.

In Japan, the prismatic concept takes the form of a pin-in-block design with a different fuel configuration and coolant path (Fig. 4). The graphite block employed in the pin-in-block design is shorter, 580 mm high, but still 360 mm across the flats, and contains 31 or 33 fuel rods. Helium coolant flows downward in the annular gap between the fuel rods and the boreholes in the graphite block. Each fuel rod consists of a graphite sleeve in which 14 prefabricated annular fuel compacts are stacked. The fuel compacts have an outside diameter of 26 mm, an inside diameter of 8 mm and are 39 mm high. Coated fuel particles are overcoated with compact matrix material, mixed with additional graphite powder and binder materials, and then hot-pressed into their annular form [10–12].

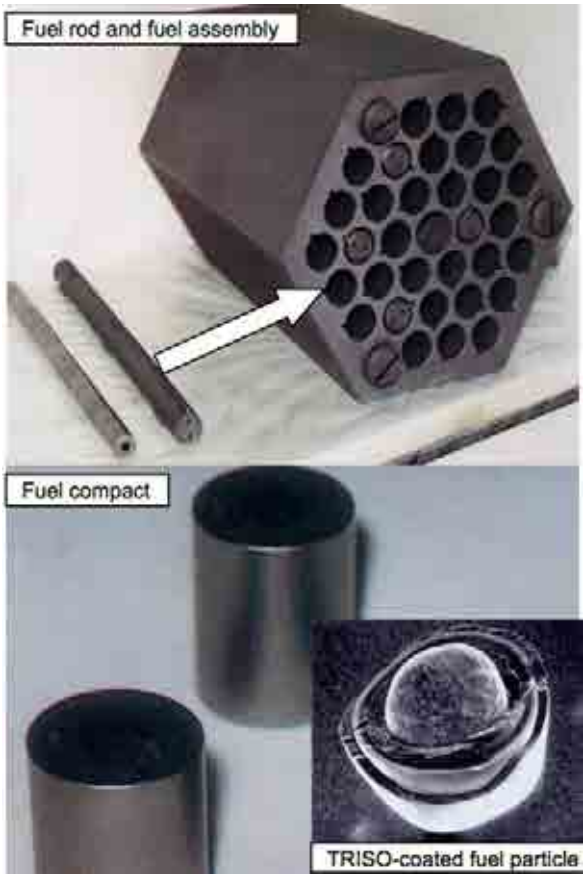

FIG. 4. Japanese fuel element, fuel rods, compacts and particle.

Although the fuel elements in the two HTR designs differ substantially, the coated particle concept is essentially the same for both element types. Coated fuel particle development has been underway since the 1960s as an international effort quite independent of differences in HTR designs. The basic fuel containing unit was originally suggested and patented by Roy Huddle [13] in 1957 and 1959. Since that time fundamental research on coated particle fuels has been conducted in Germany, the United Kingdom, France, Belgium, the United States of America, Russian Federation, India, Japan, China, South Africa, and the Republic of Korea. Some of these countries, namely China, Germany, Japan, the United Kingdom and the United States have produced fuel particles and elements on a large scale for use in operating HTRs.

Three experimental reactors were designed and built in the 1960s and were subsequently operated using thorium fuels. The first two of these operated for a period of over 7 years Peach Bottom 1 Reactor in the USA and the Dragon Reactor in the United Kingdom, and a

third, the AVR for 21 years in Germany [14]. The main features of HTRs are shown in Table 1. These reactors were operated

The 46 MW(th) AVR was operated from 1966 to 1988 with a large number of different fuel spheres that majority of which contained thorium (Table 2). ^{232}Th and ^{232}U decay products in the AVR GO1 type fuel sphere with 1.00 g ^{235}U and 5 g Th initial loading are quantitatively listed [15] in Table 3 and plotted in Fig. 5.

TABLE 1. MAIN FEATURE OF HISTORIC AND OPERATIONAL HTRs

Country	USA	UK.	Germany	USA	Germany	Japan	China
Name	Peach Bottom	Dragon	AVR	FSV	THTR	HTTR	HTR-10
Fuel	Th	Th, U	Th, U	Th	Th	U	U
Reactor type	Early Experimental			Prototype		Modern Experimental	
First Criticality	1967	1964	1966	1974	1983	1998	2000
Out of operation	1974	1975	1988	1988	1988	Still op.	Still op.
Thermal power MW(th)	115	20	46	842	750	30	10
Electric power MW(e)	40	0	15	330	300	0	2
Power density, MW(th)/m^3	8.3	14	2.6	6.3	6	2.5	2
He inlet / outlet temp.(°C)	377/ 750	350/ 750	270/ 850, 950	405/ 784	270/ 750	385/ 850, 950	250, 350/ 700, 900
He pressure (MPa)	2.5	2.1	1.1	4.9	3.9	4.0	3.0
FE type	Pin	Pin	Sphere	Prismatic	Sphere	Pin-in-block	Sphere
Fuel	Carbide	Oxide	Carbide Oxide	Carbide	Oxide	Oxide	Oxide
Enrichment	HEU	HEU, LEU	HEU, LEU	HEU	HEU	LEU	LEU

TABLE 2 APPROXIMATE AMOUNT OF THORIUM FUEL [7] USED IN HTR

HTR	Thorium (kg)
Dragon, UK	100
AVR, Germany	1360
Peach Bottom, USA	3500
THTR-300, Germany	6400
Fort St. Vrain, USA	26 500*

*The prismatic design of Fort St. Vrain requires much higher initial heavy metal loading than the pebble-bed design of THTR that has no burnable poisons and where the fissile loading is only gradually increased.

TABLE 3. ^{232}Th AND ^{232}U DECAY PRODUCTS DECAY IN AVR FUEL SPHERE OF TYPE GO1

g/FE type AVR-GO1	Burnup		
isotope	5% FIMA	10% FIMA	15% FIMA
Tl-208	3.01E-15	4.16E-14	2.17E-13
Pb-208	2.49E-10	9.57E-09	1.15E-07
Pb-212	1.75E-12	2.41E-11	1.26E-10
Bi-212	1.65E-13	2.30E-12	1.20E-11
Rn-220	2.66E-15	3.68E-14	1.92E-13
Ra-224	1.52E-11	2.10E-10	1.18E-09
Ra-228	2.18E-10	5.30E-10	9.46E-10
Ac-228	2.28E-14	5.53E-14	9.88E-14
Th-228	3.09E-09	4.08E-08	2.13E-07
Th-232	4.93E+00	4.85E+00	4.73E+00
Pa-231	1.05E-05	2.39E-05	3.89E-05
Pa-233	3.85E-03	2.95E-03	2.64E-03
U-232	1.00E-06	5.68E-06	1.74E-05
U-233	3.51E-02	7.20E-02	9.47E-02
U-234	1.07E-02	1.37E-02	2.12E-02
U-235	6.61E-01	3.34E-01	1.07E-01
U-236	6.17E-02	1.18E-01	1.49E-01
U-238	6.41E-02	6.20E-02	5.86E-02
Pu-238	5.51E-05	7.20E-04	3.16E-03
Pu-239	4.97E-04	6.12E-04	9.76E-04
Pu-240	2.23E-04	4.88E-04	8.10E-04
Pu-241	5.76E-05	2.20E-04	3.92E-04
Pu-242	8.53E-06	1.13E-04	4.36E-04
Am-241	8.37E-07	9.27E-06	2.83E-05
Am-242m	6.24E-09	1.01E-07	3.44E-07
Am-243	2.47E-07	9.97E-06	8.26E-05
Cm-242	4.18E-08	9.53E-07	3.51E-06

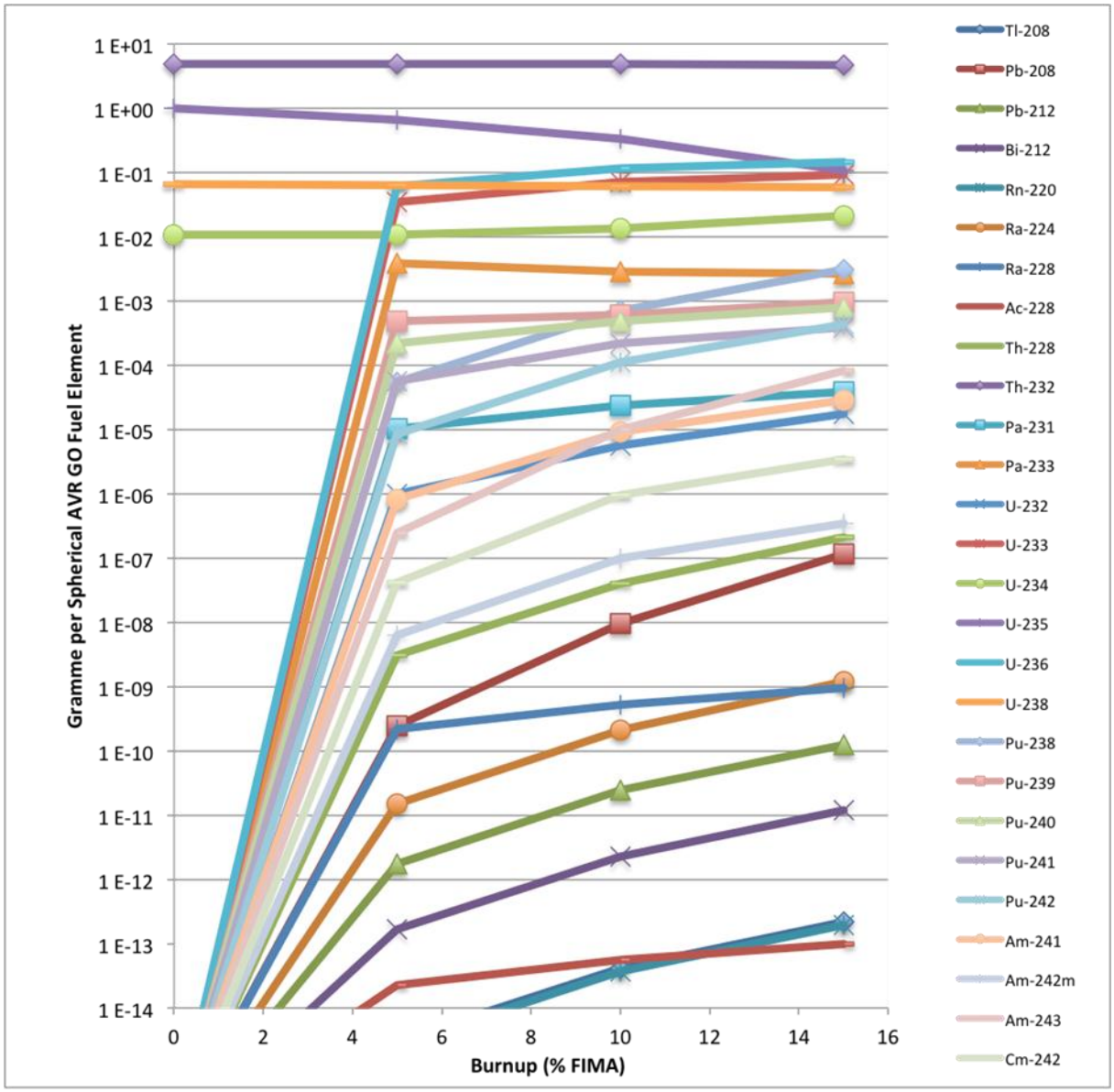

FIG. 5. ^{232}Th and ^{232}U decay products in the AVR fuel sphere of type GO1 with 1.00 g ^{235}U and 5 g Th initial loading.

Various options for the utilization of thorium in present day HTRs [16] are presented in Table 4.

TABLE 4. OPTIONS FOR THE UTILIZATION OF THORIUM IN PRESENT HTR

Cycle		Th/U 93%		Th/U-233		Th/U 20%		LEU	
Enrichment of feed fuel	w%	8.04		6.54		10.76		10.82	
Fuel residence time	Years	3.8		3.8		3.8		3.8	
Target burnup	MWD/KgHM	**77.2**		**77**		**77.5**		**77.4**	
	GWd/KgHM	0.0772							
Conversion ratio		0.462		0.557		0.519		0.487	
U_3O_8 requirement	Kg/GWd(th)	278		-		359		357	
Separative work	SWU/GWd(th)	243		-		284		263	
Loading → unloading		Load	Unload	Load	Unload	Load	Unload	Load	Unload
Fissile: U-233	Kg/GWd(th)	0.00	0.23	0.85	0.31	0.00	0.14	0.00	0.00
U-235	Kg/GWd(th)	1.06	0.16	0.00	0.02	1.39	0.50	1.40	0.52
	Kg/MWd(th)	1060.0	160.0	0.0	20.0	1390.0	500.0	1400.0	520.00
Pu-239 + Pu-241	Kg/GWd(th)	0.00	0.00	0.00	0.00	0.00	0.11	0.00	0.17
	Kg/MWd(th)	0.00	0.00	0.00	0.00	0.00	110.00	0.00	170.00
Fertile: Th-232	Kg/GWd(th)	11.79	11.24	12.07	11.46	5.90	5.65	0.00	
U-238	Kg/GWd(th)	0.07	0.06	0.00	0.00	5.62	5.25	11.51	10.95
Pu-240	Kg/GWd(th)	0.00	0.00	0.00	0.00	0.00	0.03	0.00	0.05
Additionally Pu-242	Kg/GWd(th)	0.00	0.00	0.00	0.00	0.00	0.01	0.00	0.02
Fractional neutron absorption									
Fissile: U-233	%	12.2		43.7		3.7		-	
U-235	%	35.8		0.9		34.4		33.3	
Pu-239 + Pu-241	%	-		-		12.9		18.5	
Fertile: Th-232	%	21.8		23.7		9.4		-	
U-238	%	0.4		-		14		20.9	
Pu-240	%	0.1		-		3.1		4.5	
Additionally Pu-242	%	-		-		0.1		0.1	
In-situ utilization of bred nuclides:									
U-233	%	57.00		78.8		40.2		-	
Pu-239 + Pu-241	%	-		-		75.6		73.4	

1.3. THORIUM COATED PARTICLE FUEL DEVELOPMENT

Coated particle fuel was developed to provide strength and fission-product containment at the relatively high fuel operating temperatures of a HTR [10–12]. The coated particles of ~1 mm diameter are in themselves miniature fuel elements with a kernel that contains the fissile material protected by a sequence of ceramic coating layers. These coatings provide the primary barrier to fission product release. Various coating designs have been proposed to fulfil distinct functions and extensively tested over the years. A reactor core with a 400–600 MW(th) power level will contain between 109 and 1010 individual coated fuel particles. The particles are embedded in a graphite matrix to form the fuel elements.

The first coatings applied to fuel kernels had little to do with fission product retention; their primary purpose was to prevent oxidation of uranium carbide kernels prior to reactor start up.

Coated particle fuel technology developed rapidly as a result of the broad international effort.

The very small size of coated particles is a distinct advantage in testing, since a statistically significant number of ‘fuel elements’ can be irradiation tested in a relatively small reactor test volume. Individual tests typically contain 103 to 105 coated fuel particles. Through properly designed fuel development and test programmes, in-service fuel performance can be predicted with a high degree of confidence. Processes that lead to loss of coating integrity have been defined and minimized either through design choices for the fuel particle design or by operating requirements for the reactor core.

Prior to 1980s, the two primary coated particle types [7] were:

— a two-layer BISO coating that consisted of a porous, low-density buffer layer around the fuel kernel, surrounded by a high density isotropic PyC layer; and

— a three-layer TRISO coating consisting of a porous, low-density buffer layer around the fuel kernel, surrounded by a SiC fission product barrier sandwiched between two layers of high-density isotropic PyC.

Both BISO and TRISO coated particles are capable of complete retention of gaseous fission products and iodine with properly designed and specified coatings. Intact TRISO particles also provide essentially complete retention of metallic fission products at current peak HTR normal operating temperatures. Because diffusive release of certain metallic fission products, in particularly caesium, strontium, and silver, occurs at elevated temperatures from BISO coatings, fuel elements with TRISO coated particles are used in all modern HTR designs (Fig. 6).

An excellent compendium of the international R&D efforts, experience and knowledge base compiled on HTR coated particle fuels has been compiled and edited by Terry Gulden and Hubertus Nickel in 1977 [17].

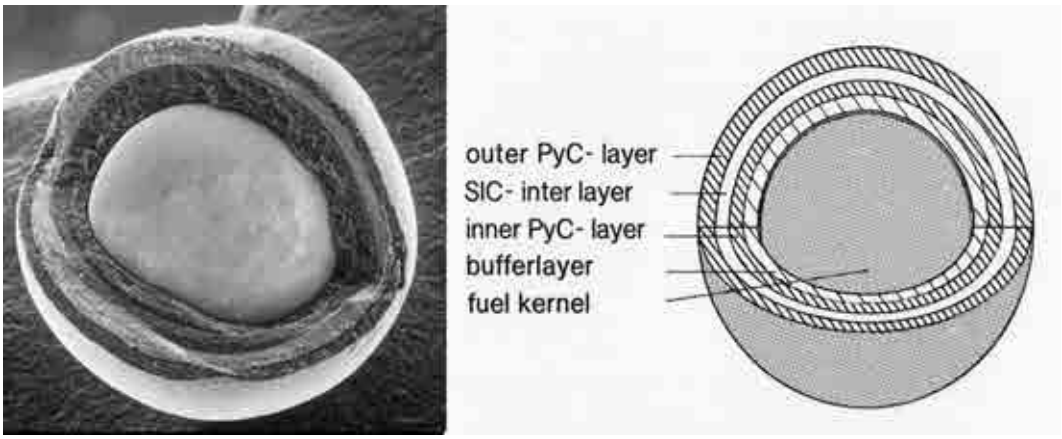

FIG. 6. Scanning electron microscope view of a HTR TRISO coated particle with an oxide fuel kernel showing the three protective pyrocarbon layers and the load bearing SiC fission product barrier. The schematic on the right depicts the fuel kernel and each of the ceramic coating layers.

The progress of HTR fuel particle development is shown schematically in Fig. 7. Coated particle development in Germany began in 1960s and, by 1972, led to a particle design qualified for use in the HTR prototype known as thorium high temperature reactor (THTR). The qualified particle design consisted of mixed thorium-uranium oxide kernel with a methane derived pyrocarbon coating. The $(Th,U)O_2$ HTI BISO coated fuel design utilized HEU (93 wt.% ^{235}U).

For advanced applications with 850°C and 950°C coolant exit temperatures, three reference particle types were suggested for the HEU-Thorium fuel cycle, $(Th,U)O_2$ HTI BISO, $(Th,U)O_2$ LTI TRISO, and the two-particle system with fissile UC_2 or UCO TRISO plus fertile ThO_2 TRISO. The HEU $(Th,U)O_2$ fuel kernels used in AVR and THTR, with a TRISO coating were eventually qualified for prototype nuclear process heat (PNP) and HTR with helium turbine (HHT)). As a further development, high density UCO kernels were considered as an alternative to the USA low density weak acid resin derived (WAR) kernels with partial

conversion. An HEU UCO (and ThO_2) production charge (~5400 elements) was introduced in reload 13-3 into the AVR core in late 1977. Around this time, uranium carbide fuel was no longer of interest due to its complicated manufacturing process, fast diffusion of U into the PyC, and the excessive release of strontium and rare earths fission products.

In the period between 1975 and 1980, the German reference particle coating design changed to the low temperature isotropic LTI TRISO coating, which afforded a greater degree of resistance to fast neutron damage and a significantly higher degree of fission product retention. The thorium cycle in use at that time used was of concern relative to fuel economics optimization and resource conservation. After a thorough study of LEU fuel particle performance, Germany and United States of America adopted LEU fuel for all future HTR projects. In Germany, LEU UO_2 was selected as the reference fuel kernel material in 1980. The reason for this action was consideration of its non-proliferation aspects (INFCE) and, therefore, the decision to cancel the reprocessing step. The LEU UO_2 particle with a 500 μm diameter kernel and a TRISO coating design (verified during the HEU fuel development effort) was selected as the German LEU reference particle design.

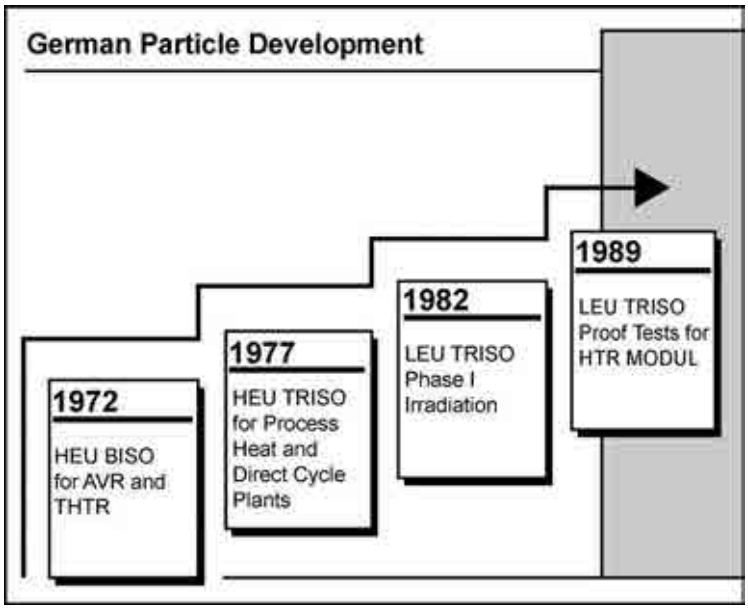

FIG.7. Sequence of major HTR fuel particle development programmes carried out in Germany.

Changing goals within the German fuel development programme have also led to a steady increase in the quality of particle coating. In the decade of the 1980s, Germany initiated a fuel development effort to qualify the reference LEU UO_2 TRISO fuel design. A first set of LEU specifications was fixed before the first large-scale production of fuel elements (24 600) were made for reload 19 for the AVR in mid-1982. This development effort led to the demonstration of fission product retention in all normal and offnormal design conditions for the LEU UO_2 TRISO particle concept. The LEU UO_2 TRISO fuel produced during this period represents 'modern HTR fuel' that can be characterized as near defect free along with a very low uranium contamination level. Improvements in coated particle and fuel element fabrication processes, quality control and characterization resulted in the production of fuel elements with defect levels less than 1×10^{-5} with similar U_{free}/U_{total} contaminations levels. The last fuel development effort in Germany was Proof Testing the LEU UO_2 TRISO fuel for the MODUL HTR requirements.

The German LEU UO_2 TRISO fuel produced by NUKEM remains the standard of excellence within the worldwide HTR community. It is shown here that the HEU fuel with 500 µm $(Th,U)O_2$ LTI TRISO particles had achieved an equivalent standard.

1.4. HTR FUEL CYCLES

The HTR has the inherent flexibility to accommodate many fuel types and to permit full cost effective optimization [18]. Due to their unique features, graphite moderated HTRs can accommodate many types of fuel cycles and permit full cost effective optimization. The HTR can meet the requirements of enhanced safety, higher efficiency, fuel cycle flexibility, competitiveness and waste management in an environmentally responsible and sustainable manner. Evaluations performed by the Generation IV International Forum (GIF) concur with this assessment.

1.4.1. HTR fuel cycle flexibility

The advantage that makes the HTR particularly attractive and distinguishes it from other reactor types is its fuel. Because of the unique arrangement of the fuel, moderator and coolant, HTRs can accommodate a variety of mixtures of fissile and fertile materials without significant modification to the core design. This flexibility is mainly due to the virtually perfect uncoupling of those parameters that determine cooling geometry, and to the fundamental parameters that characterize neutronic optimization; i.e. the moderation ratio within the HTR core. It is possible to modify the packing fraction of coated particles (up to a theoretical value of ~60%) within the graphite matrix without changing the basic dimensions of the fuel elements. It is also possible to change the diameter of the fuel particle kernel, or the relative proportions of the various particle types containing different nuclear materials. Hence, many degrees of freedom exist to optimize the HTR core to achieve fuel cycle management objectives.

There are other physical reasons that contribute to the fuel cycle adaptability of HTRs as compared to light water reactors. For example, the moderator void coefficient limits the plutonium content of pressurized water reactor (PWR) mixed oxide (MOX) fuels. In the event of complete loss of coolant in a PWR, the neutron spectrum becomes very ‘fast’ (the neutrons exhibit a very high average speed since they are no longer slowed down by a moderator). Under these conditions, the neutron multiplication factor, due to the presence of plutonium fissile isotopes, increases considerably (the reproduction factor increases significantly for fast neutrons). Clearly, this is not a constraint for graphite-moderated reactors. Note also that an HTR core has a significantly better neutron economy than a PWR core because there is much less parasitic capture in the moderator (the capture cross section of graphite is 100 times less than that of water), in internal structures (there are no metal materials to capture neutrons) and by fission products (the HTR spectrum is harder and fission products tend to capture more neutrons as they become thermalized).

The performance of TRISO coated particles of plutonium or uranium fuels is such that they are capable of attaining very high burn-ups, ranging upwards of hundreds GWd/tHM. This capability has been confirmed by various irradiation tests conducted since the inception of the particle fuel concept [19]. In assessing the various fuel cycles that may be used in an HTR [20], the starting point is to find a comprehensive set by considering all combinations of the basic components of a nuclear fuel, that is: (i) the fissile material, which may be ^{235}U, ^{233}U or plutonium; and, (ii) the fertile material, which may be ^{238}U or ^{232}Th. This systematic approach leads to a list of several possible fuel cycles that are grouped into four categories:

— ‘Low enriched uranium’ (LEU) fuel cycle;
— ‘Mixed oxide’ (MOX) fuel cycle;
— ‘Plutonium only’ fuel cycle;
— ‘Thorium based’ fuel cycle.

1.4.1.1. Low enriched uranium (LEU) cycle

The LEU cycle actually uses uranium with a range of enrichments from 5 to 16% depending on the reactor type. These enrichments are actually high compared to other thermal reactors. This is primarily due to a rather diluted and homogeneous uranium distribution in HTR fuels which favours resonance captures by fertile nuclei (in this case ^{238}U nuclei).

The LEU cycle was studied in the USA, Germany, UK and France during the 1960s and 1970s. This cycle appears as the most appropriate cycle for near term commercial deployment. It has already been employed in HTRs, but its main advantage is that the use of uranium oxide (UO_2) fuel benefits from the huge commercial experience base as LEU UO_2 is used in almost all of the power reactors in operation worldwide. Consequently, the LEU cycle has been selected as the reference cycle for all the ongoing HTR commercial projects. The exception is the GT-MHR project developed between the US and Russia that, in its initial development stage, addresses the consumption of weapons-grade plutonium.

1.4.1.2. Mixed oxide (MOX) cycle

As in LWRs, deployment of a mixed plutonium/depleted uranium fuel can also be envisioned. This mixture currently takes the form of a mixed oxide (MOX), but it could also take a different form, such as carbide compounds, or even nitride compounds.

The MOX type of cycle has never really been realized in HTRs; however, the CEA has conducted some exploratory neutronic studies [21]. Even if HTRs offer more flexibility for plutonium consumption than MOX fuel cycles in LWRs, this cycle for HTRs does not offer significant advantage compared to the ‘plutonium only’ cycle.

1.4.1.3. Plutonium only cycle

As part of the search for solutions enabling improved ‘control’ of plutonium in the medium term, current efforts are focused on maximizing plutonium consumption. Studies [22] have been conducted, to assess the feasibility and performance of plutonium cores containing no fertile material at all. This solution of ‘plutonium only’ cores, a unique feature of HTRs, is being investigated by the USA and the Russian Federation as part of the GT-MHR project to examine consumption of excess weapons grade plutonium.

This cycle would need an extensive research and development programme to develop and qualify a fuel capable of reaching the burnup levels currently envisaged, although experimental fuels have already been tested at such high burnup levels in reactors in the past (for example — the DRAGON reactor [23] and the Peach Bottom reactor [24].

The costs and lead times involved in developing such plutonium fuels for HTRs led to the USDOE decision not to consider this solution as a means of ‘burning’ weapons grade plutonium in the USA [25]. Moreover, the neutron related difficulties which could potentially arise with ‘plutonium-only’ cores should not be underestimated. Some of the problems encountered in studies for prismatic element cores concern control of changes in reactivity

(using erbium type poisons), moderator temperature coefficient (risk of positive coefficient), low fraction of delayed neutrons, increased residual heat, etc.

1.4.1.4. HEU/thorium (cycle with or without ^{233}U recycle)

The main advantage of the HEU/Thorium fuel cycle is the significant reduced consumption of natural uranium when operating in a closed cycle. The HEU/Thorium cycle is particularly well-suited for this type because it can potentially reach very high conversion factors and, with ^{233}U recycling, reduce natural uranium requirements by a factor of 2 or more. The HEU/Thorium cycle was extensively studied in early HTRs and considered as the reference cycle from the beginning of HTR development in both the USA and Germany. Four HTRs, two experimental reactors and two prototype power reactors, operated on fuel cycle: the AVR and the THTR in Germany, Peach Bottom and Fort Saint Vrain in the USA. It should be noted that AVR was not solely dedicated to the use of HEU/Thorium fuel cycle but was used to test other fuel cycles as well.

The future use of the HEU/Thorium cycle may require additional research and development and heavy industrial investment. Furthermore, barring a shortfall in natural uranium supply, commercial development of this fuel cycle will be isolated to countries with very unique nuclear situations. A prime example is India, a country that has factors favouring development of the HEU/Thorium cycle like significant thorium resources.

The competitiveness of the HEU/Th cycle is not necessarily clear today, particularly given the considerable uncertainty regarding estimates of thorium cycle costs, not the least of which is the cost of thorium itself, since the market for this material is practically non-existent. The main technical hurdle for ^{233}U recycle is the significant gamma activity emitted by some daughter products of ^{232}U (i.e. ^{208}TI, ^{212}Bi, see Fig. 1), which is present as an admixture with ^{233}U. This means, in practice, that the recycled fuel has to be fabricated remotely in shielded cells. Technically, this is feasible but a significant research and development effort would be necessary to implement it on an industrial scale. Regardless of the potential technical merits of this fuel cycle, it would be near-impossible to market in the current climate, given the use of HEU and ^{233}U, and their associated problem of proliferation.

1.4.1.5. Medium enriched uranium (MEU)/thorium cycle

Studies of this intermediate cycle began in the USA in the late 1970s as a result of the non-proliferation policy initiated in the US. The aim was to investigate fuel cycles capable of minimizing proliferation risks associated with the use of fissile materials suitable for the manufacture of nuclear weapons. The HEU cycle in HTRs was considered to be highly proliferating. Therefore ‘denatured’ cycles with limited uranium enrichment levels of 20% ^{235}U (or 12% ^{233}U), with a certain quantity of thorium were investigated. This cycle complicates the management of heavy nuclei from both uranium and thorium, and therefore, does not offer any significant advantages compared to other fuel cycles.

1.4.1.6. Thorium-plutonium (Th/Pu) cycle

The idea of using plutonium as the only fissile material in place of highly enriched uranium (but still with ^{232}Th as a fertile material) was considered at a very early stage in HTR development. Initial studies were conducted in the UK in the early 1960s as part of the DRAGON European project [26]. Studies were continued in the USA in a joint programme with General Atomics and the Edison Electric Institute that included the manufacture of experimental $(Th,Pu)O_2$ test specimens and their successful irradiation in the Peach Bottom

HTR [24]. The Th/Pu Cycle could be of interest in a transition period to the full use of a thorium fuel cycle. Plutonium from available stockpiles or from reprocessing LWR fuels could serve as the feed fissile material to initiate a closed thorium cycle. Justifying such an option in today's market is not possible, therefore this cycle could be considered only as a possible long term option. However, it is to be noted that HTR cores, operating on a Th/Pu fuel cycle, may have attractive features such as a more uniform power distribution (thus an increase of outlet temperature), an increase of average power density, and a reduction of reactivity control measures.

1.4.2. Reprocessing of spent ^{232}Th/^{233}U fuels

Nuclear energy utilization worldwide is based on the two fuel cycles: the uranium/plutonium and the thorium/uranium cycles. Without using the breeding processes of either ^{238}U, with fast neutrons leading to ^{239}Pu, or ^{232}Th, with thermal neutrons leading to ^{233}U, the world reserves of the naturally occurring fissile U-235 nuclide will be exhausted in the future. For many years now the ^{238}U/^{239}Pu breeding process occurs in the LWRs using slightly enriched ^{235}U (3% to 5%). Reprocessing plants located in some industrial countries extract the bred ^{239}Pu from the spent fuel and refabricate this fissile nuclide into fresh fuel [e.g. (U,Pu)O_2]. These mixed oxide (MOX) fuels are then reintroduced into reactors like LWRs or fast breeder reactors (FBRs).

Thorium generates ^{233}U, which is by far the best fissile isotope for thermal spectrum reactors because of its nuclear characteristics. Typically, in a thermal spectrum like that of HTRs (and LWRs), the neutron reproduction factor, η (the average number of neutrons produced for each neutron absorbed in a fissile isotope), is 2.29 for ^{233}U, compared to 2.05 for ^{235}U, and only 1.80 for ^{239}Pu. This makes breeding theoretically possible in a thermal reactor using ^{233}U fuel. This possibility was demonstrated under experimental conditions in the Shipping port reactor in the early 1970s, although the technological configuration used would be difficult to transfer to power reactors [27].

The use of the ^{232}Th/^{233}U cycle has an advantage for thermal reactors. Therefore, with the development of the HTRs using thermal neutrons this fuel cycle should be used. An optimum utilization of a fuel cycle utilizing thorium is the availability of a recycle technology, i.e., the capability to separate the bred ^{233}U and refabricate it into fresh fuel elements. In the 1960s and early 1970s, many activities in Germany and the US were focused on closing the Th/U fuel cycle. For reprocessing of the spent fuel in HTRs and recovery of ^{233}U, the wet-chemical process with solvent extraction, the so-called THOREX process (similar to the PUREX process used for U/Pu fuel reprocessing) was developed in ORNL, USA and in the Forschungszentrum Jülich in Germany.

For burning the fuel matrix graphite before applying the THOREX process, the 'Burning-Head-End' step was developed and successful demonstrated in Germany in the test facility 'juelicher pilotanlage for thorium element reprocessing' (JUPITER).

Grenèche discussed an assessment of the reprocessing issue for HTR fuels and its feasibility [28].

2. HIGH QUALITY THORIUM TRISO MANUFACTURE

2.1. INTRODUCTION

High quality HEU $(Th,U)O_2$ TRISO coated particle batches are identified in Table 5. The four specific $(Th,U)O_2$ LTI TRISO particle batches have similar characteristics [7] such as fuel kernel diameter, enrichment, composition, and a TRISO coating design shown in Table 6. This particle is different from the earlier $(Th,U)O_2$ HTI BISO particle manufactured in large numbers for AVR and THTR and the UO_2 HTI TRISO in Dragon and the UK.

TABLE 5. HIGH QUALITY $(Th,U)O_2$ LTI TRISO COATED FUEL PARTICLE BATCHES

Particle batch	Particle kernel			Sphere irradiation tests	No. particles per fuel sphere
	N=Th/^{235}U	enrichment [^{235}U wt%]	diameter [µm]		
EO 1607	5.01	89.57	494	R2-K12 FRJ2-K11	10 830
AVR XV BP-S1 (HT 150-160, 162-167)	5.00	92.46	500	AVR XV	10 480
EO 1674	10.02	89.01	496	R2-K13	20 050
AVR XX BP-S1, AVR XX BP-S2	4.97	92.39	495	AVR XX	10 660

TABLE 6.NOMINAL DIMENSIONS OF $(Th,U)O_2$ LTI TRISO PARTICLE DESIGN

TRISO Particle Component	Dimensions [µm]
$(Th,U)O_2$ kernel diameter	500
buffer layer thickness	90
iPyC layer thickness	40
SiC layer thickness	35
oPyC layer thickness	40

2.2. THORIUM KERNEL MANUFACTURE

Increasing quality and performance requirements favour wet chemical processes over dry agglomeration processes employed in the 1960s and early 1970s, and were used to produce fissile, fertile, and mixed oxide fuel kernels. The flow sheet described in Fig. 8 represents the process to produce 500 µm diameter ThO_2 and HEU $(Th,U)O_2$ fuel kernels in the TRISO coating batches.

Aqueous solutions containing uranium and/or thorium nitrate with additives are transformed into droplets by vibrating nozzles. In the kernel forming process as shown in Fig. 9, droplets pre-consolidate while falling through gaseous ammonia into an aqueous solution of ammonia.

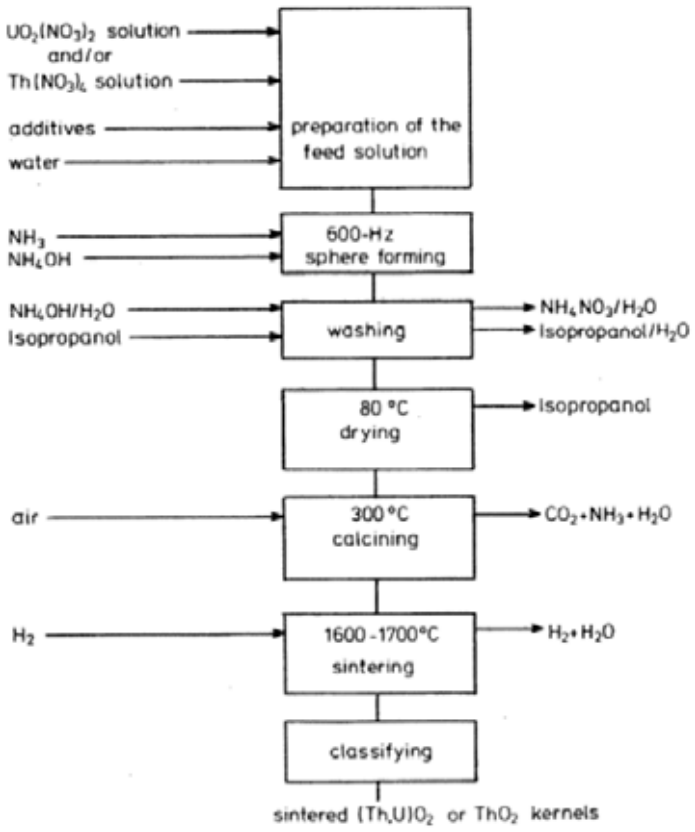

FIG. 8. Flow sheet for ThO_2 or $(Th,U)O_2$ fuel kernel manufacture.

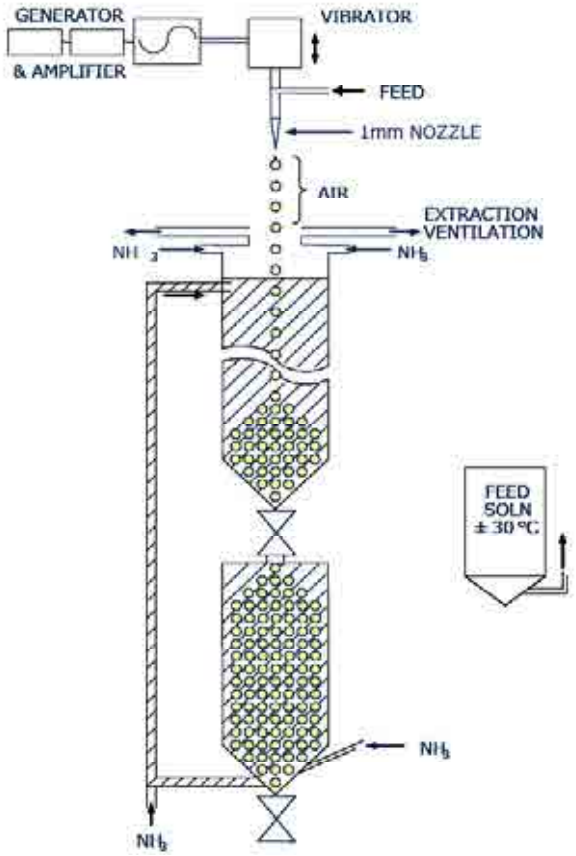

FIG. 9. Schematic diagram of the German kernel casting process.

The reaction with ammonia produces thorium hydroxide and ammonium nitrate that is removed from the kernel in a subsequent washing step. The kernels are then dried, calcined and sintered to produce a dioxide kernel. Characteristics of the HEU $(Th,U)O_2$ fuel kernels produced with the process are listed in Table 7. Also added are the respective coating properties.

TABLE 7. MEASURED PARAMETERS FOR HEU $(Th,U)O_2$ FUEL KERNELS AND LTI TRISO COATINGS OF PARTICLE BATCHES

	HEU $(Th,U)O_2$ LTI TRISO particle batch characteristics			
	EO 1607	AVR XV BP-S1 (HT 150-160, 162-167)	EO 1674	AVR XX BP-S1 / AVR XX BP-S2
HEU $(Th,U)O_2$ kernel characteristics				
Kernel diameter				
mean [$\bar{x}$, µm]	494	500	495	495
Enrichment [^{235}U wt%]	89.57	92.48	89.01	92.39 / 92.47
Density [g/cm^3]	10.12	10.08	10.10	10.18
N-value (Th/^{235}U)	5.01	5.00	10.02	4.97 / 4.97
LTI TRISO coating characteristics				
Buffer layer				
mean thickness [$\bar{x}$, µm]	85	91	89	94 / 100.2
density [g/cm^3]	1.09	n.m.	1.06	n.m.
iPyC layer				
mean thickness [$\bar{x}$, µm]	39	45	37	40 / 41
density [g/cm^3]	1.93	1.90	1.90	1.90 / 1.91
anisotropy (BAF_o)	1.030	1.018	1.029	1.04 / 1.03
SiC layer				
mean thickness [$\bar{x}$, µm]	37	33	33	35 / 35
density [g/cm^3]	3.20	3.20	3.19	3.20 / 3.20
defect fraction (burn-leach)	$< 0.4\times10^{-6}$	$< 2\times10^{-6}$	$< 2\times10^{-6}$	$< 2\times10^{-6}$
oPyC layer				
mean thickness [$\bar{x}$, µm]	39	39	39	39 / 39
density [g/cm^3]	1.93	1.91	1.90	1.91 / 1.91
anisotropy (BAF_o)	1.017	1.018	1.013	1.03 / 1.02

n.m. = not measured

2.3. TRISO COATING TECHNOLOGY

The process schematic for the uninterrupted TRISO coating deposition [29] is given in Fig. 10. The four coating layers are deposited on kernels in a fluidized-bed coating furnace (Fig. 11), in a process called spouted bed chemical vapour deposition (CVD) [30]. The flowing gases forced into the furnace suspend the kernels so that they form a fluidized-bed. Coating gases were selected which decompose and deposit, at temperatures up to 1600°C, certain of their constituents onto the surfaces of the partially coated fuel kernels. The materials of the layers formed by this process are described as pyrolytic, because they are

formed by pyrolysis (thermochemical decomposition) of an organic material, brought about by heat.

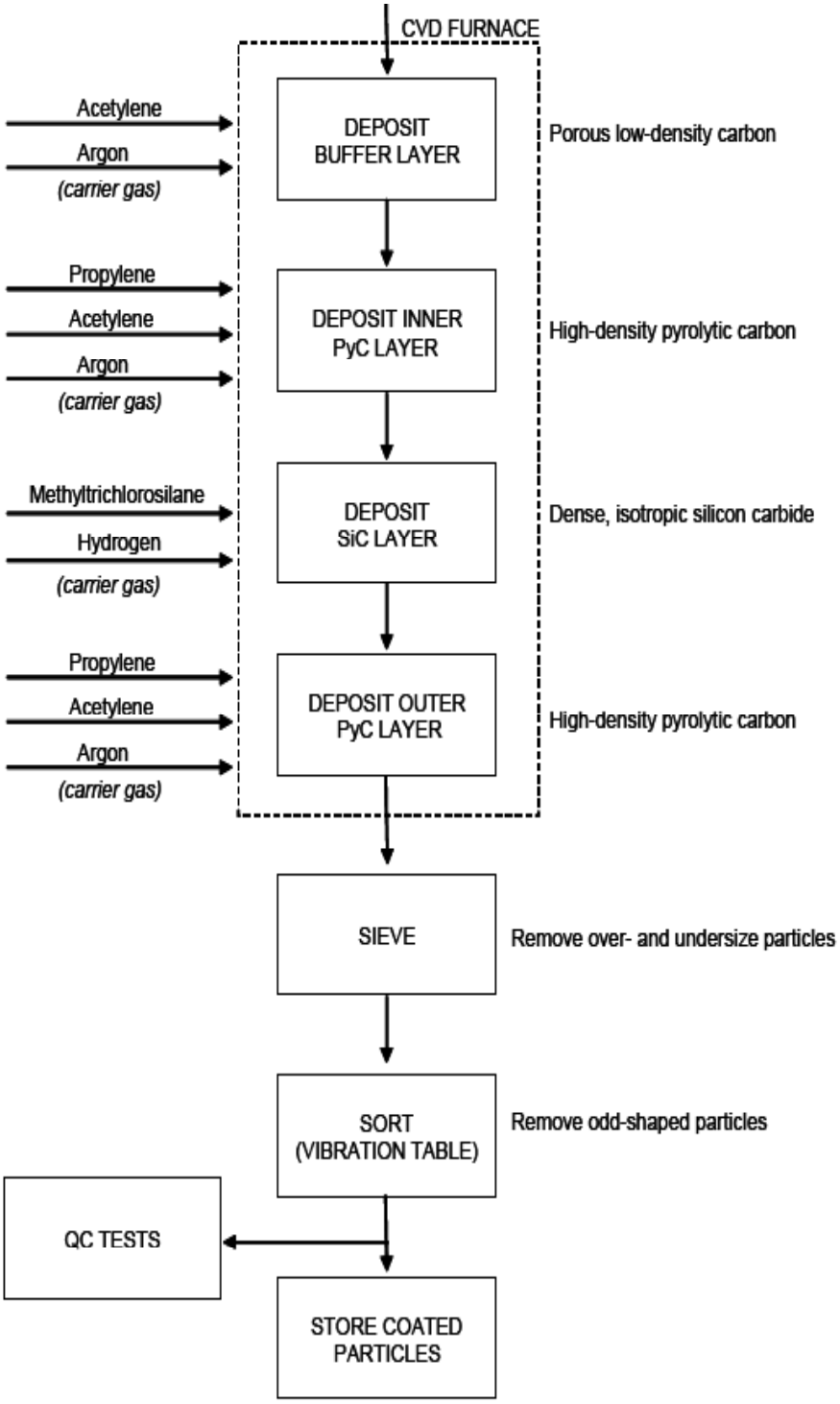

FIG. 10. Flow sheet for the LTI TRISO coating deposition process [12].

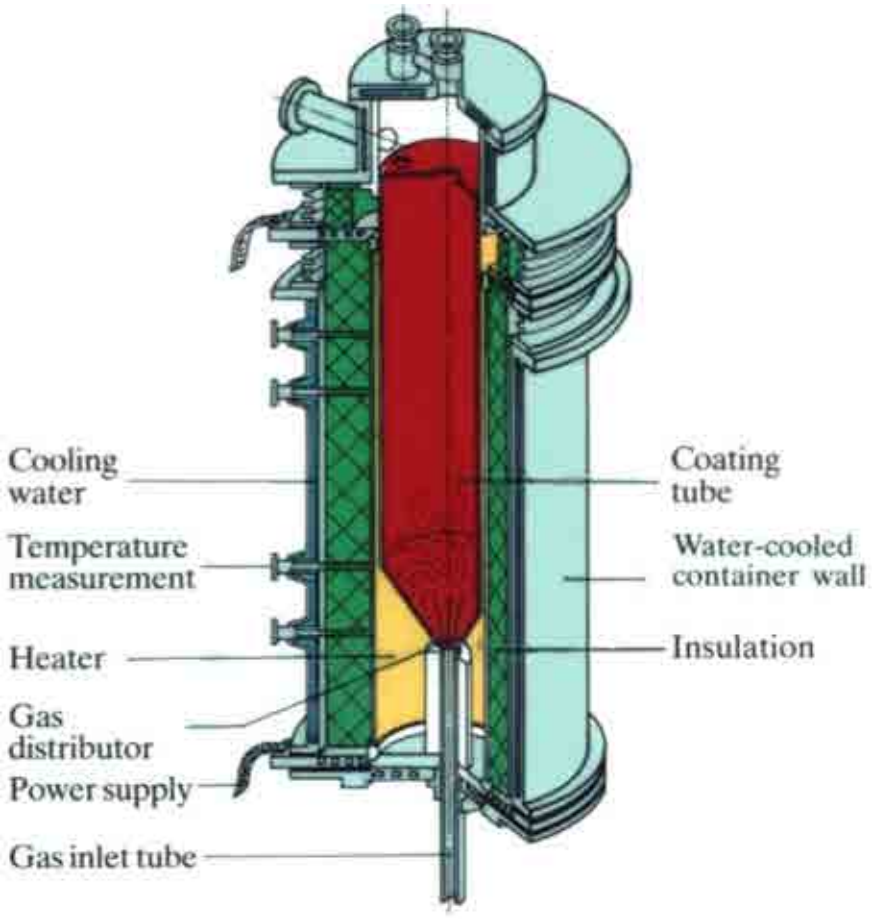

FIG. 11. Schematic diagram of a high temperature fluidized-bed chemical vapour deposition coating furnace used in HTR fuel fabrication [12].

The process for depositing the four LTI TRISO coating layers is as follows:

— Deposit the buffer layer onto the fuel kernels by the decomposition of ethyne, C_2H_2, according to the reaction:

$$C_2H_2(g) \rightarrow 2\ C(s) + H_2(g)$$

— Deposit an inner, dense layer of isotropic pyrocarbon (iPyC) onto the porous buffer layer by the decomposition of a mixture of propene, C_3H_6, and ethyne:

$$C_3H_6(g) \rightarrow 3\ C(s) + 3\ H_2(g)$$

$$C_2H_2(g) \rightarrow 2\ C(s) + H_2(g)$$

— Deposit a dense, isotropic layer of SiC onto the iPyC layer by the decomposition of methyltrichlorosilane, CH_3SiCl_3, according to the reaction:

$$CH_3SiCl_3\ (g) \rightarrow SiC(s) + 3\ HCl\ (g)$$

— Deposit an outer, dense layer of isotropic pyrocarbon (oPyC) onto the SiC layer by the decomposition of propene and ethyne (same as iPyC).

Nominal values of the key process parameters used to deposit the four layers that make up a LTI TRISO coating are provided in Table 8.

TABLE 8. TYPICAL PROCESSING PARAMETERS FOR DEPOSITION ON LTI TRISO COATING ONTO A HEU $(Th,U)O_2$ FUEL KERNEL

Coating layer	Decomposition gas	Carrier gas	Deposition temperature [°C]	Deposition rate [μm/min]
Low density carbon	C_2H_2	Argon	1 250	10
Inner dense isotropic PyC	Mixture of C_3H_6 and C_2H_2	Argon	1 300	5
Isotropic SiC	CH_3SiCl_3	Hydrogen	1 500	0.2
Outer dense isotropic PyC	Mixture of C_3H_6 and C_2H_2	Argon	1 300	5

All four layers of the LTI TRISO coating are deposited in an uninterrupted sequential process in the same fluidized-bed coating furnace. The conditions under which layer deposition takes place are very important as they determine the material properties of the coated particles formed. Parameters such as time, temperature, pressure, gas composition and gas ratios all play an important role in fixing the coated particle properties.

Major key material property requirements [7] for good irradiation performance for the dense isotropic PyC layers and the optimum SiC layer are:

PyC layer:

— Impermeable;

— Stable in neutron irradiation;

— Isotropic texture;

— Deposited at low enough temperature to avoid heavy metal contamination.

SiC layer:

— β-SiC with a cubic structure of type 3C;

— Density > 3.19 g/cm^3;

— Equiaxed microstructure with fine grains and few flaws;

— Strength of PyC-SiC interfaces.

The characteristics of the TRISO coatings applied to the four HEU $(Th,U)O_2$ particle batches were listed in Table 6 along with the key $(Th,U)O_2$ kernel characteristics. All of the coating batches exhibit PyC coatings with typically high densities, low anisotropy and thicknesses close to the nominal values. Similarly, the SiC layers in each of the batches have thicknesses close to the nominal value of 35 μm, densities ≥ 3.19 g/cm^3, and SiC defect fractions, as

measured by the burn-leach procedure, typically in the low 10^{-6} range. The similarity from coating batch to coating batch are indications that the deposition process together with adherence to strict process control of the conditions listed in Table 9 results in reproducible TRISO coatings of reproducible quality.

Ceramographic sections of one particle from coating batch EO 1607 in one of the R2-K12 fuel elements are shown in Fig. 12. These ceramographic sections are typical for the high quality HEU (Th,U)O_2 LTI TRISO fuel particle design.

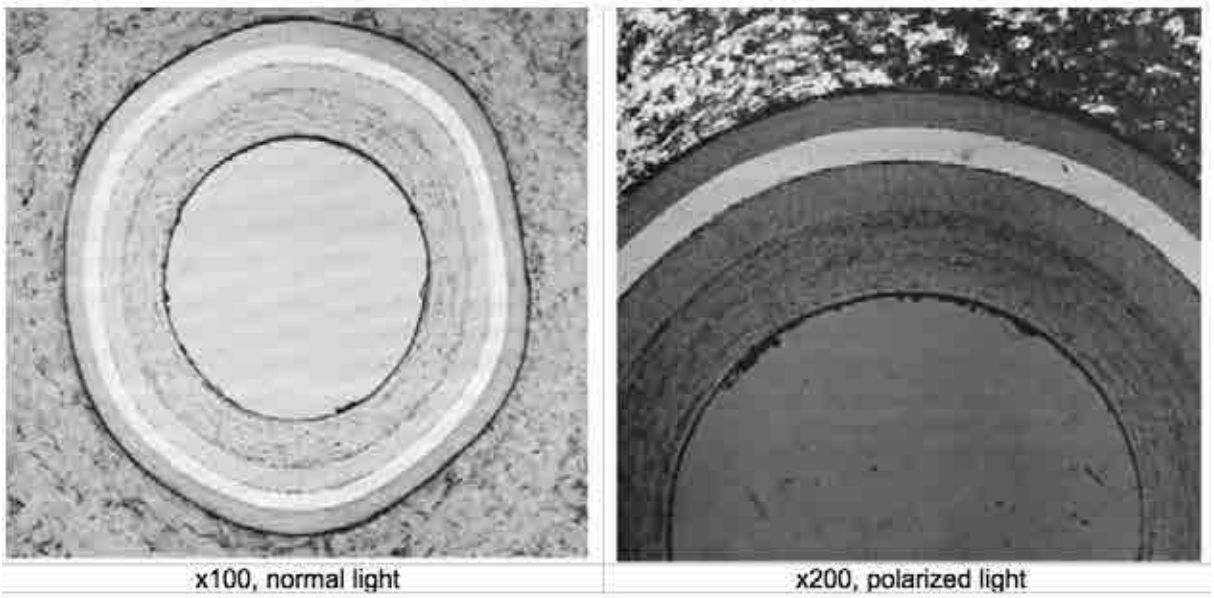

FIG. 12. Single particle from coating batch EO 1607 photographed in bright (left) and polarized (right) and photographs taken from ceramographic section of companion spherical fuel element manufactured for irradiation test R2-K12 [31].

The most important aspects of good high quality SiC are shown in Fig. 13.

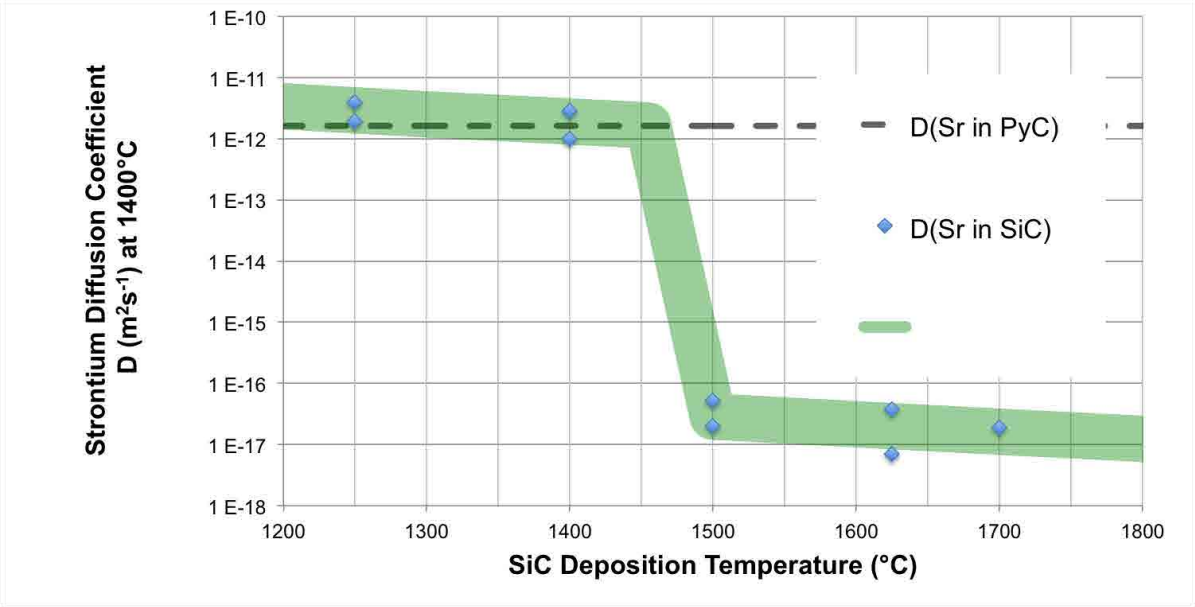

(a) Diffusion coefficient of Sr in SiC and PyC at 1400°C showing superior retention capability of SiC over PyC for optimum SiC deposited at ≥ 1500°C. Diffusion data for D (Sr in SiC) from Chinaglia [32].

(b) SEM pictures of SiC surfaces deposited at 1300, 1500, 1600 and 1700°C.

(c) Etched SiC ceramographic sections deposited at 1300, 1500, 1600 and 1700°C.

FIG. 13. SiC performance, characterization and properties; (a) shows both the massive reduction of the Sr diffusion coefficient at 1400°C and its superior retention capability over PyC for optimum SiC deposited at 1500 – 1550°C; (b) and (c) show SiC surfaces and sections of SiC deposited at 1300, 1500, 1600, and 1700°C in a 3-inch coating furnace [33].

TABLE 9. PROCESSING CONDITIONS AND PROPERTIES OF SiC DEPOSITED AT DIFFERENT TEMPERATURES [33]

Deposition temperature	°C	1300	1500	1600	1700
MTS concentration	vol. %	1.8	2.55	1.87	2.12
Deposition Rate	µm/min	.27	.59	.55	.50
Density	g.cm-3	3.07	3.19	3.20	3.20
Free Si	weight %	17	*bdl	bdl	bdl
α-SiC	%	10	bdl	bdl	bdl

*below detection limit

The final production steps are sieving to remove any under and oversized particles, followed by sorting to remove any odd shaped particles. Sorting is performed on a vibrating table that is slightly inclined to allow spherical particles to roll downhill following a parabola while oddshaped particles, twins etc. are removed.

2.4. FABRICATION OF SPHERICAL FUEL ELEMENTS FOR PEBBLE-BED HTRS

The fabrication process for HTR spherical fuel elements, described in the flowchart of the individual fabrication steps in Fig. 14, was developed and optimized by NUKEM. A pictorial display of the process is provided in Fig. 15. The primary steps in spherical fuel element processing are:

— resinated graphitic matrix powder preparation;

— overcoating of particles;

— pre-moulding of fuel zone;

— high-pressure isostatic pressing of the complete fuel element;

— machining to size;

— carbonization at 800°C; and

— final heat treatment at 1950°C.

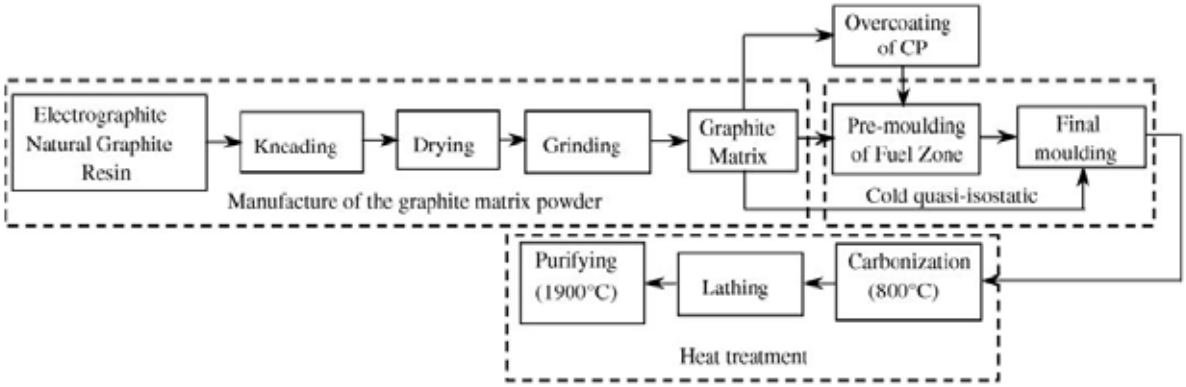

FIG. 14. Flow chart of individual processes involved in spherical fuel element fabrication [34].

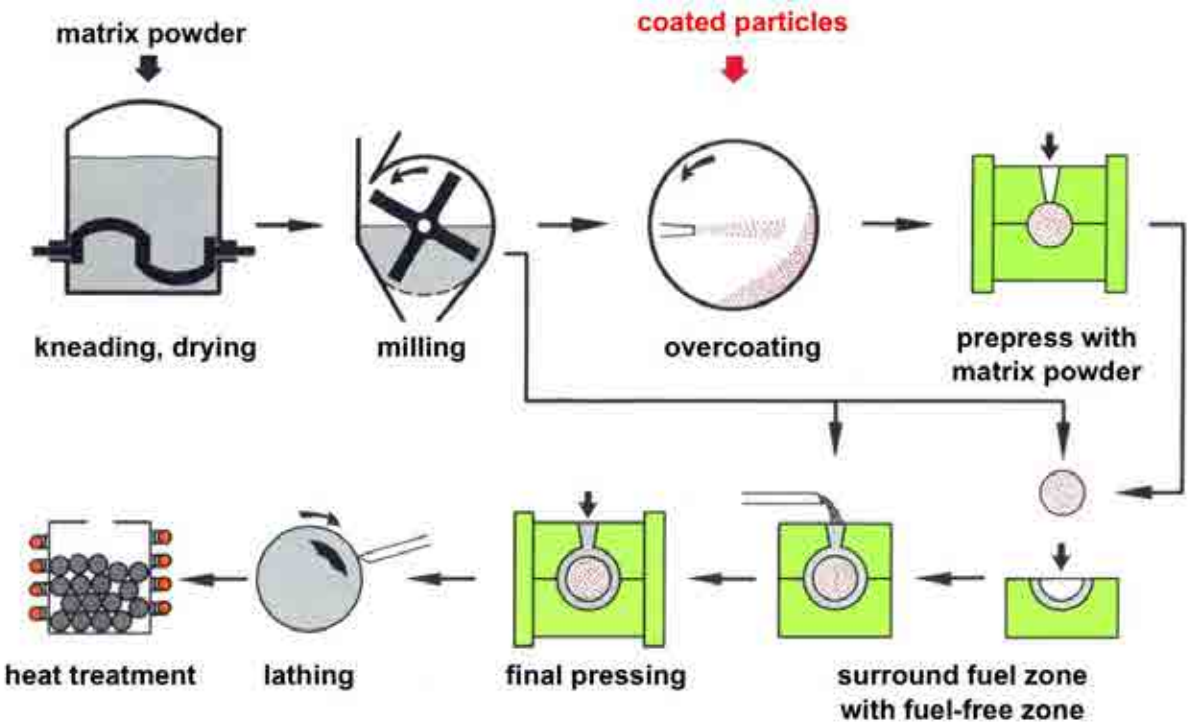

FIG. 15. Illustration of the fabrication method for spherical fuel elements [35, 36].

Same or similar spherical fuel element fabrication processes have been used in the past in Russia and South Africa, and are currently being employed in China for fabrication of reference 60 mm diameter fuel elements for the HTR-PM concept [37].

2.4.1. Preparation of resinated graphitic matrix powder

Two types of sphere matrix graphite [38] designated A3-3 and A3-27 were developed by NUKEM for spherical fuel element production. The composition and fabrication differences between the two matrix types are illustrated in Table 10. Both matrix types are based on the same filler components — natural graphite and artificial electro-graphite. The primary difference is in the type of binder employed and how it is processed or synthesized. In general, the matrix graphite for spherical fuel elements consists of 64% natural graphite, 16% electro-graphite powders, and 20% phenolic resin binder.

The manufacturing process steps for the graphitic matrix powder are:

1. Natural graphite and electro-graphite powders are mixed in a four to one ratio in a conical mixer.

2. Depending on the type of matrix required, either A3-3 or A3-27, the binder materials are added in different manner and the binder is synthesized differently:
   -- standard A3-3 matrix, a phenolic resin is dissolved in methanol to form the binder in a separate process step, added to the natural- and electro-graphite powders and then the mixture homogenized. This mixture is then fed into a kneading machine.
   -- A3-27 matrix, all of the raw materials — the natural and electro-graphite powders, are warm-mixed together with the binder components — phenol and hexamethylenetetramine at a temperature of 130ºC where the binder synthesized. This process eliminates the need for kneading and steps 3 and 4 below.

3. The paste-like mixture is extruded through a punched screen creating strings that are cut into small pieces.

4. These small pieces are placed in drying trays which are heated to 100°C.

5. The dried graphitic mass is transferred into a hopper that feeds a hammer mill used to grind the material into powder of the desired grain size.

6. The milled powder is homogenized and ready for pressing.

TABLE 10 COMPOSITION AND PARAMETERS FOR TWO TYPES OF GRAPHITE MATRIX MATERIALS USED IN SPHERICAL FUEL ELEMENT FABRICATION

Material and fabrication	Standard matrix A3-3	Matrix with synthesized resin A3-27
Composition of raw materials [wt%]:		
natural graphite	64	62.4
petroleum coke graphite	16	15.6
resin binder	22	22.0
Binder	Phenolic resin pre-fabricated from phenol and formaldehyde	Resin synthesized from phenol and hexamethylenetetramine during matrix formation
Moulding method	Quasi isostatic cold moulding	
High-temperature treatment [°C]		
fuel elements	1800 or 1950	1950
fuel-free matrix spheres	1800	1950

* for AVR fuel elements: A3-3 and A3-27, for THTR fuel elements: A3-3.

Table 11 shows the properties for A3-3 and A3-27, the two types of graphite matrix used in the fabrication of fuel spheres [35, 36]. After initial use of A3-3, there was a test and development phase with A3-27 matrix, but finally A3-3 was chosen as the overall reference for future HTRs.

TABLE 11 MATERIAL PROPERTIES FOR, the TWO TYPES OF GRAPHITE MATRIX (A3-3 & A3-27) USED IN FABRICATIONOF FUEL SPHERES

Property		A3-3		A3-27	Generic specification
Final heat treatment temperature		1800°C	1950°C	1950°C	
Geometrical density [g/cm^3]		1.70	1.73	1.74	≥ 1.70
Young's modulus [10^4 Kn / m^2]	∥	1020	1000	1070	
	⊥	991	970	1020	n.s.
Thermal expansion coefficient 20–500°C [10^{-6}/K]	∥	2.80	2.89	2.43	
	⊥	2.92	3.45	2.69	≤ 5
Thermal conductivity [W/m/K] @ room temperature:	∥	59	70	69	n.s.
	⊥	63	63	64	n.s.
@ 1000°C:	∥	38	41	44	≥ 30
	⊥	38	37	39	≥ 30
Specific electrical resistance [10^{-3} Ω cm]	∥	1.56	1.46	1.43	n.s.
	⊥	1.60	1.48	1.48	n.s.
Falling strength (no. of falls from 4 m onto A3-3 spheres until fracture)		521	437	652	≥ 50
Corrosion rate (@ 1000°C, 0.1 MPa in He with 1 vol.% H_2O for 10 h [mg/cm^2/h])		1.19	0.97	0.73	≤ 1.5
Abrasion [mg/h per sphere]		1.81		2.89	≤ 6
Anisotropy factor in thermal expansion		1.19			≤ 1.3
Crushing strength [kN]	∥	24.9		23.7	≥ 18
	⊥	23.1		26.3	
Impurities [µg/g]		60 (S:36; Si:6)		32 (Cl:16; Ca:7)	
Ash		50		30	≤ 300
B equivalent		–		–	≤ 1.3
Li		–		–	≤ 0.05

|| = parallel, ⊥ = perpendicular to equatorial plane of matrix sphere;
n.s. = not specified

2.4.2. Over coating the TRISO particles

Overcoating of the TRISO particles takes place in a rotating drum as shown in Fig. 16. The photograph on the left is the old manual overcoating drum that was used at NUKEM in the production of the HEU (Th,U)O_2 TRISO coated particles. The photograph on the right is a new, automated overcoating facility [39] located at the Institute of New and Nuclear Energy Technology (INET), Tsinghua University, China.

FIG. 16. Old manual overcoating drum that was used by NUKEM in the production of the HEU (Th,U)O_2 and LEU UO_2 TRISO coated particles (left); new automated overcoating facility used at present by INET in the production of LEU UO_2 TRISO particles (right).

The purpose of the overcoating is to prevent direct particle-to-particle contact which may induce cracking of the particle coating layers during sphere formation. The overcoating is circa 200 μm thick on the rigid TRISO coated particles and of the same composition as the fuel element graphite matrix. The dry resinated graphitic matrix material and a solvent are added simultaneously into the rotating drum in order to maximize adherence and obtain a uniform thickness. The moist overcoated particles are then dried at 80°C to remove any of the remaining solvent. The dried overcoated particles are sieved to select the proper sized particles within the range of 1.1 mm and 1.5 mm and are once again sorted on an inclined vibrating table to remove oddly shaped, twin, or non-spherical overcoated particles.

Figure 17 shows the typical diameter distribution of overcoated particles, as measured after overcoating and also as predicted after cold isostatic sphere pressing with 300 MPa whereby the overcoating density is increased from 1.5 to 1.9 g/cm^3. Later, after final heat treatment, the density is reduced again to values in the range 1.70–1.75 g/cm^3.

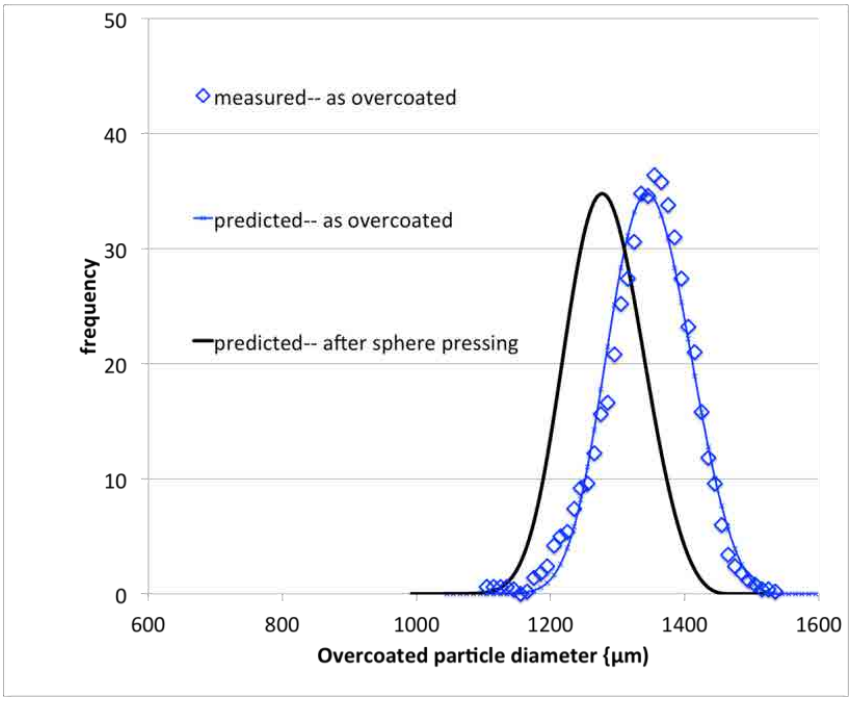

FIG. 17. Typical frequency distribution of overcoated particles with TRISO particle diameter 909 ± 27.8 µm

2.4.3. Moulding and pressing of fuel spheres

Fuel spheres are manufactured by quasi-isostatic pressing at room temperature using silicon rubber moulds.

Figure 18 is a photograph of the sphere pressing line, based on the NUKEM process that is currently in place at the INET at Tsinghua University in China [39]. Figure 19 presents a photograph of silicon rubber moulds [40] for fuel spheres.

FIG. 18. Moulding and pressing line for green fuel spheres at the INET in China.

FIG. 19. Silicon rubber dies for fuel spheres.

The sphere moulding and pressing process consists of the following steps:

— Combine over coated particles with matrix graphite powder to form the fuel zone. The matrix graphite powder volume is carefully controlled along with the overcoated particle volume and the mixture is homogenized.

— The homogenized mixture is injected into the pre-pressing mould and pressed at 5 MPa pressure.

— The pressed fuel zone spheres are then transferred into the final mould. The lower half of the final mould contains matrix graphite powder. The fuel zone sphere is placed into the centre of the bottom mould and the second half of the mould is placed on top. More matrix material is added through a feeder tube to completely fill the internal annulus between fuel zone sphere and top final mould. Final pressing process is performed at 300 MPa pressure.

After pressing, the green fuel spheres are transported to the lathing equipment where they are machined in a two-step process to obtain uniform spheres with exactly 60 mm diameter.

After machining, the spheres are heat-treated in two distinct processes; carbonization and annealing. In the carbonizing process, the green fuel spheres are heated to 800°C in an inert argon atmosphere furnace to carbonize the phenolic resin binder to provide strength and to remove all organic material.

The annealing process is carried out under vacuum at 1950°C for one hour to eliminate residual impurities in the matrix graphite. This final heat treatment step is also important for the coated particle, and the strength and corrosion resistance of the sphere.

Exemplary data for the property changes during these processing steps are shown in Fig. 20.

Table 11 summarizes fuel particle and fuel element characterization data related to the manufacture of high quality TRISO thorium reference fuel spheres [7] irradiated in MTR experiments and in the high quality HEU TRISO AVR reloads, AVR XV and AVR XX.

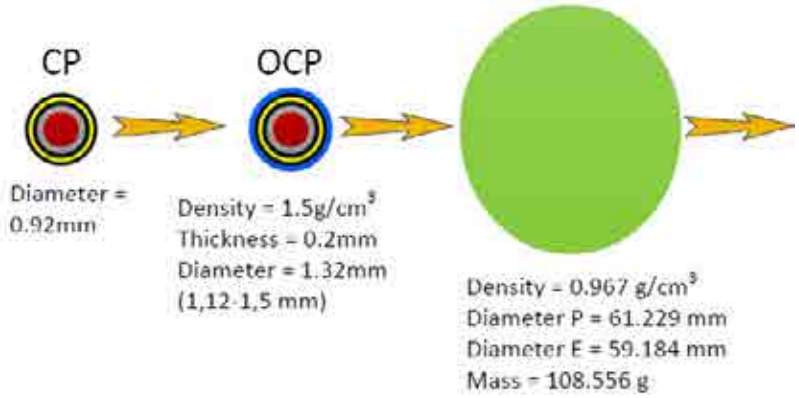

a) Coated particle, overcoated particle and sphere fuel zone in the green state

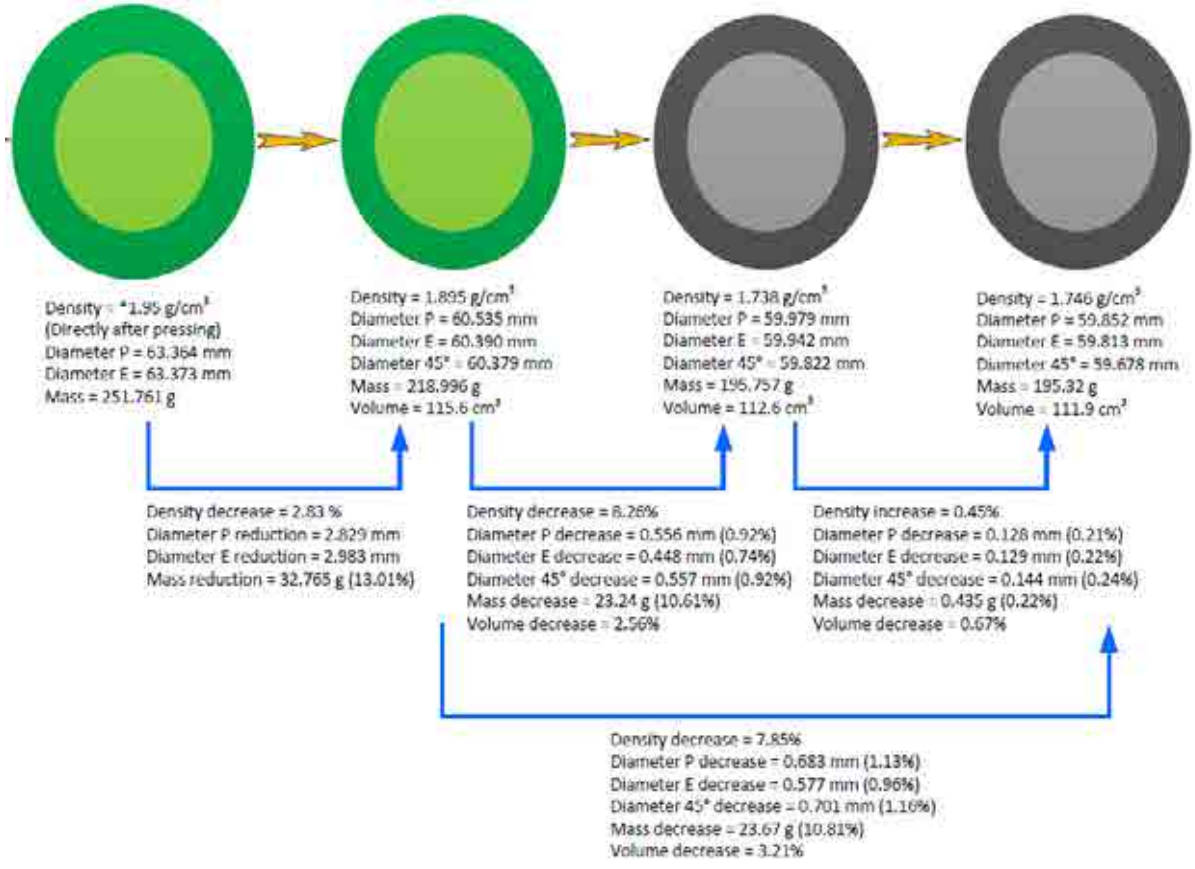

b) Pressed, machined, carbonized and annealed sphere characteristics

FIG. 20. Sphere manufacturing product characteristics (source: NECSA, data of A3-3 spheres with 1950°C final heat treatment).

TABLE 11. FUEL PARTICLE AND FUEL ELEMENT CHARACTERIZATION DATA RELATED TO THE MANUFACTURE OF SPHERICAL ELEMENTS IRRADIATED IN MTR EXPERIMENTS AND IN AVR FROM TWO RELOADS–AVR XV AND AVR XX

	R2-K12	R2-K13	AVR XV & FRJ2-K11	AVR XX
TRISO coating batch	EO 1607	EO 1674	AVR XV BP-S1 (HT 150-167)	AVR XX BP-S1 AVR XX BP-S2
$(Th,U)O_2$ kernel				
Diameter [µm]	494	495	500	495
N=Th/^{235}U	5.01	10.02	5.00	4.97 / 4.97
Enrichment [wt% ^{235}U]	89.57	89.01	92.48	92.39 / 92.47
Density [g/cm^3]	10.12	10.10	10.08	10.18
Weight [µg]	639	645	660	646
Spherical Fuel Element				
Fuel matrix type	A3-27	A3-27	A3-27	A3-27
Final heat treatment temperature [°C]	1950	1950	1950	1950
Weight [g]				
^{235}U	1.002	1.020	1.000	1.000
U_{tot}	1.119	1.146	1.081	1.081
Th	5.021	10.221	5.000	4.97
$(Th,U)O_2$	6.983	12.931	6.918	6.885
Total element	203.2	207.9	200.4 – 201.0	201.7 – 203.6
Particles/FE	10,830	20,050	10,480	10,660
SiC defect fraction*	$< 0.4\times10^{-6}$	$< 2\times10^{-6}$	3.4×10^{-5}	$< 9.5\times10^{-6}$
Particle volume loading in fuel zone [vol%]	7.8	14.4	7.5	7.6

* R2-K12, R2-K13 SiC defect fraction from burn-leach on TRISO fuel particle batches; AVR XV, AVR XX SiC defect fraction data from burn-leach on as-fabricated spherical elements.

2.4.4. Burn leach testing

One of the essential characterization techniques for quality assurance is the burn-leach testing of HTR fuel. During a 'burn and leach' test, the graphite of the sample to be measured (loose coated particles, spherical element, fuel compact or coupon) is burnt away in a combustion chamber at 800°C in air down to the SiC layer of the coated particles. This process is complete when the sample weight remains constant which is typically 90 hours for a spherical fuel element. The residual of ash and particles is treated with a nitric acid solution at 100°C and the amount of dissolved uranium and thorium analysed. Since the SiC layer is corrosion resistant, the heavy metal found in the solution includes the natural U/Th content of the matrix material and the U/Th content of those particles with a defective SiC layer. Also particles with an incomplete coating will be identified. The test results are presented as the ratio of the measured free uranium to the total uranium contained in the spherical element, U_{free}/U_{total}. The detection limit is typically at a level of $1–3 \times 10^{-6}$ depending on the U/Th content of the

sample. This uncertainty is much lower than the heavy metal content of a single defective coated particle which is on the order of 60 to 104 μg.

Tables 12 and 13 contain the burn-leach results from the AVR type GO2 fuel elements with HEU (Th,U)O_2 LTI TRISO particles from AVR Reload XV manufactured in the year 1978 and AVR Reload XX manufactured in the year 1983.

Tables 14 and 15 show defect particle fractions in comparison to later AVR Reloads XIX and XXI, which contained the AVR types GLE3 and GLE4 elements, respectively. The AVR type GLE3 and GLE4 spherical elements were manufactured with LEU UO_2 LTI TRISO particles in 1981 and 1985. All of the burn leach results are well suited for a modern, inherently safe, small modular HTR. However, the extremely low burn-leach levels of AVR XX with the equivalent of zero defects and AVR XXI/2 with a defect fraction 9×10^{-6} are of the highest quality recorded for any HTR fuel production campaign.

TABLE 12 FREE URANIUM FRACTION AND THE EQUIVALENT NUMBER OF DEFECTIVE PARTICLES FROM 16 BURN LEACH TESTS CONDUCTED ON AS FABRICATED FUEL SPHERES FROM AVR RELOAD XV [41]

	AVR XV Lot #1	AVR XV Lot #2	AVR XV Lot #3	AVR XV Lot #4
	U_{free}/U_{total} from burn leach in percentage figures			
Sphere 1	0.002	0.002	0.001	0.001
Sphere 2	0.001	0.024	0.015	0.001
Sphere 3	0.001	0.001	0.001	0.001
Sphere 4	0.001	0.001	0.001	0.001
	Number of defective particles			
Sphere 1	0	0	0	0
Sphere 2	0	3	2	0
Sphere 3	0	0	0	0
Sphere 4	0	0	0	0

TABLE 13 FREE URANIUM FRACTION AND THE EQUIVALENT NUMBER OF DEFECTIVE PARTICLES FROM 16 BURN LEACH TESTS CONDUCTED ON AS FABRICATED FUEL SPHERES FROM AVR RELOAD XX [42]

	AVR XX Lot #1	AVR XX Lot #2	AVR XX Lot #3	AVR XX Lot #4	AVR XX Lot #5
U_{free}/U_{total} from burn-leach in percentage figures					
Sphere 1	< 0.001	< 0.001	< 0.001	< 0.001	< 0.001
Sphere 2	< 0.001	< 0.001	< 0.001	< 0.001	< 0.001
Sphere 3	< 0.001	< 0.001	< 0.001	< 0.001	< 0.001
Sphere 4	< 0.001	< 0.001	< 0.001	< 0.001	< 0.001
Sphere 5	< 0.001	< 0.001	< 0.001	< 0.001	< 0.001
Number of defective particles					
Sphere 1	0	0	0	0	0
Sphere 2	0	0	0	0	0
Sphere 3	0	0	0	0	0
Sphere 4	0	0	0	0	0
Sphere 5	0	0	0	0	0

TABLE 14. EVALUATION OF FREE URANIUM AND DEFECTIVE SiC LAYERS IN GERMAN HEU $(Th,U)O_2$ TRISO AND LEU UO_2 TRISO FUEL ELEMENTS

Designation of FE population	AVR XV HEU	AVR XX HEU	AVR XIX LEU	AVR XXI LEU	AVR XXI/2 LEU
Production year	1978	1983	1981	1983	1985
No. FE lots	4	6	14	11	8
No. FEs produced	6250	12 000	24 600	20 500	14 000
^{235}U enrichment [wt%]	92.5	92.4	9.8	16.7	16.7
N = Th/^{235}U ratio	5.00	4.97	–	–	–
Number of particles/FE	10 480	10 660	16 400	9560	9560
Evaluation of free uranium from burn-leach measurements					
Mean value [ppm]	34	< 10	51	43	8
Number of FEs tested in burn-leach	16	30	70	55	40
No. FEs with 0 part. defects	0	0	31	42	38
No. FEs with 1 part. defects	0	0	26	8	1
No. FEs with 2 part. defects	1	0	9	2	1
No. FEs with 3 part. defects	1	0	4	2	0
No. FEs with 4 part. defects	0	0	0	0	0
No. FEs with 5 part. defects	0	0	0	0	0
No. FEs with 6 part. defects	0	0	0	1	0
No. FEs with ≥7 part. defects	0	0	0	0	0
No. defect particles observed	5	0	56	24	3
Equivalent ppm U_{free} from the number of defects observed	30	0	49	46	8

FE = fuel element

TABLE 15. BURN LEACH MANUFACTURING STATISTICS FOR ALL MODERN OXIDE TRISO FUELS FABRICATED IN AVR RELOAD CAMPAIGNS OVER THE PERIOD 1977–1985

Type		No. particles tested N	No. defective particles (n)	Expected defect fraction (n/N)	Upper 95% limit defect fraction*
HEU	AVR XV	167 680	5	3.0×10^{-5}	6.3×10^{-5}
	AVR XX	319 800	0	0	9.4×10^{-6}
LEU	AVR XIX	1 148 000	56	4.9×10^{-5}	6.1×10^{-5}
	AVR XXI	525 800	24	4.6×10^{-5}	6.4×10^{-5}
	AVR XXI/2	382 400	3	7.9×10^{-6}	2.0×10^{-5}

2.5. RANDOM PARTICLE PACKING

In an attempt to understand manufacturing defects, we look at the distances between nearest particles in the HTR fuel sphere. Modelling particles as random points in the fuel zone: when we model N particles in the fuel zone with R_f = 23 mm as dimensionless mathematical points, then the probability p of finding the nearest neighbour [43] at radius r is given by

$$p(r) = \frac{d}{dr}\left\{1 - \exp\left[-N\left(\frac{r}{R_f}\right)^3\right]\right\}.$$

This is a Weibull distribution with modulus m = 3. The point distance distributions as obtained by Monte-Carlo simulations are shown in Figs 21 and 22.

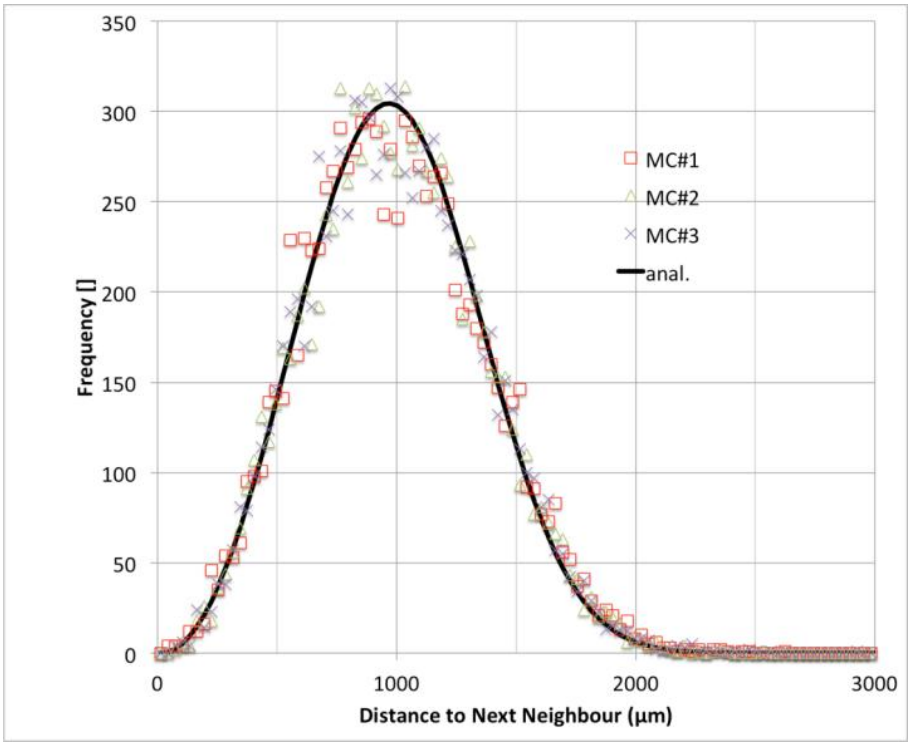

FIG. 21. Frequency distribution of nearest neighbour with N=9409 points in the spherical volume with radius R_f=23 mm. Three Monte-Carlo simulation runs and comparison to analytical solution.

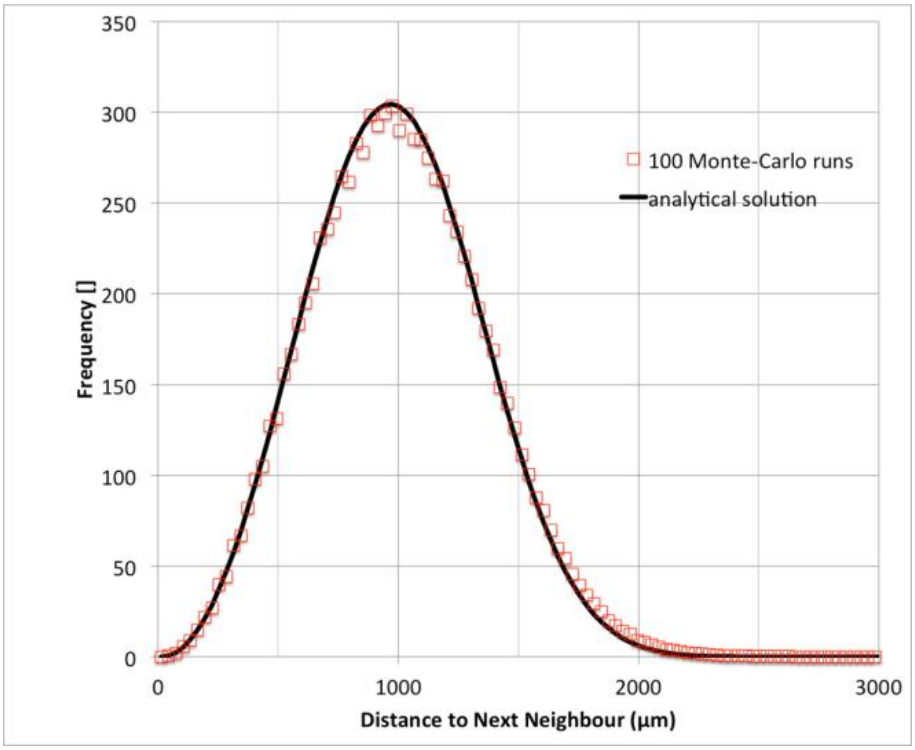

FIG. 22. Frequency distribution of nearest neighbour with N=9409 points in the spherical volume with radius Rf=23 mm. Mean value of 100 Monte-Carlo simulation runs and comparison to analytical solution.

With the finite dimension of coated particles of diameter, d = 920 µm, we can use the analytical distance correlation to predict the fraction of particles that may touch each other after cold isostatic pressing the HTR spherical fuel element (Table 16).

TABLE 16. TRISO FUELS MANUFACTURED IN GERMANY DURING 1978-1988

Spherical Fuel Elements FE	Particle	N part. in FE	*Fraction of particles touching each other
AVR Reload XXI GLE4	LEU UO_2 LTI TRISO	9 560	0.46
AVR Reload XV GO2	HEU (Th,U)O_2 LTI TRISO	10 480	0.49
AVR Reload XX GO2	HEU (Th,U)O_2 LTI TRISO	10 660	0.49
Proof Test Fuel	LEU UO_2 LTI TRISO	14 600	0.61
AVR Reload XIX GLE3	LEU UO_2 LTI TRISO	16 400	0.65

*Despite low volume loadings, quite large fractions of particles touch each other.

Modelling particles as solid spheres with 920 µm diameter: the distance distributions shown in Figs 21 and 22 will be shifted to the right with real solid particles of diameter 920 µm. In the process of cold isostatic pressing of the sphere with 300 MPa, a certain small fraction ψ of the touching particles will be broken, must likely in the rare cases where the protection by the overcoating layer is not perfect. This leads to the proposal to predict the fraction of defects per sphere by the following expression:

$$n_{def} = \psi N \left[1 - e^{-N\left(\frac{d}{R_f}\right)^3} \right]$$

The evaluation of all burn-leach measurements of all TRISO fuel elements leads to values of the impact parameter ψ:

$\psi_{old} = 7.86 \cdot 10^{-5}$ for AVR reload 15, 19 and 21/1;

$\psi_{new} = 1.70 \cdot 10^{-5}$ for AVR reload 20, 21/2 and Proof Test fuel

and the predicted manufacturing defects per fuel sphere are listed in the last column of Table 17 and are shown in Fig. 23.

TABLE 17. EXPERIMENTAL RESULTS OF BURN-LEACH TESTS OF TRISO FUELS MANUFACTURED IN GERMANY DURING 1978-1988

Spherical Fuel Elements FE	Particle Type	Year of Manuf	N part. in FE	No. burn-leach tests	Meas. n_{def}	n_{def} per FE	
						meas.	pred.
AVR Reload XV GO2	HEU (Th,U)O_2 LTI TRISO	1978	10 480	16	5	0.31	0.40
AVR Reload XIX GLE3	LEU UO_2 LTI TRISO	1981–1983	16 400	70	56	0.80	0.84
AVR Reload XXI/1 GLE4	LEU UO_2 LTI TRISO	1983	9560	55	24	0.44	0.34
AVR Reload XX GO2	HEU (Th,U)O_2 LTI TRISO	1983	10 660	30	0	0.00	0.09
AVR Reload XXI/2 GLE4	LEU UO_2 LTI TRISO	1985–1987	9560	40	3	0.08	0.07
Proof Test Fuel	LEU UO_2 LTI TRISO	1988	14 600	10	3	0.30	0.15

* The experimental results of the burn-leach tests on complete spherical fuel elements indicate two quality levels in manufacture. The more recent 3 productions runs show superior results due to systematic tabling of kernels, of particles and of overcoated particles and an advanced automatic overcoating drum design.

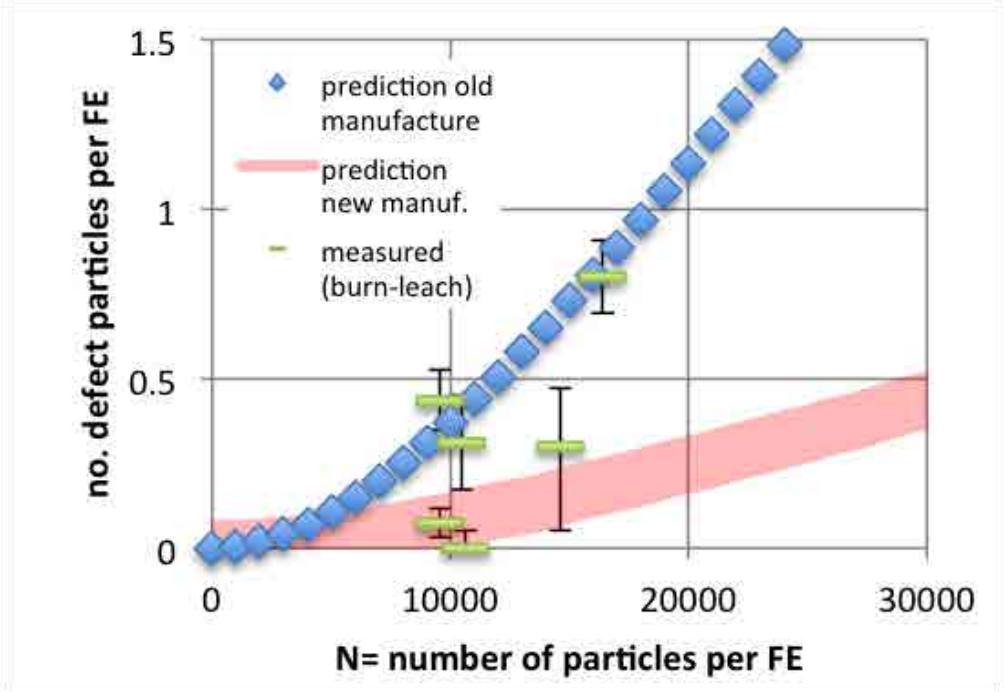

FIG. 23. Measured particle defects per fuel sphere by burn-leach and prediction of defects for the old process (1978–82) and the new manufacturing process (1983–88).

Based in detailed knowledge of typical coated particle diameters and their statistical distribution, of overcoated particles and their statistical distributions and the knowledge of material properties during sphere pressing, a Monte-Carlo simulation model has been developed [44] whereby the distribution of particles in the fuel zone is simulated, the amount of overcoating compression is modelled and limited only when the theoretical density of the matrix material is reached. Overall modelling predictions are obtained by repeating the Monte-Carlo simulations for a large number of spheres.

One of the model predictions is the distance distribution of nearest particle neighbours and the prediction is depicted by the large red circles in Fig. 24. X ray tomography measurements of 16 spheres with nominal 14 580 particles in the fuel element are also shown [45]. The good agreement provides confidence that the Monte-Carlo simulation model can be used for quantitative predictions.

The model predictions for the mean nearest neighbour distances have been extended to the range between 5000 and 34 000 overcoated particles per sphere (Fig. 25). Assuming perfect overcoatings, the number of particles is not limited in this range. However, from an early NUKEM study [46]. “Die Grenzen des Kaltpressverfahrens”, a decrease of sphere strength has to be expected for large particle numbers in the sphere.

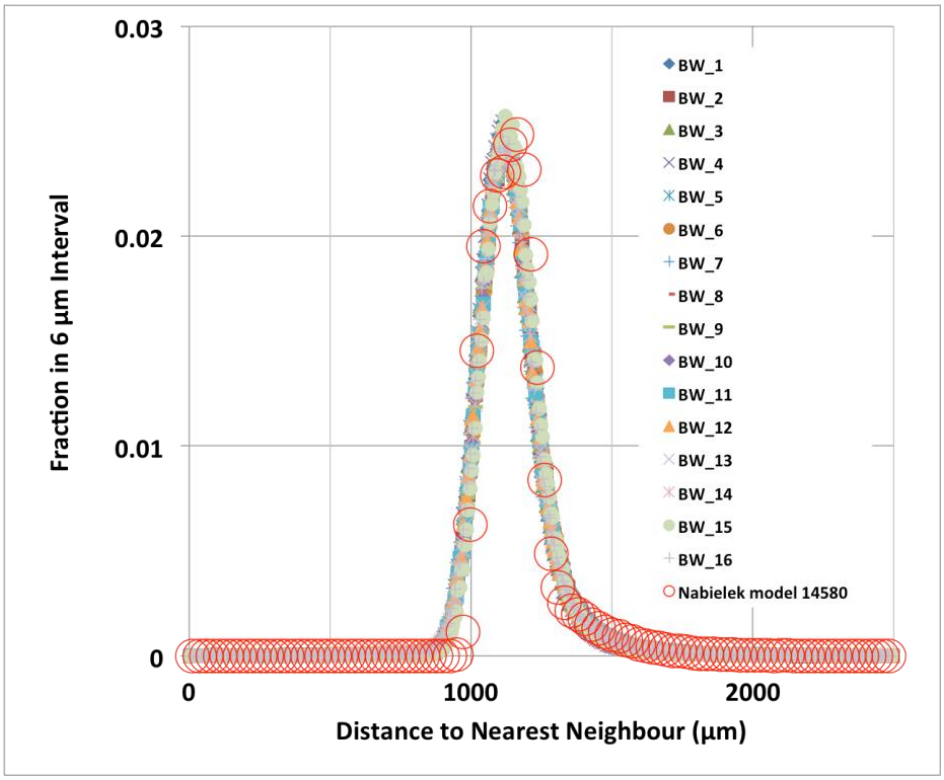

FIG. 24. Model prediction of the distance distribution of nearest TRISO particle neighbours in spheres with 14 580 particles.

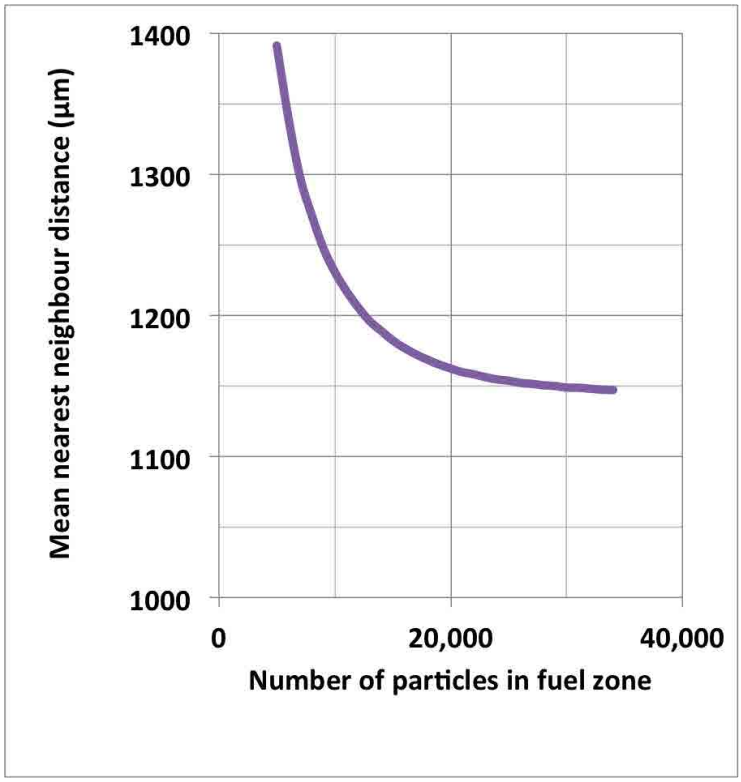

FIG. 25. Prediction of mean nearest neighbour distances of overcoated TRISO particles in the fuel zone of the spherical element for the range between 5000 and 34 000 particles per sphere.

3. IRRADIATION AND ACCIDENT TESTING, PERFORMANCE EVALUATION

For the HTR fuel performance assessment, the following steps are performed [7]:

— Manufacture of statistical significant amount of fuel fulfilling prior specifications

— Irradiation testing of fuel spheres in Material Test Reactors (MTRs) to significant levels of burnup, temperature and fast fluence. Additional testing in real HTRs like the AVR.

— Accident condition testing of irradiated spherical fuel elements at characteristic accident temperatures (now mostly 1600°C) for typical accident times and beyond.

All these have been performed in a systematic way with both HEU $(Th,U)O_2$ TRISO and LEU UO_2 TRISO fuels. The Thorium + HEU work is reported here.

3.1. MTR TESTING

The typical setup for the irradiation testing of fuel spheres is shown in Figs 26 and 27.
During irradiation testing of fuel spheres, Kr and Xe fission gas release rates are measured continuously in a sweep loop to determine particle failure. Solid fission product release is obtained from measuring the sphere surrounding graphite cups and capsule walls after irradiation.

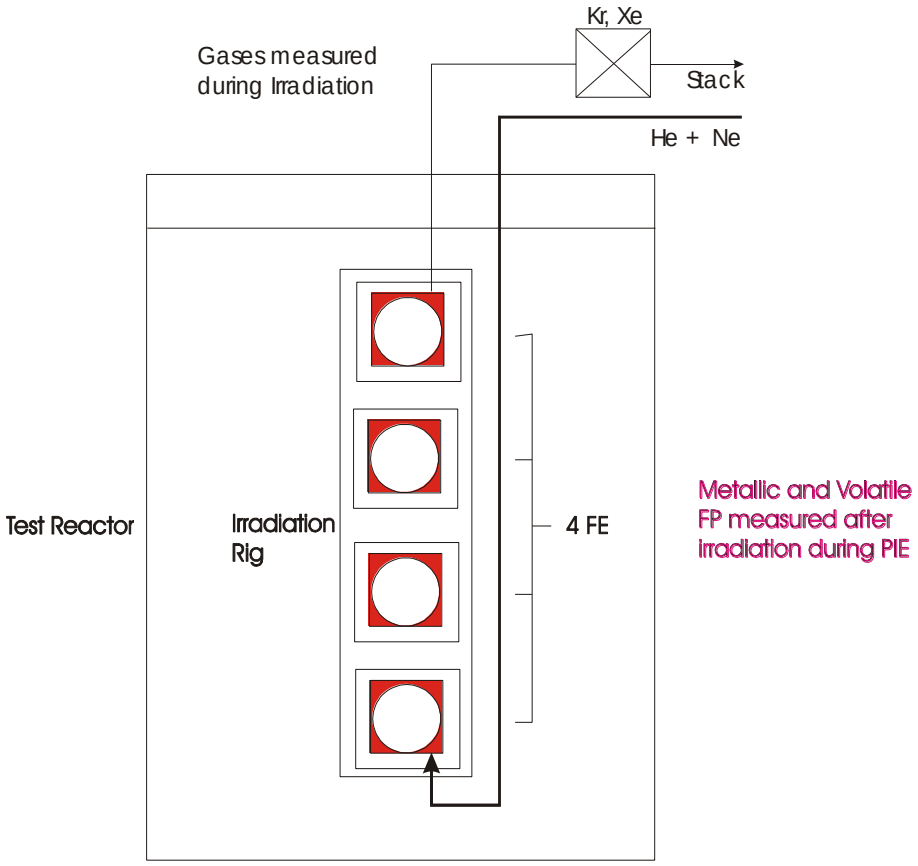

FIG. 26. The typical setup for the irradiation testing of fuel spheres.

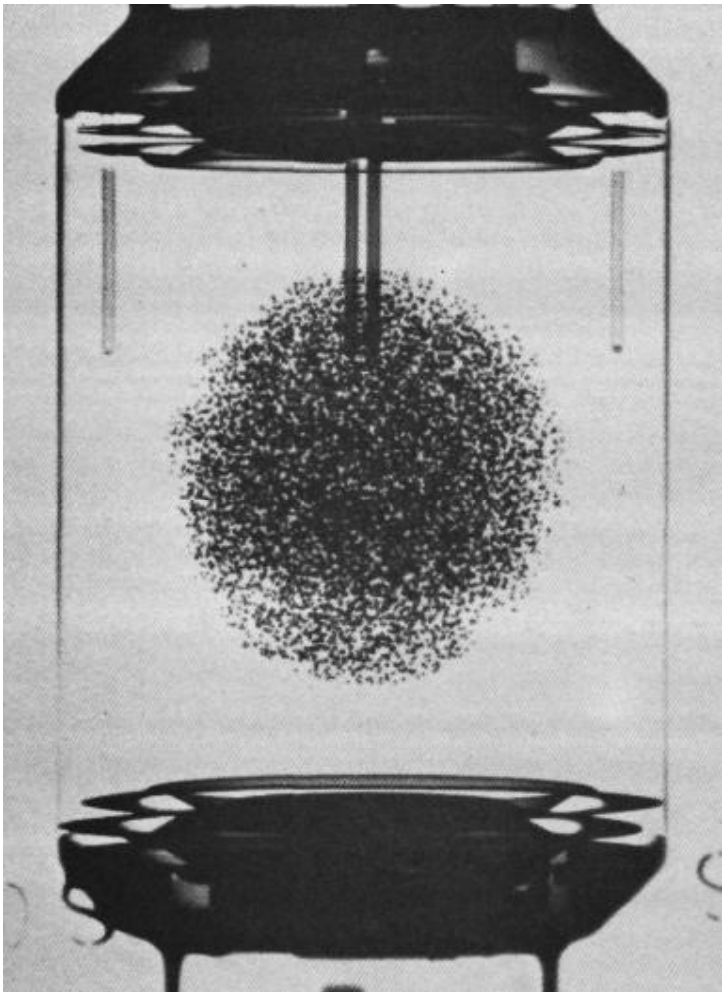

FIG. 27. X Ray image of a spherical fuel element built into one of the four capsules in the R2-K12 test rig [31].

At the time of high quality Thorium TRISO development, irradiation targets were derived from the requirements of a 950°C exit process heat reactor PNP and the 850°C exit direct cycle gas-turbine system HHT (Table 18).

TABLE 18. PNP AND HHT REQUIREMENTS ON HTR FUEL [47]

Operating parameter	Nominal maximum for PNP and HHT
Fuel element central temperature	1020°C
Fuel burnup	11% FIMA
Accumulated neutron fluence	4.5×10^{25} n/m^2 (E > 16 fJ)

Tables 19 and 20 list the Thorium TRISO tests of fuel spheres in the Studsvik R2 reactor and in the Jülich FRJ2 ‘DIDO’ material test reactor.

TABLE 19. ACCLERATED MTR IRRADIATION TESTS OPERATING CONDITIONS FOR HEU (Th,U)O_2 TRISO FUEL SPHERE TESTING [48, 49]

Fuel sphere	Operating temperature range [°C]	Burnup [% FIMA]	Fluence [10^{25} n/m^2, E > 16fJ]	^{85m}Kr release rate to birth rate Ratio (R/B)	
				Start	End-of-irr.
R2-K12/					
1	950 – 1100	11.1	5.6	3.9×10^{-9}	3.2×10^{-8}
2	1120 – 1280	12.4	6.9	3.5×10^{-9}	3.4×10^{-8}
FRJ2-K11/					
3	950 – 1166	9.0	0.062	1.7×10^{-9}	2.7×10^{-7}
4	940 – 1162	8.5	0.051		
R2-K13/					
1	960 – 1170	10.2	8.5	2.2×10^{-9}	2.1×10^{-7}
4	750 – 980	9.8	6.8	1.5×10^{-9}	1.9×10^{-7}

TABLE 20. DESCRIPTION OF FUEL SPHERES IN MTR IRRADIATION TESTS FOR QUALIFICATION OF HIGH QUALITY HEU (Th,U)O_2 TRISO PARTICLES

Irradiation test (Dates)	Duration (full power days)	(Th,U)O_2 TRISO fuel batch	Particles per fuel sphere	Total number of particles
R2-K12/ 1, 2 (11/78 – 2/80)	308	EO 1607	10 830	21 660
FRJ2-K11/ 3, 4 (4/79 – 6/80)	260	HT 150–160, 162–167	10 480	20 960
R2-K13/ 1, 4 (4/80 – 9/82)	517	EO 1674	20 050	40 100

3.1.1. Derivation of failure fraction from measured gas release rates in MTRs

All of the MTR accelerated tests have the capability to measure the release rates of gaseous fission products from the fuel under irradiation. By comparing release rates of short lived fission gases like ^{85m}Kr or ^{88}Kr to the rates expected from a defective or failed particle, we derive the failure fraction:

$$\eta = \frac{\left(R_i / B_i\right)_{EOL}}{\left(R_i / B_i\right)_f}$$

where

η is the fraction of failed particles;

$\left(R_i/B_i\right)_{meas.}$ is the measured normalised release rate for isotope i;

$\left(R_i/B_i\right)_f$ is the normalised release rate for a defective or failed particle for isotope i as obtained from an earlier calibration test or from a verified and validated release model.

The number of failed particles present at the end of an irradiation experiment is then the product of the failure fraction η and the particle population that the R/B measurement represents.

Figure 28 shows measured release rates in comparison to predictions of release rates from heavy metal contamination. The deviation towards the end may conservatively be due to the failure of 2 particles.

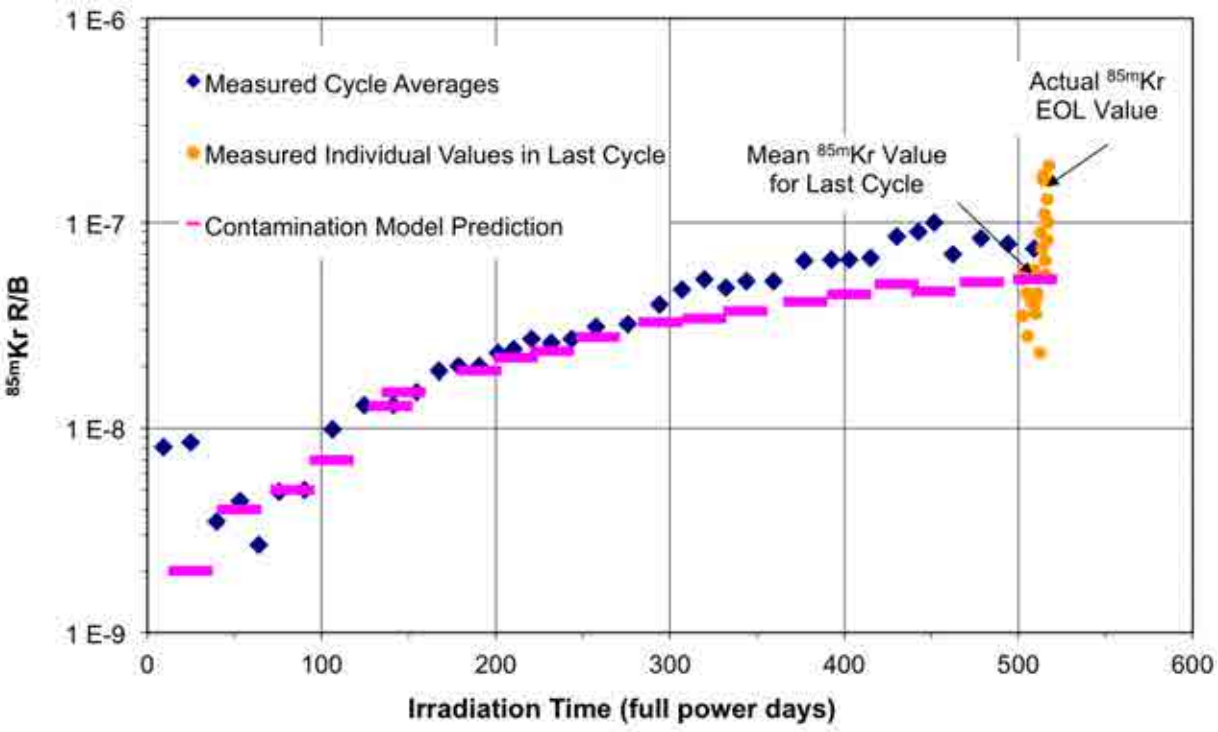

FIG. 32. Measured ^{85m}Kr release rates during irradiation of R2-K13/4.*

*Comparison to (heavy metal only) predicted data for R2-K13/4 as a function of irradiation time. Individual ^{85m}Kr R/B data for last irradiation cycle are shown for reference. The assumption is that there are two particle failures by the end of the irradiation

Using this procedure, we derive the number of in-irradiation failed particles in the high quality Thorium TRISO irradiation tests (Table 21).

TABLE 21. FUEL PERFORMANCE EVALUATION IN ACCLERATED MTR IRRADIATION TESTS BASED ON MEASURED ^{85m}Kr R/B VALUES

Fuel sphere	Beginning		End-of-Irradiation		
	$\left(R/B\right)^{Kr-85m}_{BOL}$	Equiv. failed particles	$\left(R/B\right)^{Kr-85m}_{EOL}$	Contrib. due to contamination	Equiv. in-reactor failed particles
R2-K12/					
1	3.9×10^{-9}	0	3.2×10^{-8}	100% **	0
2	3.5×10^{-9}	0	3.4×10^{-8}	100% **	0
FRJ2-K11/					
3 and 4	1.7×10^{-9}	0	2.7×10^{-7}	~50%	1
R2-K13/					
1	2.2×10^{-9}	0	2.1×10^{-7}	100% **	0
4	1.5×10^{-9}	0	1.9×10^{-7}	negligible	2

**A portion of noble gas release is due to the breeding of fissile material into the initial uranium and thorium contamination in fuel matrix and capsule graphite materials.

3.2. AVR PEBBLE-BED REACTOR IN JÜLICH, GERMANY

The AVR ($46MW_{th}$) was used to test the Pebble Bed Reactor concept, the fuel, and the components. Fuelling of the first core started on 14 July 1966 with 30 000 first core fuel elements, 70 000 moderator graphite balls, and 3000 absorber balls. The last day of power operation was 31 December 1988. Over the whole operational lifetime, more than 290 000 spherical fuel elements of five different types and 15 variants (carbide/oxide, BISO/TRISO, HEU/LEU) with more than 6 billion coated fuel particles plus about 80 000 graphite moderator balls were inserted into the core [50–55]. The detailed fuel composition of the reactor core and its evolution during time is shown in Fig. 29 and listed in Table 22. Modern high quality thorium TRISO fuels are shown in Table 23.

The first modern type of pressed A3 sphere appeared with type GK in April 1969. It took until February 1981 to insert spherical fuel elements with near-perfect high quality, high performance (Th,U)O_2 LTI TRISO particles with GO2. These were followed by very high quality UO_2 LTI TRISO fuels GLE-3 in July 1982 and GLE-4/1 in February 1984. Final perfection was achieved with TRISO particles in the GO2/ Reload XX and GLE-4/2 production.

Using high enriched mixed carbide/oxide fuel at the beginning, the reactor core was, since mid-1982, gradually converted to low enriched fuel. The composition of the reactor system inventory of totally ~110 000 fuel spheres remaining in the core at the end of operation was about 50% of HEU and 50% LEU fuel.

The AVR maximum fuel element temperature frequency distribution, much higher than originally assumed, is shown in Fig. 30. Based on the melt-wire measurement results, two Gaussian distributions with peak temperatures of 1100 ± 66°C and 1220 ± 100°C were found and that define the variation of momentary maximum fuel element surface temperatures in the AVR between the inner core and outer core locations. Peak central temperatures are 37°C and

76°C higher for fuel spheres at the inner and outer locations, respectively. Typical release rates of short-lived fission gases in AVR, Table 24 and Fig. 31, are characteristic for poor quality BISO fuels in the AVR-GO and AVR-GK fuel elements that have a typical heavy metal contamination level of 3×10^{-4}. Modern TRISO fuels are two orders of magnitude lower in contamination.

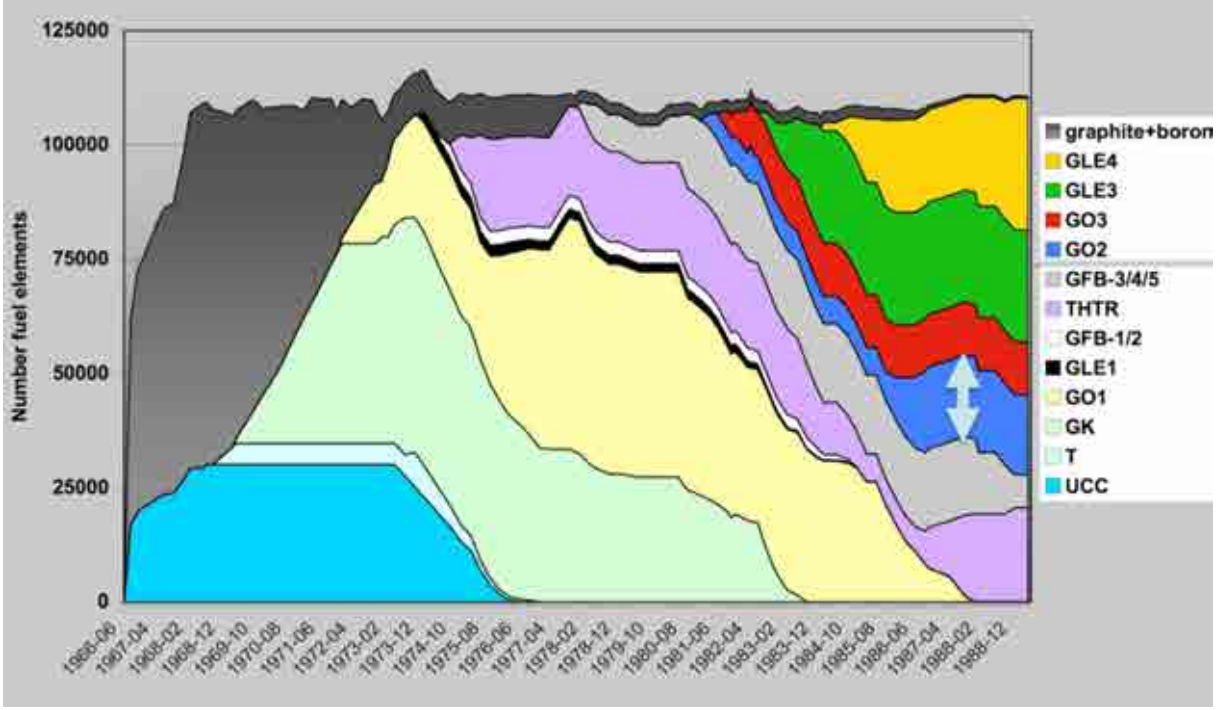

FIG. 29. Distribution of fuel types in the AVR core as a function of operating history [55] [56].

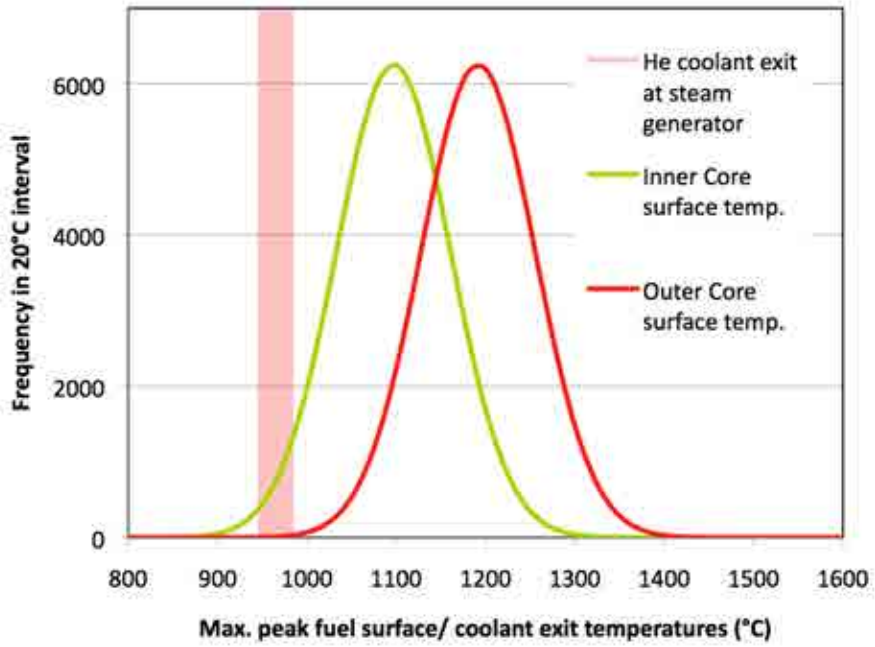

FIG. 30. AVR fuel spheres surface temperatures: peak maxima that are temporarily reached at the surface of the pebble bed core.

TABLE 22. FUEL ELEMENTS INSERTED IN AVR REACTOR

Fuel element	Reload	Begin insertion	No. fuel elements	Fuel kernel	Coating	Particles per fuel element
UCC	0	Jul 1966	30 155	HEU 200 µm $(Th,U)C_2$	HTI BISO	171 000
T	1-1 1-2	Oct 1968 Aug 1973	4550 2954	HEU 400 µm $(Th,U)C_2$	HTI BISO	23 700
GK	3 4 5-1	Apr 1969 Jul 1970 Nov 1970	17 770 6210 26 814	HEU 400 µm $(Th,U)C_2$	HTI BISO	23 700
GO-1	5-2 7 6-1	Dec 1971 Jan 1973 Oct 1973	39 662	HEU 400 µm $(Th,U)O_2$	HTI BISO	20 800
	12 14	Mar 1976 Nov 1976	11 325 9930			
GO-2	15 20	Feb 1981 Oct 1985	6083 11 850	HEU 500 µm $(Th,U)O_2$	LTI TRISO	10 480 10 660
GO-3	18	Jul 1981	11 546	HEU 400 µm $(Th,U)O_2$	HTI BISO	20 800
GO-THTR(22 = KAHTER)	9 10 11 22	Sep 1974 Dec 1974 Dec 1974 Sep 1986	5145 10 022 5000 15 248	HEU 400 µm $(Th,U)O_2$	HTI BISO	38 600
GFB-1	8-1	May 1974	1440	HEU 200 µm UO_2 600 µm ThO_2	LTI BISO	24 500 10 100
GFB-2	8-2	May 1974	1610	HEU 200 µm UO_2 600 µm ThO_2	LTI TRISO LTI BISO	24 500 10 100
GFB-3	13-1	Dec 1977	6076	200 µm UC_2 500 µm ThO_2	LTI TRISO LTI BISO	7 500 8000
GFB-4	13-2	Jul 1980	5860	HEU 200 µm UC_2 530 µm ThO_2 + additives	LTI TRISO LTI BISO	27 100 8600
GFB-5	13-3	Dec 1977	5354	HEU 200 µm UCO 500 µm ThO_2	LTI TRISO LTI TRISO	28 700 9100
GLE-1	6-2	Dec 1973	2400	LEU 600 µm UO_2	LTI BISO	8000
				U_{nat} 600 µm UO_2		9500
GLE-3	19	Jul 1982	24 611	LEU 502 µm UO_2	LTI TRISO	16 400
GLE-4/1	21	Feb 1984	20 350	LEU 502 µm UO_2	LTI TRISO	9560
GLE-4/2	21-2	Oct 1987	8740	LEU 502 µm UO_2	LTI TRISO	9560
		Σ =	290 729			

TABLE 23. HIGH QUALITY THORIUM TRISO FUEL ELEMENTS INSERTED IN AVR REACTOR

Fuel	AVR type	Reload	Initial insertion	No. of fuel elements in campaign
HEU (Th,U)O_2 TRISO	GO2	AVR XV AVR XX	Feb. '81 Oct. '85	6087 11 854

TABLE 24. MEASURED RELEASE RATES OF SHORT LIVED FISSION GASES [54]

*Krypton	R/B	*Xenon	R/B
^{85m}Kr	6.2×10^{-6}	^{133}Xe	4.3×10^{-6}
^{85}Kr	4.4×10^{-6}	^{135}Xe	2.6×10^{-6}
^{88}Kr	3.4×10^{-6}	^{135m}Xe	1.4×10^{-6}
^{89}Kr	1.2×10^{-6}	^{137}Xe	8.0×10^{-7}
^{90}Kr	2.0×10^{-8}	^{138}Xe	4.0×10^{-7}
^{91}Kr	6.2×10^{-6}	^{139}Xe	2.0×10^{-7}

*recorded at full power and maximum operation temperature. Typical values in the period from 1984 to 1987.

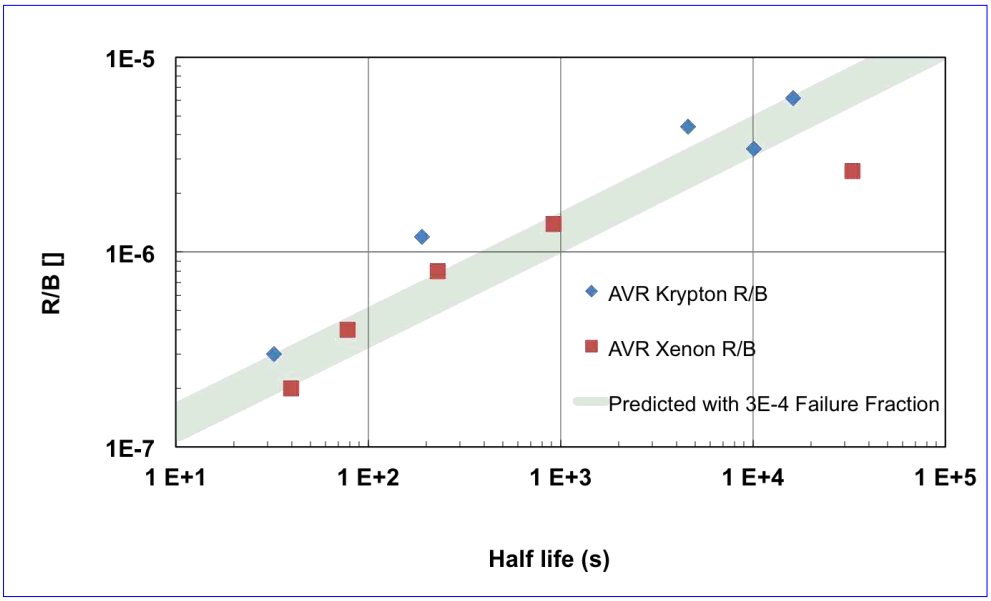

FIG. 31. Measured AVR release rates of short-lived fission gases normalized to respective birth rates as a function of half- life [54] (typical values from the AVR operation period 1984–87. At this stage total primary circuit fission gas activity was 1.04 × 10^{12} Bq. Comparison with release predictions assuming a 3 × 0^{-4} level of contamination or failed particle fraction. Modern HTRs are two orders of magnitude lower in contamination [10]).

3.2.1. AVR in-reactor fuel performance

Due to the large number of different fuel types and qualities, the whole AVR R/B measurements cannot be used to derive individual fuel performance, particularly because the large number of releasing spheres is dominating the releases from modern high quality TRISO fuels by several orders of magnitude. To assess the performance of the AVR GO2 fuel elements with HEU (Th,U)O_2 TRISO fuel particles, a methodology was developed by Michael J Kania [59] based upon fission gas release measurements made during the gradual heatup in the early phase of accident condition testing. This heatup process begins at room temperature, progresses over a series of heating-ramps to specific temperatures (300°C, 1050°C, and 1250°C) and hold periods until the desired simulation temperature is reached. Two of these hold points, 1050°C, and 1250°C, are designed to equilibrate the irradiated fuel particles in the fuel element at or near their prior irradiation temperature. This allows the fuel to develop a stable internal environment before being heating to an elevated temperature, not previously experienced by the fuel particles. The 1050°C hold point was considered the mean working temperature for fuel specimens from accelerated MTR irradiation tests, and the 1250°C hold point was considered the typical working temperature for AVR fuel elements.

Throughout the accident simulation test, the test furnace is purged with a sweep gas and continuously monitored for release of the long-lived ^{85}Kr (10.76 yr half-life) fission gas. Detection of any significant activity in the sweep gas represents release from the fuel element and may be an indicator of the presence of failed or defective fuel particles.

Table 25 is a detailed list of fuel elements containing HEU (Th,U)O_2 TRISO fuel elements that were subjected to accident simulation testing. Of these, nine were used to analyse AVR irradiation performance. The two remaining elements are one element each from the MTR accelerated irradiation tests FRJ2-K11/3 and R2-K13/1. Also shown are MTR irradiated UO_2 LTI TRISO results that demonstrate fully consistent behaviour.

TABLE 25. ^{85}Kr RELEASE FRACTIONS MEASURED DURING HEATUP PHASE IN ACCIDENT SIMULATION TESTS ON AVR IRRADIATED HEU $(Th,U)O_2$ FUEL ELEMENTS AND IRRADIATED SPHERES FROM MTR TESTS R2-K13 AND FRJ2-K11

Fuel element*	Burnup (% FIMA)	Measurement temperature of ^{85}Kr release (°C)	^{85}Kr release fraction	Peak temperature of accident simulation test (°C)
KÜFA isothermal accident simulation tests				
AVR 70/26	8.2	1610**	$\leq 1.0 \times 10^{-6}$	1610
R2-K13/1	10.3	1250	$\leq 3.4 \times 10^{-7}$	1600
Graphite furnace tests				
AVR 70/15	7.1	1250	$\leq 7.0 \times 10^{-7}$	1500
AVR 70/7	7.3	1500**	$\leq 6.3 \times 10^{-7}$	1500
AVR 69/13	8.6	1800**	$\leq 5.4 \times 10^{-7}$	1800
AVR 74/24	11.2	1250	$\leq 5.4 \times 10^{-7}$	2100
AVR 74/20	11.9	1250	$\leq 1.6 \times 10^{-7}$	1900
FRJ2-K11/3	10.0	1600**	$\leq 5.1 \times 10^{-6}$	1600
Ramp accident simulation tests in graphite furnace				
AVR 69/28	6.8	1530**	$\leq 6.8 \times 10^{-7}$	2150
AVR 70/18	7.1	2130**	$\leq 6.5 \times 10^{-6}$	2400
AVR 74/17	10.3	1250	$\leq 1.4 \times 10^{-7}$	2500
Accident simulation tests on LEU UO_2 MTR and HTR-Modul Proof Test elements				
HFR-K3/1	7.7	1250	$< 5.6 \times 10^{-8}$	1600
HFR-K3/3	10.2	1250	1.5×10^{-7}	1800
FRJ2-K13/2	8.1	1250	5.3×10^{-7}	1600
FRJ2-K13/4	7.8	1250	4.5×10^{-8}	1600 / 1800
HFR-K6/2	9.7	1050	1.0×10^{-8}	1600
HFR-K6/3	9.8	1050	3.2×10^{-6}	1600

* The AVR Sample No. represents the sequential sample of elements withdrawn for the AVR core for surveillance purposes; the Specimen No. is the order in which this element was withdrawn.
** No detectable release at 1250°C.

Figure 32 presents the fractional release data: all results are at a level well below the characteristic values for one defective or failed fuel particle. Earlier tests of this type had determined up to 50% particle failure in AVR-GLE1 fuel elements.

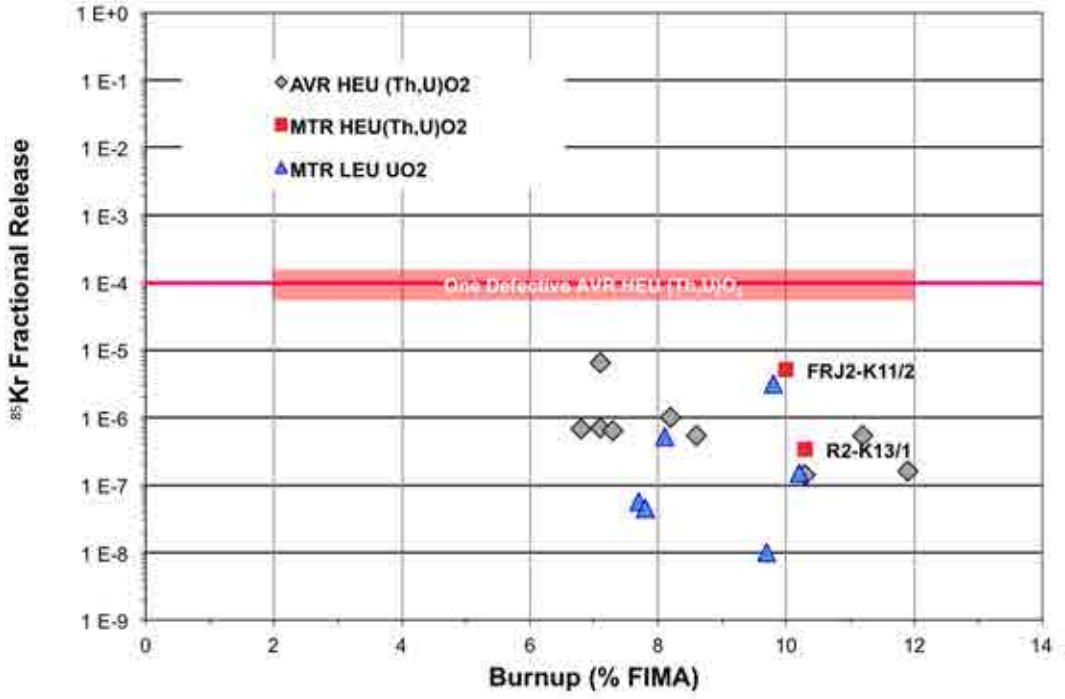

FIG. 32. Noble gas ^{85}Kr fractional release monitored during accident simulation testing of AVR type GO2 fuel elements with HEU (Th,U)O_2 TRISO fuel (black symbols) compared with similar data obtained in MTR tests (red + blue symbols).

Figure 33 shows the ^{85}Kr fractional release measured on the three AVR GO2 fuel elements subjected to constant rate heating ramp tests up to 2150°C–2500°C. The level of one particle failure is 9.5×10^{-5} (black horizontal line).

Collectively, the nine AVR GO2 fuel elements represent a population of 94 320 HEU (Th,U)O_2 TRISO coated particles, with no observed in-reactor failure at discharge.

For the in-reactor performance in MTRs and AVR, we combined the results to the observation of three particles failures in an assembly of 177 040 particles. The expected failure limits and the confidence limits are shown in Table 26, combined with previous results on low enriched UO_2 LTI TRISO fuels [58, 59].

In both cases, failure levels are well below 2×10^{-4} level that were originally requested [66]. The superior upper confidence limit results of the LEU fuels is partially due to the much larger sample size in testing.

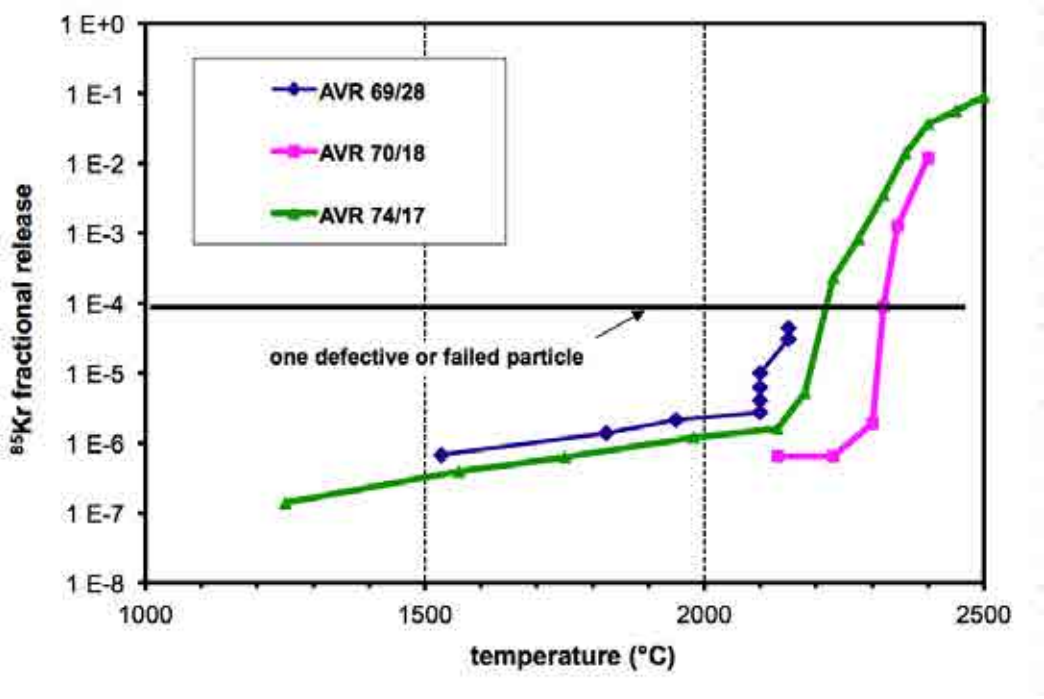

FIG. 33. Fractional release of ^{85}Kr measured during accident simulation temperature ramp testing of AVR-GO2 fuel elements containing HEU (Th,U)O_2 TRISO fuel as function of heating temperature [60, 61].

TABLE 26. IRRADIATION TESTING PERFORMANCE OF SPHERICAL FUEL ELEMENTS WITH HEU (Th,U)O_2 TRISO AND LEU UO_2 TRISO PARTICLES [59]

		No. fuel spheres	No. coated particles (N)	No. in-reactor failed particles (n)	Expected failure fraction (=n/N)	One-sided upper 95% confidence limit
			HEU (Th,U)O_2 TRISO			
*Irradiation testing	MTRs	6	82 720	3		
	AVR	9	94 320	0		
	Total	15	177 040	3	1.7×10^{-5}	4.4×10^{-5}
			LEU UO_2 TRISO			
*Irradiation testing	MTRs	19	276 680	0		
	AVR	24	393 600	0		
	Total	43	670 280	0	0	4.5×10^{-6}

3.3. ACCIDENT SIMULATION

Accident testing is done by simulating the characteristic elevated temperature sequence with irradiated fuel elements with on-going measurement of fission product release [57–64]. For the large HTRs, the hypothetical unrestricted core heatup can go to fuel temperatures as 2500°C or higher. In contrast, the small modular HTRs with their tall, small diameter core automatically limit the maximum temperature to less than 1600°C.

Accident simulation is accomplished by externally heating irradiated spherical fuel elements under a purged helium environment. The helium purge circuit has the capability for continuous online measurement of ^{85}Kr release from the heated fuel in external cold traps (Fig. 34) as an indicator of particle failure.

Prior to 1984, a graphite high-temperature furnace described in the left of Fig. 35 was the primary furnace employed. This provides the capability to reach temperatures as high as 2500°C. Continuous fission gas release monitoring is possible, but the release of solid fission products can only be estimated by measuring the difference in key solid fission product inventories before and after the accident simulation test.

In the 1980s, at the Forschungszentrum Jülich, a new accident simulation facility was designed to demonstrate the passive safety characteristics of small, modular HTRs. The high temperature furnace in this facility was a tantalum furnace allowing heating tests up to 1800°C with a built-in cold-finger apparatus (KÜFA=**KÜ**hl**F**inger-**A**nlage). Inclusion of the cold finger assembly added the capability of a quasi-continuous measurement of solid fission product release in addition to the continuous gas release monitoring without having to interrupt the heating test. The right of Fig. 35 is a schematic of the tantalum heating furnace showing the cold-finger apparatus, fuel element placement within the furnace heating zone, and the major components of the KÜFA facility. In the meantime, the KÜFA facility has been relocated to Karlsruhe and many more tests have been performed.

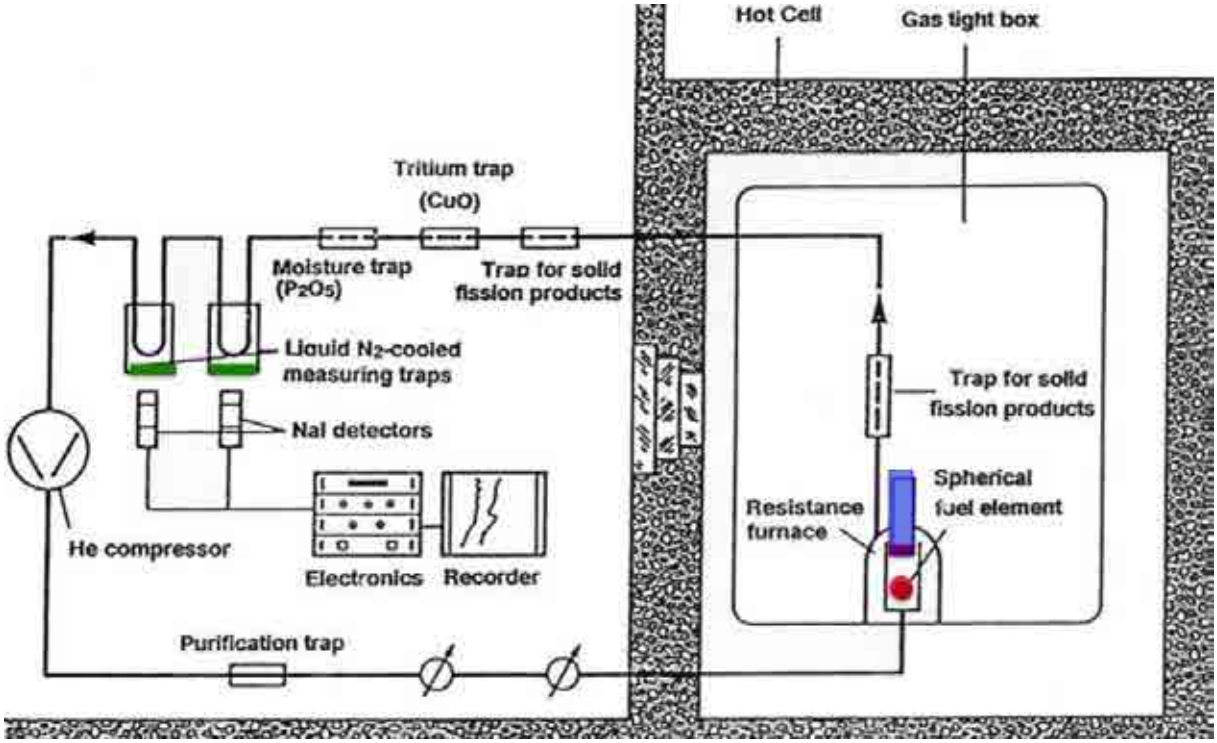

FIG. 34. Accident simulation tests with irradiated fuel elements. Kr release is measured outside, solid fission product release at the cold finger inside the Hot Cell.

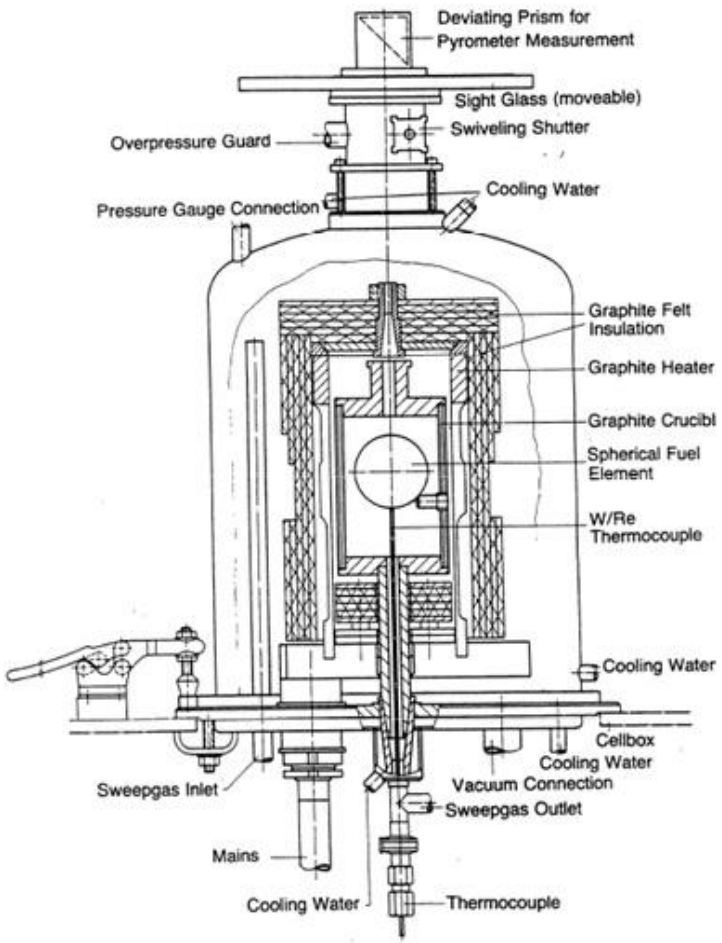

Graphite furnace for isothermal and temperature ramp tests up to 2500°C

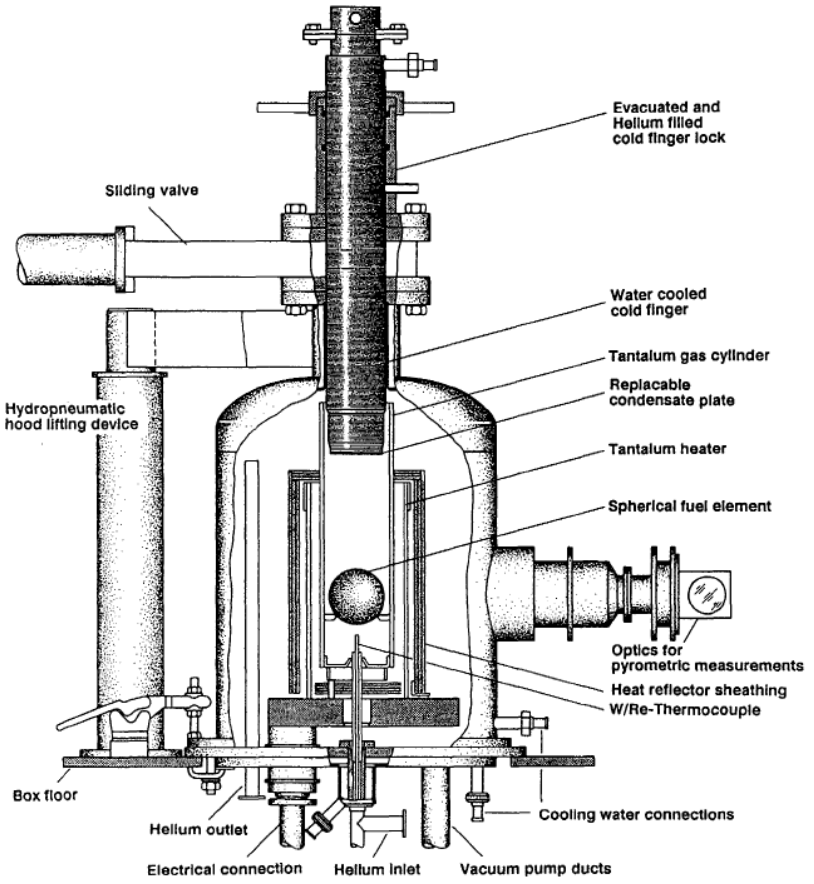

Tantalum furnace of heating tests up to 1800°C with the addition of the cold finger ("KÜFA") for quasi-continuous measurements of solid fission product release.

FIG. 35. The design of accident condition heating furnaces.

Typically the heating profile for small, modular HTRs like the HTR-Modul would be limited to 1600ºC or 1800ºC (Fig. 36). The hold points at 1050ºC and 1250ºC were established for equilibration to re-adjust the fuel to their prior irradiation conditions. The ^{85}Kr gas release data measured at these hold point temperatures can be used to estimate the fuel element's irradiation performance.

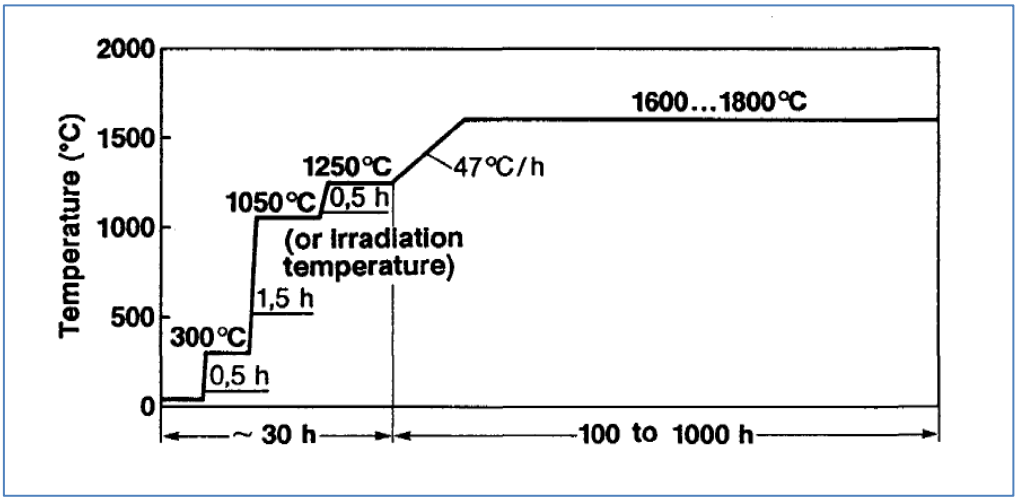

FIG. 36. Typical temperature sequence in accident condition testing for small modular reactors.

The accident simulation tests conducted with HEU $(Th,U)O_2$ TRISO fuel elements [7] include:

— Two isothermal accident simulation tests performed in the KÜFA test facility at temperatures of 1600ºC;

— Five isothermal accident simulation tests in the graphite furnace at temperatures of 1500ºC (2x), 1600ºC, 1800ºC, 1900ºC, 2100ºC; and

— Three temperature ramp tests in the graphite furnace – one element each to 2150ºC, 2400ºC and 2500ºC.

A total of ten irradiated fuel elements with $(Th,U)O_2$ TRISO fuel were subjected to accident conditions tests and are characterized along with their irradiation conditions prior to the heating tests in Table 27.

The complete set of fission product release data obtained from accident simulation tests on irradiated fuel elements containing HEU $(Th,U)O_2$ TRISO fuel particles are given in Table 28. The ^{85}Kr release results were obtained from the cold traps in the gas circuit. Solid fission product releases were measured in two different ways: in tests performed in the KÜFA facility, measurements were made on the cold finger plates; in tests performed in the graphite furnace, the loss of inventory was obtained by measurement of the spherical fuel element inventory before and after the heating procedure and their sensitivity is limited to the percentage range.

TABLE 27. HIGH QUALITY HEU $(Th,U)O_2$ TRISO FUEL IN ACCIDENT CONDITION SIMULATION TESTS

Fuel element	$(Th,U)O_2$ particle batch	Irradiation conditions			Peak temperature of accident simulation test [ºC]
		Temperature [ºC]	Burnup [% FIMA]	Fluence [10^{25} n/m^2, E>16 fJ]	
Tantalum KÜFA test facility					
AVR 70/26	HT 150–160, 162–167	900–1200	8.2	2.0	1610
R2-K13/1	EO 1674	1000–1200	10.3	8.3	1600
Graphite furnace test facility					
AVR 70/15	HT 150–160, 162–167	900–1200	7.1	1.7	1500
AVR 70/7	HT 150–160, 162–167	900–1200	7.3	1.8	1500
AVR 69/13	HT 150–160, 162–167	900–1200	8.6	2.1	1800
AVR 74/24	HT 150–160, 162–167	900–1200	11.2	2.7	2100
AVR 74/20	HT 150–160, 162–167	900–1200	11.9	2.9	1900
AVR 69/28	HT 150–160, 162–167	900–1200	10.0	1.7	2150
AVR 70/18	HT 150–160, 162–167	900–1200	6.8	1.7	2400
AVR 74/17	HT 150–160, 162–167	900–1200	7.1	2.5	2500

TABLE 28. RELEASE RESULTS FROM ACCIDENT TESTING OF HIGH QUALITY HEU $(Th,U)O_2$ TRISO FUEL ELEMENTS FROM ISOTHERMAL AND RAMP TESTS

Fuel element	Burnup [% FIMA]	Heating programme			Release fractions				
		T_{max} [ºC]	1250ºC to T_{max} [h]	Heating time [h]	^{85}Kr	^{134}Cs	^{137}Cs	^{90}Sr*	^{110m}Ag*
AVR 70/7	7.3	1500	1.5	100	$< 7 \times 10^{-6}$	$< 2 \times 10^{-2}$	$< 2 \times 10^{-2}$		
		1500	1.5	50	$< 7 \times 10^{-6}$	$< 2 \times 10^{-2}$	$< 2 \times 10^{-2}$		
		1500	1.5	50	$< 7 \times 10^{-6}$	$< 2 \times 10^{-2}$	$< 2 \times 10^{-2}$		
				total: 200	$< 2 \times 10^{-5}$	$< 2 \times 10^{-2}$	$< 2 \times 10^{-2}$	–	–
AVR 70/15	7.1	1500	7	90	$< 8 \times 10^{-5}$	$< 2 \times 10^{-2}$	$< 2 \times 10^{-2}$		
		1500	1.5	50	$< 3 \times 10^{-6}$	$< 2 \times 10^{-2}$	$< 2 \times 10^{-2}$		
				total: 140	$< 8 \times 10^{-5}$	$< 2 \times 10^{-2}$	$< 2 \times 10^{-2}$	–	–
AVR 70/26	8.2	1610	1.5	312	$< 1 \times 10^{-5}$	**	$< 3 \times 10^{-5}$	$< 1.7 \times 10^{-5}$	$< 1.9 \times 10^{-2}$
R2-K13/1	10.3	1600	7.5	1000	$< 3.5 \times 10^{-4}$	$< 1.6 \times 10^{-2}$	$< 1.5 \times 10^{-2}$	$< 1.2 \times 10^{-3}$	~1
AVR 69/13	8.6	1800	14	10	$< 1 \times 10^{-6}$	$< 1 \times 10^{-2}$	$< 1 \times 10^{-2}$		
			2.5	10	$< 1 \times 10^{-6}$	$< 1 \times 10^{-2}$	$< 1 \times 10^{-2}$		
			3.5	22	$< 3 \times 10^{-5}$	$< 1 \times 10^{-2}$	$< 3 \times 10^{-2}$		
			12	50	$< 9 \times 10^{-3}$	5×10^{-1}	4.8×10^{-1}	–	–
				total: 92	9.0×10^{-3}	5.0×10^{-1}	4.8×10^{-1}		
AVR 74/20	11.9	1900	15	50	$< 2.1 \times 10^{-2}$	$< 4.2 \times 10^{-1}$	$< 4.3 \times 10^{-1}$	–	–
AVR 74/24	11.2	2100	18	30	$< 1 \times 10^{-1}$	$< 5.0 \times 10^{-1}$	$< 5.0 \times 10^{-1}$	–	–
AVR 69/28	6.8	2150	58	6	$< 4 \times 10^{-5}$	$< 2.2 \times 10^{-1}$	$< 2.2 \times 10^{-1}$	–	–
AVR 70/18	7.1	2400	28	Ramp	$< 1.2 \times 10^{-2}$	**	$< 8.2 \times 10^{-1}$	–	–
AVR 74/17	10.3	2500	27	Ramp	$< 1.2 \times 10^{-1}$	$< 8.3 \times 10^{-1}$	$< 8.3 \times 10^{-1}$	–	–

*Measured only in two tests conducted in KÜFA facility.

**Not evaluated/inexact measurement

Ramp test results are illustrated in Fig. 37. At temperatures above 2100ºC, the release quickly reaches a level indicative of catastrophic particle failure and this occurs in the (Th,U)O_2 TRISO fuel as well as in the UO_2 TRISO fuel at nearly the same temperature. This dramatic change in performance is due to a serious deterioration of the TRISO coatings on fuel particles caused by the onset of SiC thermal decomposition [63]. However, high burnup thorium fuels are superior to high burnup UO_2 fuels in ramp tests.

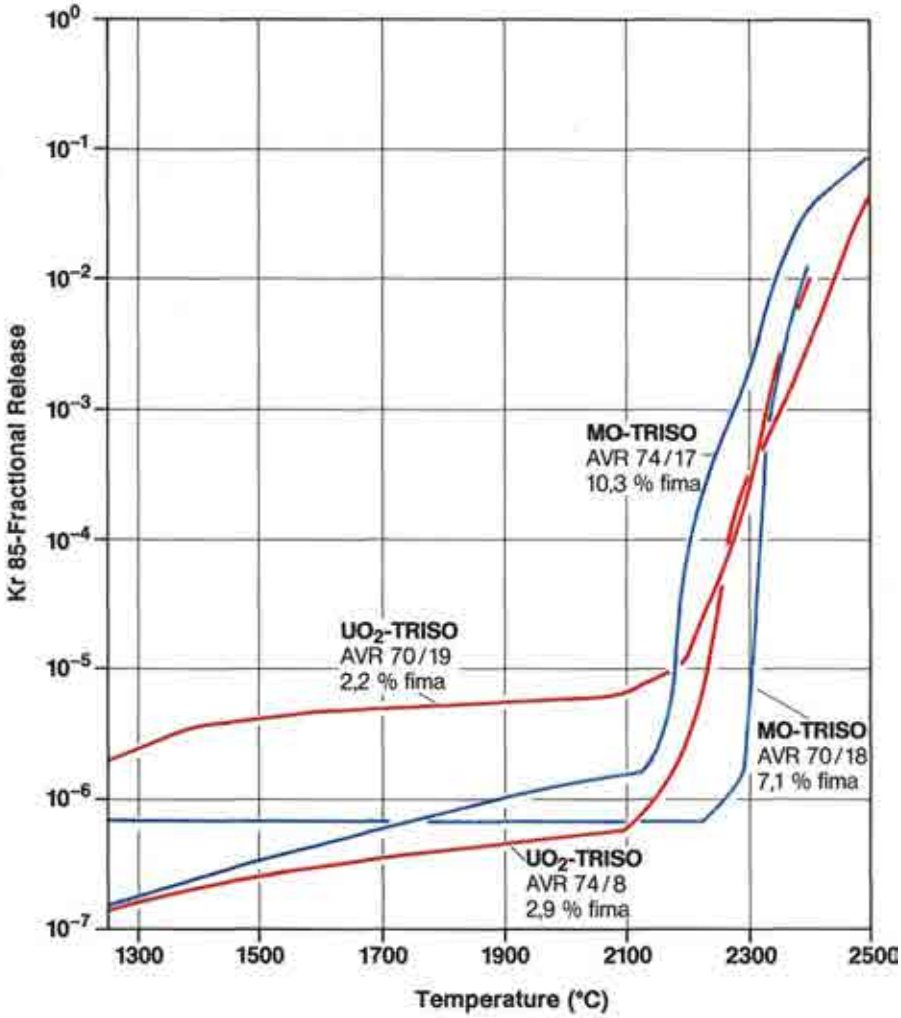

FIG. 37. Comparison of the ^{85}Kr fractional release from irradiated AVR GO2 [HEU (Th,U)O_2 TRISO] and AVR GLE3 [LEU UO_2 TRISO] fuel elements as a function of temperature during accident simulation ramp tests.

Five isothermal accident simulation tests were conducted in the graphite furnace on AVR GO2 fuel elements AVR 70/15, AVR 70/7, AVR 69/13, AVR 74/24, AVR 74/20 with burnups ranging from 7.1% to 11.9% FIMA. Figure 38 shows the ^{85}Kr fractional release data for all of these elements as a function of accident simulation temperature. All of these release data are consistent with the ramp test results.

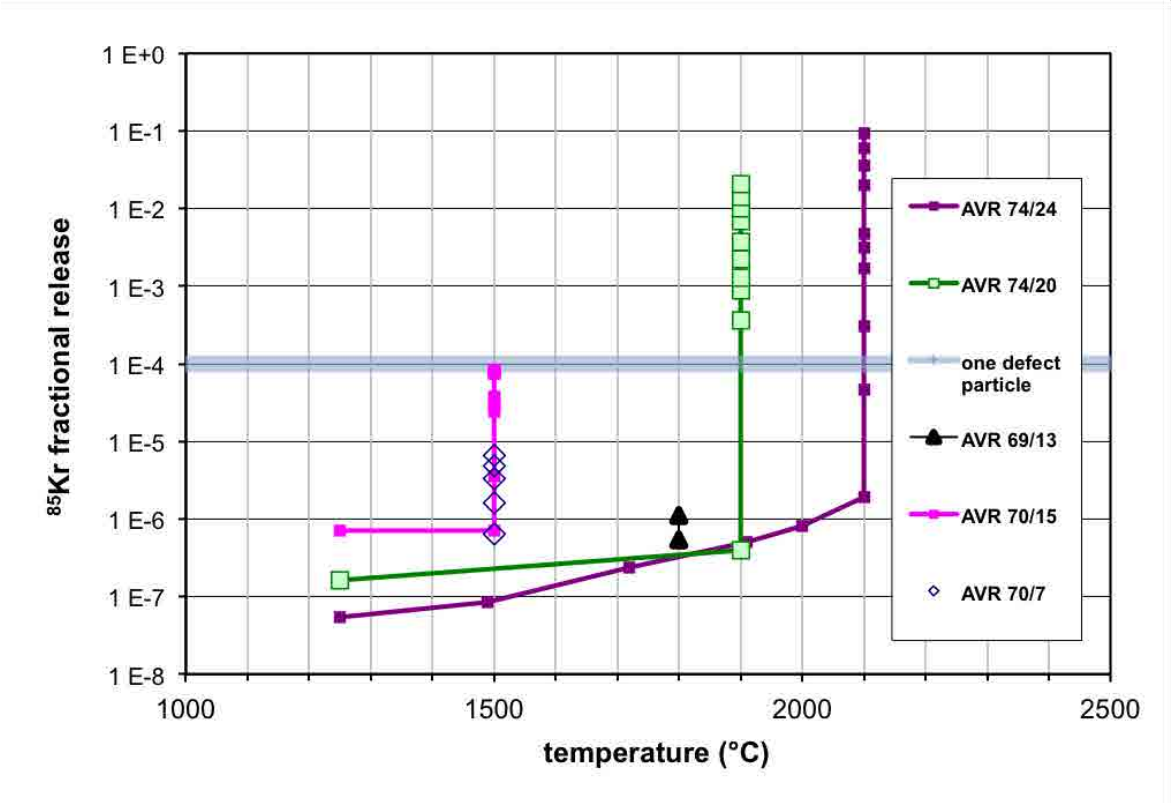

FIG. 38. ^{85}Kr fractional release measured during isothermal accident simulation tests conducted on six AVR type GO2 fuel elements with high quality HEU (Th,U)O_2 TRISO fuel particles.

Figure 39 is a ceramographic section of AVR GO2 element 69/13 after completing its accident simulation test. The ceramography showed no evidence of corrosion in the SiC layer or any detrimental effects due to the 92 hr exposure at temperatures of 1800ºC consistent with the good results in gas release.

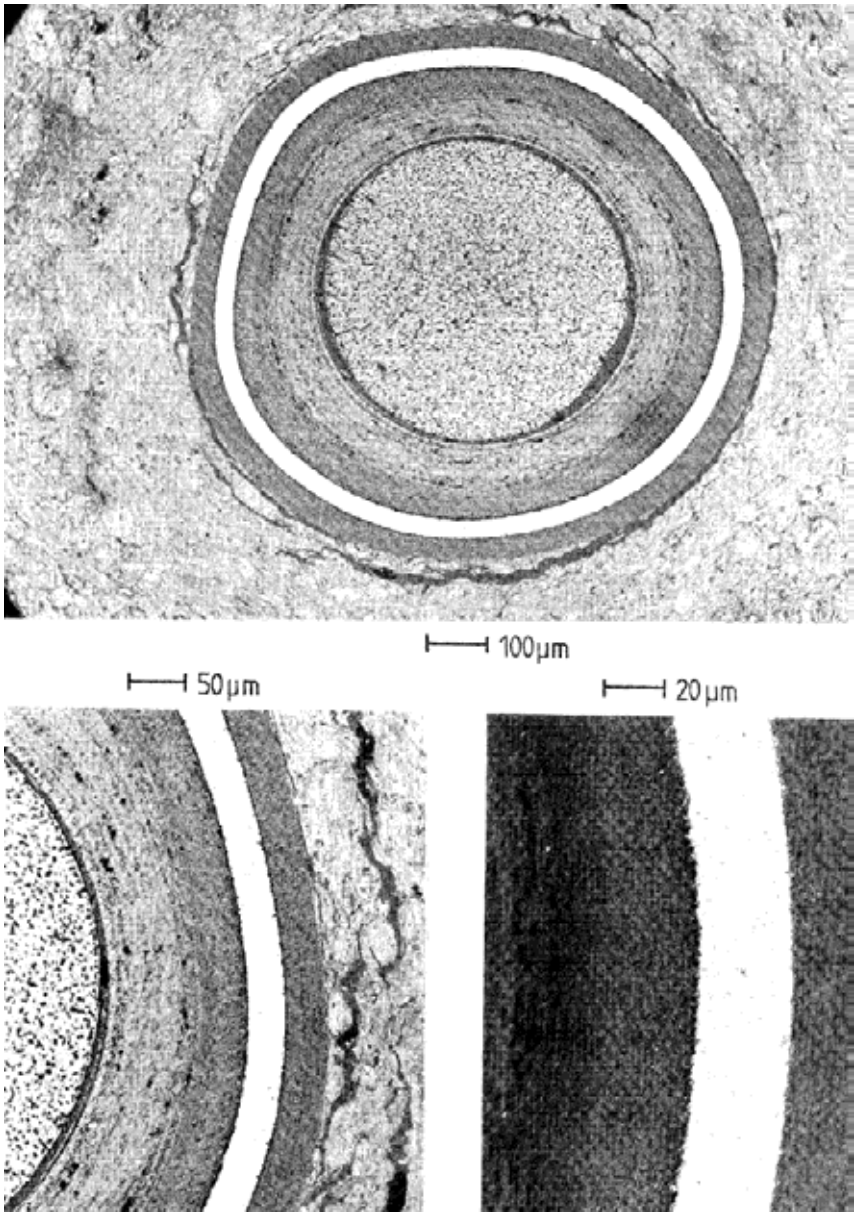

FIG. 39. Ceramographic sections through high quality HEU (Th,U)O_2 TRISO particles from AVR GO2 fuel element 69/13 irradiated to 8.6% FIMA and heated for 92 hours at 1 800°C [62].

Two 1 600°C isothermal KÜFA heating tests were performed on the GO2 fuel element AVR 76/20 and the fuel element from R2-K13/1. The fractional release results for the key fission products ^{85}Kr, ^{90}Sr, ^{137}Cs, and ^{110m}Ag are shown in Fig.40. At the beginning of the isothermal heatup phase the ^{85}Kr, ^{90}Sr, and ^{137}Cs release fractions are all significantly < 10^{-5}. Considering the characteristic accident time of less than 100 hrs, all release are very low with the exception of ^{110m}Ag. Silver is known to be released fast even from high quality SiC in TRISO particles [65].

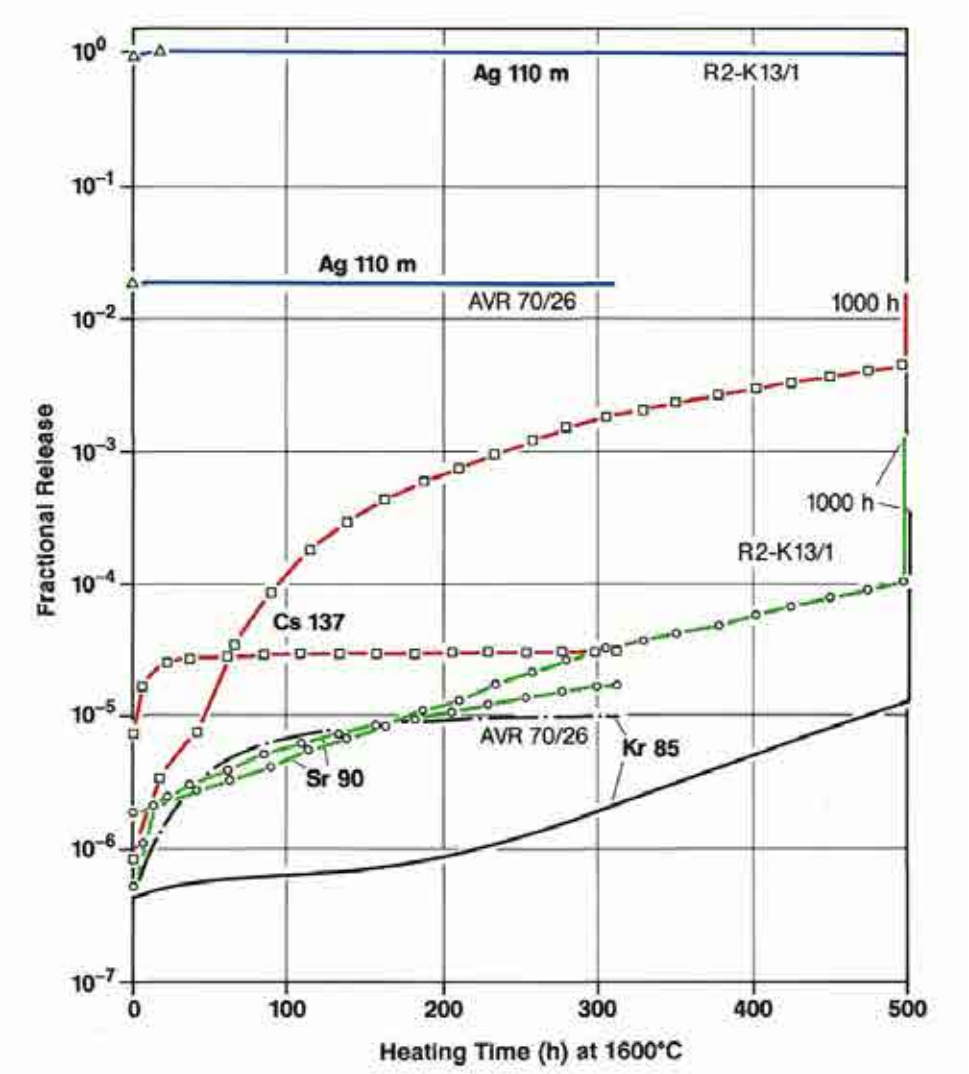

FIG. 40. Fission product release fractions measured during 1000 h (R2-K13/1) and 312 h (AVR 70/26) isothermal heatup tests at 1600°C from fuel elements with HEU (Th,U)O_2 TRISO particles [61].

Figure 41 presents the ^{85}Kr fractional release for AVR 70/26 and R2-K13/1 for the first 200 hours of their 1600ºC isothermal accident simulation tests. The fractional release for AVR 76/20 remained < 10^{-5} for the duration of its 312 hours of isothermal heating. In R2-K13/1, the ^{85}Kr fractional release started out at < 10^{-6} and remained below 10^{-6} for the first 200 hours. The ^{85}Kr fractional release data from other AVR GO2 type elements subjected to accident condition simulation tests with HEU (Th,U)O_2 TRISO fuels are also shown; the release fractions for R2-K13/1 is significantly lower than for the AVR GO2 fuel elements for the first 200 hours of heating at 1600°C.

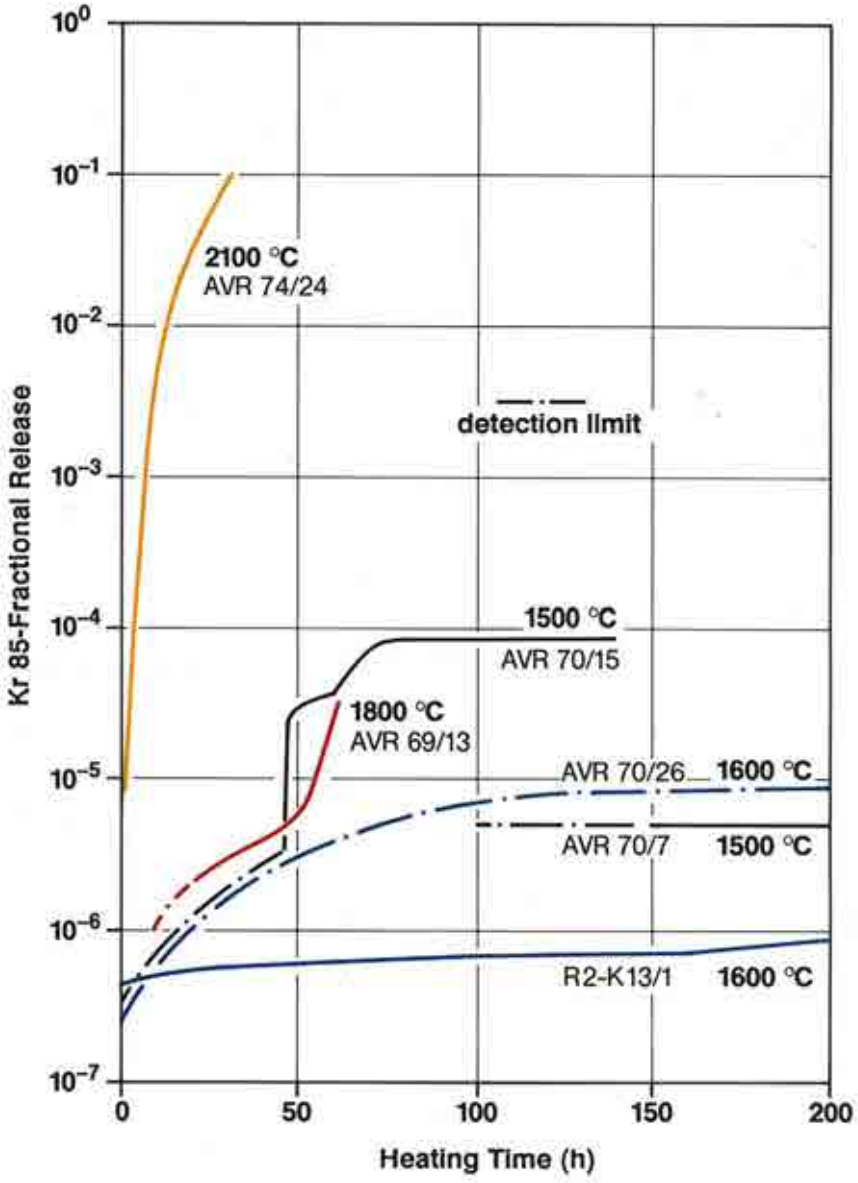

FIG. 41. ^{85}Kr fractional release for AVR 70/26 and R2-K13/1 remained < 10^{-5} well beyond 200 hours at 1600ºC indicating no particle failure in either element.

3.3.1. Accident condition performance assessment

HEU (Th,U)O_2 TRISO fuel element accident condition performance is characterised:

— The graphite furnace has a solid fission product detection limit of one or several percent of the inventory. Furthermore, some results from the 1400ºC-1800°C isothermal accident simulation tests are unreliable because of uncertainty in the temperature determination caused by repeated failures in the automated temperature control system (therefore a new furnace had been built — the KÜFA).

— AVR GO2 fuel elements (and other modern HTR fuel elements) are soaked with caesium on the surface because of the large number of releasing elements that remained in the AVR from early poor quality fuel element production. However, they do not actively release Cs during prolonged heating from the particles within the elements.

— Spherical fuel elements irradiated in MTRs are much cleaner and release fission product at a much lower level as compared to AVR irradiated elements. However, with continued heating, these elements with higher operating temperatures and higher accumulated fast fluences exhibit active diffusive release of solid fission products from intact TRISO particles within the fuel elements.

— Typically, krypton fractional releases always lag behind the caesium release because of the additional holdup provided by the PyC layers in TRISO coatings.

The statistical evaluation of particle failure is summarized in Table 29. While the accident test results are extremely good, the coincidence of the late construction of the KÜFA furnace with the change-over to LEU resulted in only two useful tests with $(Th,U)O_2$ TRISO fuel elements. Future thorium programmes should consider additional accident testing.

Table 29. Statistical evaluation of HEU $(Th,U)O_2$ TRISO fuel particle failure fractions at 1600°C during accident simulation tests.

Spherical elements with HEU $(Th,U)O_2$ TRISO particles		No. fuel bodies	No. coated particles N	No. in-reactor failed particles n	Expected failure fraction =n/N	One-sided upper 95% confidence limit
Accident testing	R2-K13/1 during the first 550 h	1	20 050	0	0	
	AVR GO2 from Reload XV*	4	41 920	0	0	
	Total	5	61 970	0	0	4.8×10^{-5}

* AVR 70/26 in KÜFA; AVR 69/28, AVR 70/18 and AVR 74/17 in ramp tests performed in the graphite furnace.

3.4. PERFORMANCE LIMITS OF THE HEU $(TH,U)O_2$ TRISO FUEL SYSTEM

Performance data on the HEU $(Th,U)O_2$ TRISO fuel system generated within the German fuel development programme during the period 1977 to 1990 were evaluated in three areas: fuel manufacture, in-reactor testing and 1600°C accident simulation testing.

Figure 42 and Table 30 present a statistical analysis of all the manufacturing, irradiation and accident testing performance results in terms on the number of defective and failed fuel particles observed in the totality of the HEU $(Th,U)O_2$ TRISO sphere tests. For comparison, LEU UO_2 TRISO data from the later development period are also included in Table 31 [58, 59].

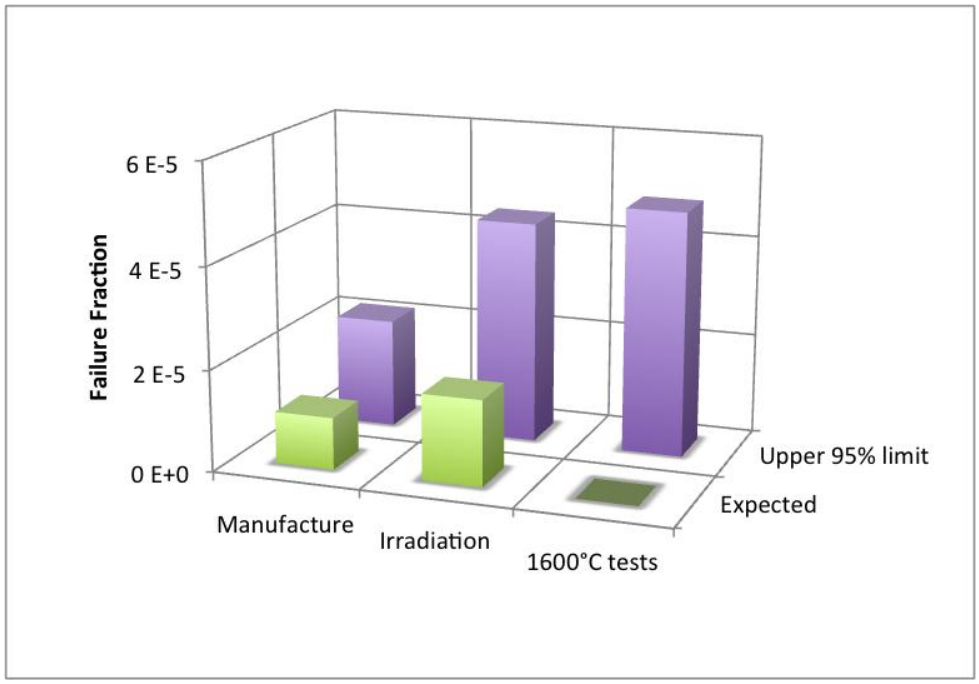

FIG. 42. Final high quality HEU (Th,U)O_2 TRISO fuel performance assessment of experimental values in manufacturing defects, irradiation and accident induced failures, and their one-sided upper 95% confidence limits.

4. SUMMARY AND CONCLUSIONS

With modern HTR fuels, present state-of-the-art requirements dictate:

— near complete retention of fission products at their source – the intact TRISO coated particles with no particle failure during normal operating conditions at temperatures < 1250°C, and for accident conditions at temperatures ≤ 1600°C;

— very low levels of contamination in the outer PyC layer ($<10^{-5}$) of the particle and in the fuel element graphitic matrix ($<10^{-5}$); and

— low levels of as-fabricated defective fuel particles ($\sim10^{-5}$) with missing or defective coatings.

In this manner, the source term in an HTR is dominated by defective fuel particles produced during manufacture and only by their failure during irradiation or in accidents. Many of the irradiation and accident conditions tests conducted between 1977 and 1990 have demonstrated excellent fuel behaviour, and their final performance assessment is limited by sampling statistics. The performance statistics for the HEU (Th,U)O_2 TRISO fuel system, as illustrated in Table 31, are in perfect concert with those state-of-the-art requirements for present-day High Temperature Reactor concepts.

TABLE 30. COMPARISON OF THE PERFORMANCE STATISTICS OBTAINED ON HEU $(Th,U)O_2$ TRISO FUEL ELEMENTS WITH SIMILAR STATISTICS ON ELEMENTS CONTAINING LEU UO_2 TRISO FUEL (see also Fig. 42).

Spherical elements with $(Th,U)O_2$ TRISO particles	Total No. fuel bodies	Total No. coated particles N	Total No. failed particles n	Expected failure fraction n/N	One-sided upper 95% confidence limit
		HEU $(Th,U)O_2$ TRISO			
Manufacture	46	487 480	5	1.0×10^{-5}	2.2×10^{-5}
Irradiation	15*	177 040*	3	1.7×10^{-5}	4.4×10^{-5}
Accident	5	61 970	0	0	4.8×10^{-5}
		LEU UO_2 TRISO			
Manufacture	175	2 202 200	86	3.9×10^{-5}	4.7×10^{-5}
Irradiation	43	670 280	0	0	4.5×10^{-6}
Accident	19	287 480	5	1.7×10^{-5}	3.7×10^{-5}

* Six MTR tests with 82 720 particles plus nine AVR tests with 94 320 particles

TABLE 31. GENERIC REQUIREMENTS OF BOTH $(Th,U)O_2$ TRISO AND UO_2 TRISO ON FUEL PERFORMANCE IN SMALL MODULAR HTRs

10^{-6} Failure Fraction ("ppm-level")	Demonstration at upper 95% Limit		Generic Requirement at 95% Level (after Hanson)
	Thorium $(Th,U)O_2$ TRISO	Uranium UO_2 TRISO	
Manufacture	22	47	140
Irradiation	44	4	200
Accidents	48	37	600

REFERENCES

[1] KASTEN, P.R., An Evaluation of Thorium Fuel Cycles", Forschungszentrum Jülich Report Juel-0276, September 1964.

[2] INTERNATIONAL ATOMIC ENERGY AGENCY, Thorium fuel cycle — Potential Benefits and Challenges, IAEA-TECDOC-1450, IAEA, Vienna (2005).

[3] INTERNATIONAL ATOMIC ENERGY AGENCY, Potential of Thorium Based Fuel Cycles to Co Plutonium and Reduce Long Lived Waste Toxicity, IAEA-TECDOC-1349, IAEA, Vienna (2003).

[4] INTERNATIONAL ATOMIC ENERGY AGENCY, Thorium Fuel Utilization: Options and Trends, IAEA-TECDOC-1319, IAEA, Vienna (2002).

[5] INTERNATIONAL ATOMIC ENERGY AGENCY, Thorium Based Fuel Options for Generation of Electricity, Development in the 1990s, IAEA-TECDOC-1155, IAEA, Vienna (2000).

[6] INTERNATIONAL ATOMIC ENERGY AGENCY, Role of Thorium to Supplement Fuel Cycles of Future Nuclear Energy Systems, IAEA Nuclear Energy Series No. NF-T-2.4, IAEA, Vienna (2012).

[7] ALLELEIN, H.J., et al., "High-Quality Thorium TRISO Fuel Performance", Forschungzentrum Jülich Energy Series Monograph, in preparation (2013).

[8] INTERNATIONAL ATOMIC ENERGY AGENCY, Consultancy Meeting on the Use of Thorium-based Fuels, Vienna, Austria (1990).

[9] http://en.wikipedia.org/wiki/Thorium_fuel_cycle.

[10] INTERNATIONAL ATOMIC ENERGY AGENCY, Fuel Performance and Fission Product Behaviour in Gas Cooled Reactors, IAEA-TECDOC-978, IAEA, Vienna (1997).

[11] INTERNATIONAL ATOMIC ENERGY AGENCY, Colak, High Temperature Gas Cooled Reactor Fuels and Materials, IAEA-TECDOC-1645, IAEA, Vienna (2010).

[12] INTERNATIONAL ATOMIC ENERGY AGENCY, Advances in HTR Fuel Technology, IAEA-TECDOC-1674, IAEA, Vienna (2011).

[13] HUDDLE, R.A.U., et al., Coated Particle Fuel for the Dragon Reactor Experiment, Dragon Project Report 116, Winfrith, October 1962.

[14] NICKEL, H., HTR Coated Particles and Fuel Elements (Historical Basis); in HTR/ECS; High Temperature Rector School, Cadarache, France, 4-8 November 2002; Training on Gas Cooled Reactor Concepts, Overview of Science and Technology of HTRs.

[15] MALY, V., WAGEMANN, R., "Daten abgebrannter HTR-Brennelemente. Teil I: Das AVR-Brennelement", AVR Report, Jülich, August 1977.

[16] VAN, S.M., "Commercialization of a Thorium Fuelled Pebble Bed Modular Reactor", Thorium Energy Conference, Shanghai, 29 Oct – 1 Nov 2012.

[17] NICKEL, H., GULDEN, T.D., "Coated Particles Fuels", Special Issue in Nucl. Techn. **35** (1977) 189–573.

[18] INTERNATIONAL ATOMIC ENERGY AGENCY, An Overview of Technical Issues and Potential. Industrial Solutions for the HTR Fuel Cycle, IAEA-TECDOC-1645, IAEA, Vienna (2010).

[19] GENERAL ATOMICS, "MHTGR Pu Consumption Study", GA-Final Report, May 1993.

[20] GRENECHE, D., et al., "The Reprocessing Issue for HTR Fuels: An Assessment of Its Interest and Its Feasibility", Global 2003 Conference, New Orleans, November, 2003.

[21] MITAUT, P., Cycles Combustibles U-Th, Pu-U Appauvri et Pu-Th dans les Réacteurs Modulaires à Haute Température, CEA Report, DMT/93-291, June 1993.
[22] BONIN, B., GRENECHE, D., Prospective Studies of HTR Fuel Cycles Involving Plutonium, HTR 2002, Petten, The Netherlands, 21-24 April 2002.
[23] HOWARD, R., et al., A Summary and Evaluation of the Achievements of the Dragon Project and its Contribution to the Development of the High Temperature Reactor, Dragon Project Report DPR 1000, Winfrith (1978).
[24] MILLER, C.W., SCHEFFEL, W.J., Postirradiation Examination and Evaluation of Peach Bottom FTE-13, GA Technologies Six-Digit Report 906939, November 1985.
[25] ANSA "Management and Disposition of Excess Weapons Plutonium, Report of the American National Science Academy, Reactor Related Options **2** (1999).
[26] DRAGON REPORT, Plutonium in High Temperature Reactors, DRAGON Project Report 899, Winfrith (1974).
[27] OLSON, G.L., et al., "Fuel Summary Report: Shippingport Light Water Breeder Reactor", INEEL/EXT-98-00799, Rev. 2, September 2002.
[28] GRENECHE, D., "HTR Fuel Cycles: A Comprehensive Outlook of Past Experience and an Analysis of Future Options"; ICAPP Conference 2003.
[29] HUSCHKA, H., VYGEN, P., "Coated Particles: Requirements and Status of Fabrication Technology", Nuclear Technology **35** (1977) 228.
[30] KADNER, M., BAIER, J., "Production of Fuel Kernels for HTR Fuel Elements", Kerntechnik **18** (1977) 413.
[31] GONTARD, R., MEHNER, A.W., "Vorbestrahlungsbericht für das Experiment R2-K12", Forschungszentrum Jülich Internal Report HBK-IB-7/81, Research Centre Jülich (1981).
[32] CHINAGLIA, B., et al., "The Diffusion of Strontium and Cesium in Pyrolytic Silicon Carbide", DRAGON Project Report 805, Winfrith (1972).
[33] GYARMATI, E., NICKEL, H., "Stationäre und dynamische Abscheidung von SiC auf beschichteten Teilchen", Forschungszentrum Jülich Report-900-RW, November 1972.
[34] ZHAO, H., et al., "Manufacture and Characteristics of Spherical Fuel Elements for the HTR-10", Nuclear Engineering and Design **236** (2006) 643.
[35] HROVAT, M., NICKEL, H., KOIZLIK, K., "Über die Entwicklung eines Matrixmaterials zur Herstellung gepresster Brennelemente für Hochtemperatur-Reaktoren", Forschungszentrum Jülich Report Jül-969 (1973).
[36] HROVAT, M., et al., "Spherical Fuel Elements for Small and Medium Sized HTRs", Nuclear Engineering and Design 109 (1988) 253.
[37] <http://www.world-nuclear news.org/ENFChinese_HTR_fuel_plant_under_construction-2103134.html> 2013.
[38] SCHULZE, R.E., SCHULZE, H.A., RIND, W., "Graphite Matrix Materials for Spherical HTR Fuel Elements", Forschungszentrum Jülich Report Jül-Spez-167 (1982).
[39] LIANG, T. X., "Recent R&D of HTR Fuel in INET", Presentation at the IAEA Technical Meeting on HTR Fuel and Fuel Cycle, Vienna, 6–9 September 2010.
[40] HEIT, W., "Pebble Bed Fuel Element Research and Development and Industrial Production in Germany", Proc. HTR-TN Int. HTR Fuel Seminar, Brussels (2001).
[41] HAUER, M., BROCKER, P., "HOBEG Abnahmeprüfzeugnis AVR XV nach DIN 50049-3.1.B, Zeugnis Nr. 716/3193/78 from 7 September 1978", HOBEG, Hanau (1978).

[42] HAUER, M., BROCKER, P., “HOBEG Abnahmeprüfzeugnis AVR XX nach DIN 50049-3.1.B, Zeugnis Nr. 57/5561/83 from 20 May 1983”, HOBEG, Hanau (1983).

[43] HERTZ, P., Über den gegenseitigen durchschnittlichen Abstand von Punkten, die mit bekannter mittlerer Dichte im Raume angeordnet sind, Math. Ann. **67** (1909) 387–398.

[44] NABIELEK, H., “The distribution of particles in a sphere and the maximum acceptable loading” Düren (in preparation) (2013).

[45] HANIA, P.R., et al., Qualification of HTR pebbles by X ray tomography and thermal analysis, Nucl. Eng. Des. **251** (2012) 47.

[46] HBK Projektbericht 1977, “Grenzen der Machbarkeit kaltgepreßter Brennelemente aus A3-3 und A3-27 Matrix”, Forschungszentrum Jülich Internal Report HBK-IB-01/78.

[47] VORREYER, M., LEUSHACKE, D.F., “Th/U-Fuel Cycle for HTGRs. ProNuclear Seminar 1978”, Forschungszentrum Jülich Internal Report, HBK-IB-2/78, Research Centre Jülich, 1978.

[48] BURCK, W., KRAUTWASSER, P., “Datensatz zum Bestrahlungsverhalten von hochangereicherten (Th,U)-Mischoxid-Brennstoffteilchen mit SiC Zwischenschicht”, Forschungszentrum Jülich Internal Report, IRW-IB-13/88, Jülich (1988).

[49] GONTARD, R., NABLEIK, H., “Performance Evaluation of Modern HTR TRISO Fuels”, Forschungszentrum Jülich Internal Report HTA-IB-05/90 (1990).

[50] WIMMERS, M., “Das Verhalten kugelförmiger HTR-Brennelemente bei der Massenerprobung im AVR-Reaktor”, PhD Thesis, Jülich, January 1977.

[51] WEBER, J., “Einbeziehung der Spaltproduktfreisetzung in die numerischen Simulation des AVR-Abbrand-Umwälzgeschehens und Vergleich mit den VAMPYR-Resultaten”, PhD Thesis, Forschungszentrum Jülich Report Juel-1579, January 1979.

[52] IVENS, G., WIMMERS, M., “The AVR as Test Bed for Fuel Elements”, 21 Years of Successful Operation for a Future Technology’, Association of German Engineers (VDI)) - The Society for Energy Technologies (Publ.), VDI-Verlag Düsseldorf (1990).

[53] GOTTAUT, H., KRUGER, K., Results of Experiments at the AVR Reactor, Nuclear Engineering and Design **121** (1990) 143.

[54] ZIERMANN, E. IVENS, G., “Abschlußbericht über den Leistungsbetrieb des AVR-Versuchskernkraftwerks”, Forschungszentrum Jülich Report Juel-3448, October 1997.

[55] VERFONDERN, K., “Status of German Spent HTR Fuel Research”, Proceedings IAEA-TM on ‘Safety Aspects of Modular HTRs’, Beijing (2007).

[56] NABIELEK, H., et. al., "Fuel and Fission Products in the Jülich AVR Pebble-Bed Reactor", Proc. 4th International Topical Meeting on High Temperature Reactor Technology (HTR-2008), Paper 58337, The American Society of Chemical Engineers (2008).

[57] SCHENK, W., “Untersuchungen zum Verhalten von beschichteten Brennstoffteilchen und Kugelbrennelementen bei Störfalltemperaturen”, Forschungszentrum Jülich Report Juel-1490, May 1978.

[58] KANIA, M J., NABLIEK, H., VERFONDERN, K., “Testing of HTR UO_2 TRISO Fuels in AVR and in Material Test Reactors”, J. Nucl. Mat. (in preparation) (2013).

[59] KANIA, M J., NABLIEK H., NICKEL, H., “Coated Particle Fuels in HTRs”, chapter 4 in Wiley book on Nuclear Materials (in preparation) (2013).

[60] SCHENK, W., “Störfallsimulation an bestrahlten Kugelbrennelementen bei Temperaturen von 1400 bis 2500°C”, Forschungszentrum Jülich Report Juel-1883, December 1983.
[61] SCHENK, W., PITZER, D., NABLIEK, H., Fission Product Release Profiles from Spherical HTR Fuel Elements at Accident Temperatures, Forschungszentrum Jülich Report Juel-2234, September 1988.
[62] SCHENK, W., NABLIEK, H., “Kugelbrennelemente mit TRISO Partikeln bei Störfalltemperaturen”, Forschungszentrum Jülich Report Juel Spez-487, January 1989.
[63] NABLIEK, H., et al., The Performance of HTR Fuel Particles at Extreme Temperatures, Nucl. Techn. **84** (1989) 62.
[64] SCHENK, W., POTT, G., NABLIEK, H, Fuel Accident Performance Testing for Small HTRs, J. Nucl. Mat. **171** (1990) 19.
[65] NABLIEK, H., et al., Silver Release from Coated Particle Fuel, Nucl. Techn. **35** (1977) 483.
[66] HANSON, D.L., GT-MHR Source Term Overview, US-NRC, 28 January 2003.

ABBREVIATIONS

AVR	Arbeitsgemeinschaft Versuchsreaktor
BISO	Bi-isotropic
BN	Beloyarsk nuclear
CVD	Chemical vapour deposition
FIMA	Fission per initial heavy metal atom
FSV	Fort St. Vrain nuclear power station
GT-MHR	Gas turbine modular helium reactor
GIF	Generation IV international forum
HEU	High enriched uranium
HHT	High temperature helium turbine reactor
HTGR	High temperature gas cooled reactor
HTI	High temperature isotropic
HTR	High temperature reactor
HTR-PM	High temperature reactor – pebble modular
iPyC	Inner pyrocarbon coating
JUPITER	Juelicher Pilotanlage for thorium element reprocessing
KUFA	Kuehlfingerapparatur (cold finger apparatus)
LEU	Low enriched uranium
LTI	Low temperature isotropic
LWBR	Light water breeder reactor
MHR	Modular high temperature reactor
MOX	Mixed uranium plutonium oxide
MTR	Material test reactor
PNP	Prototype nuclear process heat
PWR	Pressurized water reactor
PyC	Pyrocarbon coating
PUREX	Plutonium uranium extraction
R/B	Release rate to birth rate ratio
THOREX	Thorium extraction
THTR	Thorium high temperature reactor
TRISO	Tri-coated isotropic
WAR	Weak acid resin

CONTRIBUTORS TO DRAFTING AND REVIEW

Basak, U	International Atomic Energy Agency
Nabliek, H	ARGE– KT, Germany

Research Coordination Meeting (RCM)

Vienna, Austria: 22–24 October 2012

IAEA
International Atomic Energy Agency

No. 23

ORDERING LOCALLY

In the following countries, IAEA priced publications may be purchased from the sources listed below or from major local booksellers.

Orders for unpriced publications should be made directly to the IAEA. The contact details are given at the end of this list.

AUSTRALIA
DA Information Services
648 Whitehorse Road, Mitcham, VIC 3132, AUSTRALIA
Telephone: +61 3 9210 7777 • Fax: +61 3 9210 7788
Email: books@dadirect.com.au • Web site: http://www.dadirect.com.au

BELGIUM
Jean de Lannoy
Avenue du Roi 202, 1190 Brussels, BELGIUM
Telephone: +32 2 5384 308 • Fax: +32 2 5380 841
Email: jean.de.lannoy@euronet.be • Web site: http://www.jean-de-lannoy.be

CANADA
Renouf Publishing Co. Ltd.
5369 Canotek Road, Ottawa, ON K1J 9J3, CANADA
Telephone: +1 613 745 2665 • Fax: +1 643 745 7660
Email: order@renoufbooks.com • Web site: http://www.renoufbooks.com

Bernan Associates
4501 Forbes Blvd., Suite 200, Lanham, MD 20706-4391, USA
Telephone: +1 800 865 3457 • Fax: +1 800 865 3450
Email: orders@bernan.com • Web site: http://www.bernan.com

CZECH REPUBLIC
Suweco CZ, spol. S.r.o.
Klecakova 347, 180 21 Prague 9, CZECH REPUBLIC
Telephone: +420 242 459 202 • Fax: +420 242 459 203
Email: nakup@suweco.cz • Web site: http://www.suweco.cz

FINLAND
Akateeminen Kirjakauppa
PO Box 128 (Keskuskatu 1), 00101 Helsinki, FINLAND
Telephone: +358 9 121 41 • Fax: +358 9 121 4450
Email: akatilaus@akateeminen.com • Web site: http://www.akateeminen.com

FRANCE
Form-Edit
5 rue Janssen, PO Box 25, 75921 Paris CEDEX, FRANCE
Telephone: +33 1 42 01 49 49 • Fax: +33 1 42 01 90 90
Email: fabien.boucard@formedit.fr • Web site: http://www.formedit.fr

Lavoisier SAS
14 rue de Provigny, 94236 Cachan CEDEX, FRANCE
Telephone: +33 1 47 40 67 00 • Fax: +33 1 47 40 67 02
Email: livres@lavoisier.fr • Web site: http://www.lavoisier.fr

L'Appel du livre
99 rue de Charonne, 75011 Paris, FRANCE
Telephone: +33 1 43 07 50 80 • Fax: +33 1 43 07 50 80
Email: livres@appeldulivre.fr • Web site: http://www.appeldulivre.fr

GERMANY
Goethe Buchhandlung Teubig GmbH
Schweitzer Fachinformationen
Willstätterstrasse 15, 40549 Düsseldorf, GERMANY
Telephone: +49 (0) 211 49 8740 • Fax: +49 (0) 211 49 87428
Email: s.dehaan@schweitzer-online.de • Web site: http://www.goethebuch.de

HUNGARY
Librotade Ltd., Book Import
PF 126, 1656 Budapest, HUNGARY
Telephone: +36 1 257 7777 • Fax: +36 1 257 7472
Email: books@librotade.hu • Web site: http://www.librotade.hu

INDIA
Allied Publishers
1st Floor, Dubash House, 15, J.N. Heredi Marg, Ballard Estate, Mumbai 400001, INDIA
Telephone: +91 22 2261 7926/27 • Fax: +91 22 2261 7928
Email: alliedpl@vsnl.com • Web site: http://www.alliedpublishers.com

Bookwell
3/79 Nirankari, Delhi 110009, INDIA
Telephone: +91 11 2760 1283/4536
Email: bkwell@nde.vsnl.net.in • Web site: http://www.bookwellindia.com

ITALY
Libreria Scientifica "AEIOU"
Via Vincenzo Maria Coronelli 6, 20146 Milan, ITALY
Telephone: +39 02 48 95 45 52 • Fax: +39 02 48 95 45 48
Email: info@libreriaaeiou.eu • Web site: http://www.libreriaaeiou.eu

JAPAN
Maruzen Co., Ltd.
1-9-18 Kaigan, Minato-ku, Tokyo 105-0022, JAPAN
Telephone: +81 3 6367 6047 • Fax: +81 3 6367 6160
Email: journal@maruzen.co.jp • Web site: http://maruzen.co.jp

NETHERLANDS
Martinus Nijhoff International
Koraalrood 50, Postbus 1853, 2700 CZ Zoetermeer, NETHERLANDS
Telephone: +31 793 684 400 • Fax: +31 793 615 698
Email: info@nijhoff.nl • Web site: http://www.nijhoff.nl

Swets Information Services Ltd.
PO Box 26, 2300 AA Leiden
Dellaertweg 9b, 2316 WZ Leiden, NETHERLANDS
Telephone: +31 88 4679 387 • Fax: +31 88 4679 388
Email: tbeysens@nl.swets.com • Web site: http://www.swets.com

SLOVENIA
Cankarjeva Zalozba dd
Kopitarjeva 2, 1515 Ljubljana, SLOVENIA
Telephone: +386 1 432 31 44 • Fax: +386 1 230 14 35
Email: import.books@cankarjeva-z.si • Web site: http://www.mladinska.com/cankarjeva_zalozba

SPAIN
Diaz de Santos, S.A.
Librerias Bookshop • Departamento de pedidos
Calle Albasanz 2, esquina Hermanos Garcia Noblejas 21, 28037 Madrid, SPAIN
Telephone: +34 917 43 48 90 • Fax: +34 917 43 4023
Email: compras@diazdesantos.es • Web site: http://www.diazdesantos.es

UNITED KINGDOM
The Stationery Office Ltd. (TSO)
PO Box 29, Norwich, Norfolk, NR3 1PD, UNITED KINGDOM
Telephone: +44 870 600 5552
Email (orders): books.orders@tso.co.uk • (enquiries): book.enquiries@tso.co.uk • Web site: http://www.tso.co.uk

UNITED STATES OF AMERICA
Bernan Associates
4501 Forbes Blvd., Suite 200, Lanham, MD 20706-4391, USA
Telephone: +1 800 865 3457 • Fax: +1 800 865 3450
Email: orders@bernan.com • Web site: http://www.bernan.com

Renouf Publishing Co. Ltd.
812 Proctor Avenue, Ogdensburg, NY 13669, USA
Telephone: +1 888 551 7470 • Fax: +1 888 551 7471
Email: orders@renoufbooks.com • Web site: http://www.renoufbooks.com

United Nations
300 East 42nd Street, IN-919J, New York, NY 1001, USA
Telephone: +1 212 963 8302 • Fax: 1 212 963 3489
Email: publications@un.org • Web site: http://www.unp.un.org

Orders for both priced and unpriced publications may be addressed directly to:

IAEA Publishing Section, Marketing and Sales Unit, International Atomic Energy Agency
Vienna International Centre, PO Box 100, 1400 Vienna, Austria
Telephone: +43 1 2600 22529 or 22488 • Fax: +43 1 2600 29302
Email: sales.publications@iaea.org • Web site: http://www.iaea.org/books

15-03901

International Atomic Energy Agency
Vienna
ISBN 978–92–0–100715–5
ISSN 1011–4289